PB80-219660

Development of a High Current Oilboom/Skimmer

Ultrasystems, Inc.
Irvine, CA

Prepared for

Industrial Environmental Research
Lab- Cincinnati, Edison, NJ Oil and
Hazardous Materials Spills Branch

Jun 80

U.S. Department of Commerce
National Technical Information Service
NTIS

TECHNICAL REPORT DATA
(Please read Instructions on the reverse before completing)

1. REPORT NO.
EPA-600/2-80-140

2.

3. RECIPIENT'S ACCESSION NO.
PB80 219660

4. TITLE AND SUBTITLE
Development of a High Current Oilboom/Skimmer

5. REPORT DATE
JUNE 1980 ISSUING DATE.

6. PERFORMING ORGANIZATION CODE

7. AUTHOR(S)
Blair A. Folsom

8. PERFORMING ORGANIZATION REPORT NO.

9. PERFORMING ORGANIZATION NAME AND ADDRESS
Ultrasystems, Inc.
Irvine, CA 92715

10. PROGRAM ELEMENT NO.
1BB610

11. CONTRACT/GRANT NO.
68-03-0403

12. SPONSORING AGENCY NAME AND ADDRESS
Industrial Environmental Research Laboratory
Office of Research and Development
U.S. Environmental Protection Agency
Cincinnati, OH 45268

13. TYPE OF REPORT AND PERIOD COVERED
Final

14. SPONSORING AGENCY CODE
EPA/600/12

15. SUPPLEMENTARY NOTES

16. ABSTRACT

A low drag oil spill recovery device has been developed to retain and recover floating oil slicks in currents up to 3.0 m/sec (6 knots) and low wave conditions typically encountered in small lakes and harbors, smooth flowing streams and other inland waterways. The streamlined oil boom/skimmer utilizes a slightly submerged slotted hydrofoil to skim a thin layer of oil and water into an attached sump where the kinetic energy of the high speed flow is dissipated and the oil and water are separated by gravity. The excess water is discarded and the oil is retained in the sump under conditions similar to a conventional low speed oil boom. The retained oil is recovered as required by a built-in secondary skimmer. Because of the system's simplicity and low drag, it can be deployed as a high speed skimmer supported by a catamaran or as a high current boom with several adjacent sections spanning a high current area.

The development effort focused on bow, sump and stability control system design and the testing of the complete streamlined oil boom system at OHMSETT. Thruput efficiencies as high as 99+ percent and 87 percent were measured under calm surface conditions at 2.0 and 3.0 m/sec (4 and 6 knots) respectively. Performance degraded in tests with waves.

17. KEY WORDS AND DOCUMENT ANALYSIS

a. DESCRIPTORS	b. IDENTIFIERS/OPEN ENDED TERMS	c. COSATI Field/Group
Water Pollution Oils Skimmers Harbors Performance Tests	Equipment Evaluation Oil Spill Cleanup Protected Waters	68D

18. DISTRIBUTION STATEMENT RELEASE TO PUBLIC	19. SECURITY CLASS *(This Report)* UNCLASSIFIED	21. NO. OF PAGES
	20. SECURITY CLASS *(This page)* UNCLASSIFIED	22. PRICE

EPA Form 2220-1 (9-73)

☆ U.S. GOVERNMENT PRINTING OFFICE: 1980--657-165/0011

United States
Environmental Protection
Agency

Industrial Environmental Research
Laboratory
Cincinnati OH 45268

EPA-600/2-80-140
June 1980

PB80-219660

Research and Development

EPA

Development of a High Current Oilboom/Skimmer

REPRODUCED BY
NATIONAL TECHNICAL
INFORMATION SERVICE
U.S. DEPARTMENT OF COMMERCE
SPRINGFIELD, VA 22161

RESEARCH REPORTING SERIES

Research reports of the Office of Research and Development, U.S. Environmental Protection Agency, have been grouped into nine series. These nine broad categories were established to facilitate further development and application of environmental technology. Elimination of traditional grouping was consciously planned to foster technology transfer and a maximum interface in related fields. The nine series are:

1. Environmental Health Effects Research
2. Environmental Protection Technology
3. Ecological Research
4. Environmental Monitoring
5. Socioeconomic Environmental Studies
6. Scientific and Technical Assessment Reports (STAR)
7. Interagency Energy-Environment Research and Development
8. "Special" Reports
9. Miscellaneous Reports

This report has been assigned to the ENVIRONMENTAL PROTECTION TECHNOLOGY series. This series describes research performed to develop and demonstrate instrumentation, equipment, and methodology to repair or prevent environmental degradation from point and non-point sources of pollution. This work provides the new or improved technology required for the control and treatment of pollution sources to meet environmental quality standards.

This document is available to the public through the National Technical Information Service, Springfield, Virginia 22161.

EPA-600/2-80-140
June 1980

DEVELOPMENT OF A HIGH CURRENT OILBOOM/SKIMMER

by

Blair A. Folsom
Ultrasystems, Inc.
Irvine, California 92715

Contract No. 68-03-0403

Project Officer

Stephen J. Dorrler
Oil and Hazardous Material Spills Branch
Industrial Environmental Research Laboratory
Edison, New Jersey 08817

INDUSTRIAL ENVIRONMENTAL RESEARCH LABORATORY
OFFICE OF RESEARCH AND DEVELOPMENT
U.S. ENVIRONMENTAL PROTECTION AGENCY
CINCINNATI, OHIO 45268

DISCLAIMER

This report has been reviewed by the Industrial Environmental Research Laboratory, U.S. Environmental Protection Agency, and approved for publication. Approval does not signify that the contents necessarily reflect the views and policies of the U.S. Environmental Protection Agency, nor does mention of trade names or commercial products constitute endorsement or recommendation for use.

FOREWORD

When energy and material resources are extracted, processed, converted, and used, the related pollutional impacts on our environment and even on our health often require that new and increasingly more efficient pollution control methods be used. The Industrial Environmental Research Laboratory - Cincinnati (IERL-Ci) assists in developing and demonstrating new and improved methodologies that will meet these needs both efficiently and economically.

This report describes the development and testing of a high speed (4 to 6 knot) skimmer for collecting floating oil from calm water. This technique will be of interest to all those interested in cleaning up oil spills in protected waters. Further information may be obtained through the Resource Extraction and Handling Division, Oil and Hazardous Materials Spills Branch, Edison, New Jersey.

David G. Stephan
Director
Industrial Environmental Research Laboratory
Cincinnati

ABSTRACT

A low drag oil spill recovery device has been developed to retain and recover floating oil slicks in currents up to 3.0 m/sec (6 knots) and low wave conditions typically encountered in small lakes and harbors, smooth flowing streams and other inland waterways. The streamlined oil boom/skimmer utilizes a slightly submerged slotted hydrofoil to skim a thin layer of oil and water into an attached sump where the kinetic energy of the high speed flow is dissipated and the oil and water are separated by gravity. The excess water is discarded and the oil is retained in the sump under conditions similar to a conventional low speed oil boom. The retained oil is recovered as required by a built-in secondary skimmer. Because of the system's simplicity and low drag, it can be deployed as a high speed skimmer supported by a catamaran or as a high current boom with several adjacent sections spanning a high current area.

The development effort focused on bow, sump and stability control system design and the testing of the complete streamlined oil boom system at OHMSETT. Thruput efficiencies as high as 99+ percent and 87 percent were measured under calm surface conditions at 2.0 and 3.0 m/sec (4 and 6 knots) respectively. Performance degraded in tests with waves.

This report was submitted in fulfillment of Contract 68-03-0403 by Ultrasystems, Inc. under the sponsorship of the U.S. Environmental Protection Agency. This report covers the period March 1, 1974 to March 31, 1980, and work was completed as of March 28, 1980.

CONTENTS

Foreword iii
Abstract iv
Figures vi
Tables vii
Abbreviations and Symbols viii
Acknowledgement x

1. Introduction 1
2. Conclusions 7
3. Recommendations 9
4. Bow Design. 11
5. Sump Design 33
6. Forces and Stability 48
7. System Integration Tests 60

References 80

Appendices

A. Phenomenological Bow Wave Theory 81
B. Detailed Test Procedures - OHMSETT System Integration Tests . . 94
C. Oil Handling and Experimental Errors - OHMSETT Systems Integration Tests 99

FIGURES

Number Page

1 Streamlined boom design with rigid sump - Phase I Tests........ 3
2 Schematic diagram of Phase I oil boom test.................... 4
3 Typical flow over a streamlined shape, shallow submergence..... 13
4 Small scale models for bow wave tests......................... 16
5 Emperical bow wave correlation verification.................. 17
6 Dimensionless bow wave flow map............................. 18
7 Dimensionless bow wave flow map with data, all solid models.... 20
8 Preliminary slotted model tests............................. 22
9 Slotted models.. 23
10 Typical flow - NACA 4415 model.............................. 25
11 Typical flow - NACA 0015 model.............................. 26
12 Correlations for bows of slotted models, NACA 4415 & NACA 0015. 27
13 Comparison of measured and calculated stagnation streamlines... 28
14 Preliminary streamlined oil boom model using NACA 0015 bow..... 29
15 Preliminary slotted bow design.............................. 30
16 Final bow design.. 32
17 Sump design concept - schematic drawing..................... 34
18 Sump test flow channel...................................... 37
19 Energy dissipation mechanisms............................... 39
20 Final streamlined oil boom/skimmer design................... 43
21 Minimum oil droplet size completely removed from final sump.... 45
22 Self-adjusting weir and secondary sump...................... 47
23 Model for Lockheed tests.................................... 49
24 Total vertical force vs. difference in free surface levels..... 51
25 Schematic diagram of streamlined oil boom supported by buoyant floatation system.. 52
26 Vertical stability as a function of net vertical force......... 54
27 Comparison of stability numbers with observed stability-OHMSETT Tests 1975.. 56
28 Streamlined oil boom model for System Integration Tests........ 61
29 Plan view of OHMSETT testing arrangement - 1976................ 63
30 Streamlined oil boom in system test at OHMSETT................. 64
31 Oil flow through streamlined oil boom system.................. 68
32 System Tests Results - Calm Surface at 3.0 m/sec (6 knots)..... 76
33 System Tests with Diversionary Boom - Flow Pattern............ 77
34 System Tests Results - Calm Water at 2.0 m/sec (4 knots)....... 79
A- 2 Fictitious Bottom Contour For Open Channel Flow Analysis....... 81
A-3 Theoretical Correlation G_3 vs. G_B............................ 83
A-4 Theoretical Correlation G_1 vs. G_B............................ 84
A-5 Three-Dimensional Flow Over Model............................ 86

FIGURES (continued)

Number Page

A-6 Dolphin Nose Model - Correlations.......................... 87
A-7 Dolphin Nose Model Data Corrected For Vortices and Data Taken with Sidewalls... 88
A-1 Turbulent Bow Wave Flow Model................................ 92
C-1 Oil Input - Schematic Diagram................................100
C-2 Oil Recovery - Schematic Diagram.............................102
C-3 Pear-Shaped Centrifuge Tube, from ASTM Designation D 96-73,API Standard 2542 - "Standard Method of Test For Water and Sediment in Crude Oils"...103
C-4 Error Associated with Minimum Calibration Divisions On Centrifuge Tube ASTM D96-73...104
C-5 Histogram of % Water in Recovered Oil Samples................106
C-6 Error Due to Oil Input Volume Measurement....................107
C-7 Histogram of Recovered Oil Volumes...........................108
C-8 Error Due to Recovered Volume Measurement....................109

TABLES

Number Page

1 Test Series Outline.. 5
2 Energy Dissipation Devices: Important Characteristics and Resultsof Tests in Sump Test Flow Channel.................. 40
3 Freeboard and Gate Position Adjustments for Optimum Performance 67
4 Test Oil Properties.. 70
5 Average Wave Heights in OHMSETT'S 1.0 Foot Harbor Chop........ 71
6 74

C-1 Oil Volume Measurement Summary - Errors Due To Minimum Calibration Divisions..110

ABBREVIATIONS AND SYMBOLS

B --freeboard

C_D --sump exit slot discharge coefficient

D --sump depth

F --Froude number based on freestream velocity and hydrofoil characteric length

F_i --Local Froude number at Station i

G_B --Reciprocal of Froude number squared based on freestream velocity and freeboard

g --acceleration of gravity

G_1 --Reciprocal of Froude number squared based on freestream velocity and freeboard

G_3 --Reciprocal of Froude number squared based on freestream velocity and flow depth over the hydrofoil's highest point.

$G_1{}^*$ --$G_1 \frac{W_1}{W_3}$

h_i --height of channel bottom above arbitrary horizontal datum line

L --characteristic length or effective sump length

Q --flowrate passing over hydrofoil per unit width

Q_0 --sump flowrate

S --flotation system stiffness

S_N --dimensionless stability number

S_W --sump exist slot width

V_1 --freestream velocity

V_i --local velocity at Station i

V_R --terminal oil droplet rising velocity in water

W --sump width

W_1 --width of flow passing over hydrofoil measured upstream

W_3 --hydrofoil width

Y_1 --depth of stagnation streamline beneath the free surface measured far upstream - the thickness of the layer skimmed

Y_3 --Flow depth over the top of the hydrofoil

Y_i --local flow depth at Station i

Y_0 --initial position of oil droplets in sump - distance above the bottom

ϵ --water level difference inside minus outside the sump

γ --fluid weight density

ACKNOWLEDGMENTS

The author wishes to thank Messrs. J. S. Dorrler and F. J. Freestone of the United States Environmental Protection Agency for their many valuable suggestions and assistance during this program. Thanks are also due to Dr. D. C. Wooten of Olson Laboratories and Messrs. G. C. Carver and C. Johnson of Ultrasystems, Inc. for their outstanding work on several aspects of the project.

SECTION 1

INTRODUCTION

Although the current generation of oil spill control equipment can clean up oil spills over a range of environmental conditions, it is inadequate to cope with spills in currents greater than 0.5 to 1.0 m/sec (1.0 to 2.0 knots).

The objective of this program was to develop an oil spill control device capable of retaining and recovering floating oil slicks in currents up to 3.0 m/sec (6 knots) and wave conditions typical of small bays, harbors and inland waterways with free surface excursions less than about 15 cm (6 inches) trough to crest. The device was to be deployable as either a boom retaining oil against a high current or as a high speed skimming craft recovering oil as it was encountered.

The streamlined oil boom concept investigated here uses a low drag streamlined hydrofoil to skim a thin layer of floating oil and water into an attached sump at high speed. In the sump the oil and water are separated under controlled conditions and the oil is retained against a barrier similar to a conventional oil boom. A built-in skimmer is operated as required to recover the retained oil.

This concept has several advantages which make it ideal for this application. The overall concept is quite simple and is amenable to fabrication as a boom spanning wide high current areas. Except for flotation/stability control and oil transfer systems, no moving parts are required and since the device is essentially two-dimensional, small easy to handle modules may be constructed separately and coupled to form a boom of arbitrarily long length. The streamlined design also reduces hydrodynamic drag to approximately 25 percent of a conventional oil boom's or other bluff body's drag significantly reducing structural requirements. But perhaps the most important advantage is that the concept has been successfully developed to retain and recover a high percentage of oil slicks in currents up to 3.0 m/sec (6 knots).

The streamlined oil boom development was performed in two phases. Phase I was a preliminary design and feasibility test of the streamlined oil boom concept and identified problem areas requiring additional development effort. Phase II focused on solving these problems through a series of developmental tests and integrating the subsystems into an operational preprototype system for testing at OHMSETT.

The initial boom design investigated in Phase I utilized an airfoil shaped leading edge section moving slightly beneath the water's surface skimming oil and water into a flexible sump. Early tests indicated that although the flow over the hydrofoil appeared promising, satisfactory control of the flexible sump shape could not be achieved.

Figure 1 shows an improved design where the sump was formed by the interior of the hydrofoil contours. This model was constructed and tested at the Lockheed Towing Basin in San Diego, California under a variety of wave and current conditions. The basic hydrofoil shape is an inverted NACA 4424 airfoil* with a 1.5 m (5 feet) chord and an adjustable slot in the ventral side. This slot, located in a low pressure region, bleeds excess water from the sump. End plates were attached to simulate two-dimensional flow and buoyancy was provided through a trailing cylindrical float and a small totally submerged control hydrofoil beneath the 1/4 chord point. The model was mounted to a force balance as shown in Figure 2 and tow tested at speeds up to 2.0 m/sec (4 knots).

The results of these tests indicated that the strealined oil boom concept was feasible for controlling oil spills in currents greater than 1 m/sec (2 knots). Thruput efficiencies** in excess of 65 to 75 percent were measured at 1.5 m/sec (3 knots) with drag coefficients substantially smaller than bluff bodies. Three design problems associated with further development were also identified:

- Bow Design - The achievement of a fundamental understanding of the oil-water flow in the vicinity of the bow wave and the design of the proper bow shape to give efficient operation under a wide variety of conditions.

- Sump Design - The development of a functional oil seperation and pumping system for handling the flow into and out of the sump.

- Stability Control System Design - Using flotation and hydrodynamic control surfaces to design a system with the proper response in combined wave and current conditions.

The Phase II development solved these problems through a balanced program of analysis to understand the important flow phenomena and iterative testing to optimize design. Table 1 describes the eight major test series performed in both phases. Following the Phase I tests at the Lockheed Towing Basin, bow wave tests were performed at small scale using open channel flow facilities. A phenomenological theory was developed as a parallel effort to correlate the results of the tests and identify scaling parameters.

---

* NACA 4424 has a 4 percent camber with the maximum 40 percent aft of the leading edge and a maximum thickness of 24 percent of the chord length. See Summary of Air Foil Data by Abbott, Doenhoff and Stives, National Advisory Committee for Aeronautics Report #825. 1945.

** Thruput efficiency in the ratio of oil volume collected to oil volume encountered as a floating oil slick.

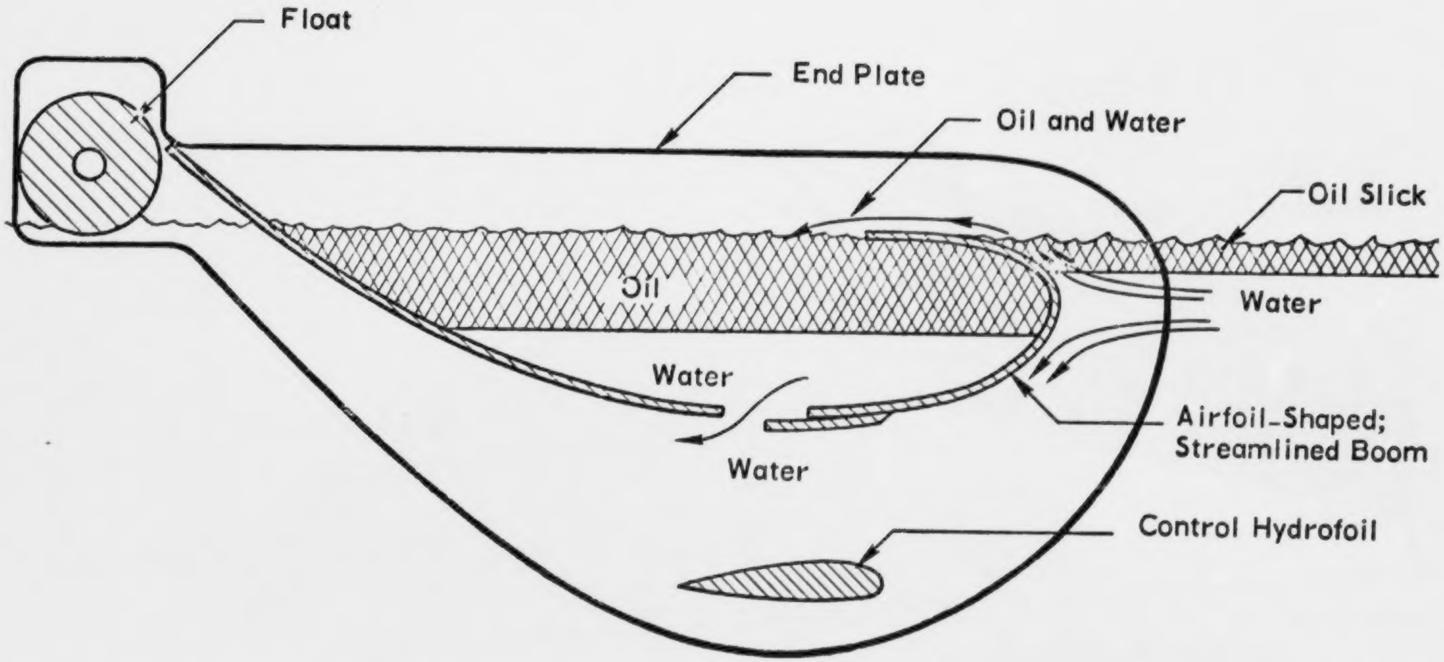
Float
End Plate
Oil and Water
Oil Slick
Oil
Water
Water
Water
Airfoil-Shaped;
Streamlined Boom
Control Hydrofoil

Figure 1. Streamlined boom design with rigid sump as an integral part of streamlined shape - Phase I Tests

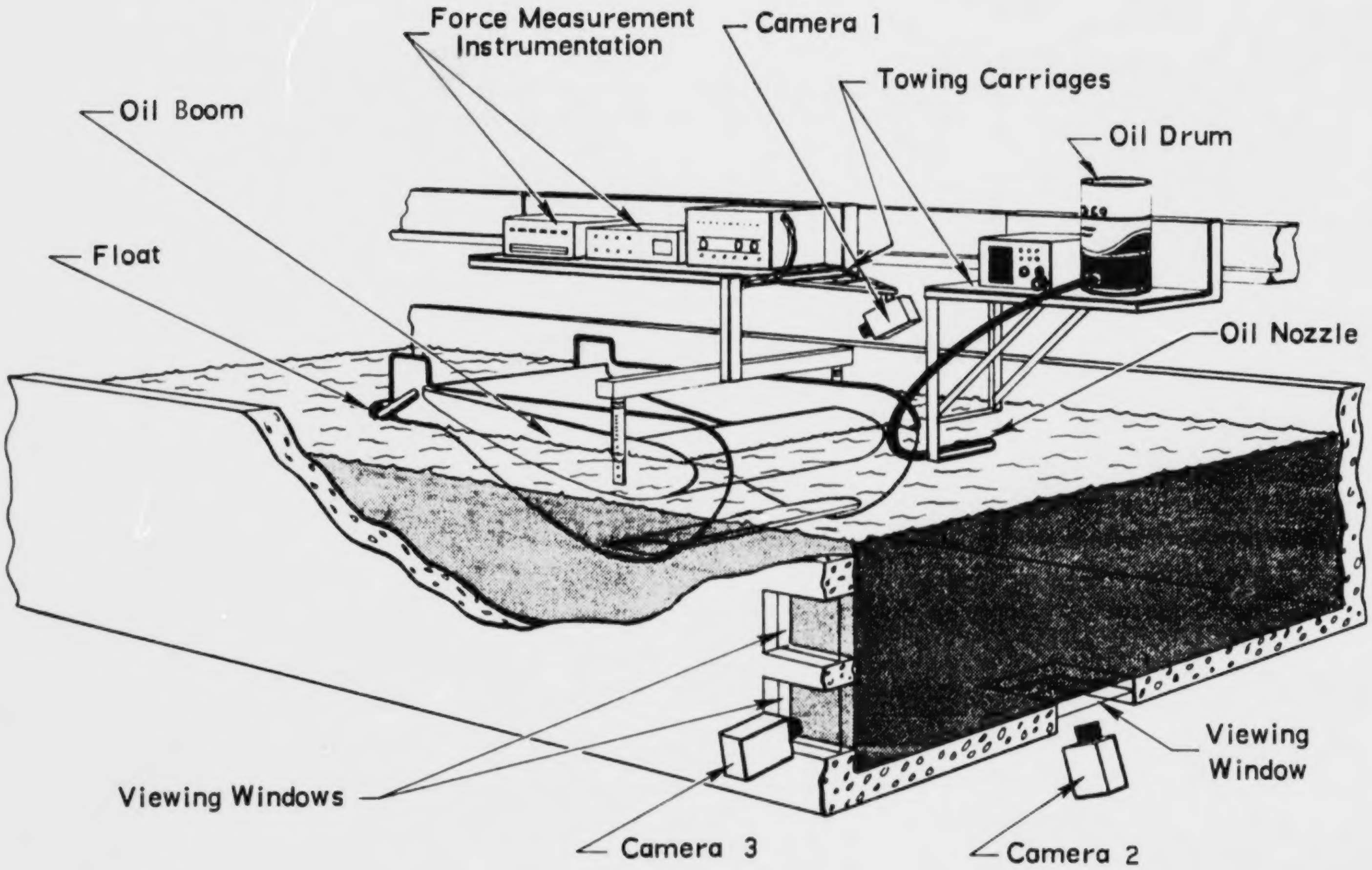
Force Measurement Instrumentation
Camera 1
Towing Carriages
Oil Drum
Oil Boom
Float
Oil Nozzle
Viewing Windows
Viewing Window
Camera 3
Camera 2

Figure 2. Schematic diagram of Phase I oil boom test

TABLE 1. TEST SERIES OUTLINE

Test Series	Scale (Vertical and flow Direction)	Model Width	Goal/Result
Tow tests at Lockheed Towing Basin, San Diego, California 5/72-11/72	Full	1.2 m (4 ft.)	Measured forces, verified system feasibility in tests with oil and identified further development needs.
Bow wave tests in small flow channels at University of California at Irvine and California State University at Fullerton 4/74-5/75	1/3	10 cm (4 in.)	Developed bow and preliminary sump designs: hydrodynamic tests, no oil
Flow channel tests in U.S. Coast Guard recirculating flow channel Richardson, Texas 5/75	Full	1.2 m (4 ft.)	Refined bow and sump designs, testing with simulated* and real oil at up to 2.5 knots
Tow tests at Lockheed Towing Basin, San Diego, California 8/75	Full	0.61 m (2 ft.)	Measured forces and refined bow and sump design in tests with simulated* oil at up to 6 knots
Tow tests at OHMSETT** (first test series) 10/75-11/75	Full	1.52 m (5 ft.)	System integration, sump design refinement, testing with oil at 3 and 6 knots, instability identified
Sump tests in specially constructed flow channel at Ultrasystems, Irvine, California 10/75-7/76	Full	8.9 cm (3.5 in.)	Refined sump design in 6-knot tests with simulated * and real oil
Catamaran supported bay tow tests in Newport Harbor, Newport Beach, California 7/76	1/3	0.51 m (20 in.)	Measured flotation requirements and developed stability control system; hydrodynamic tests, no oil
Tow tests at OHMSETT** (second test series) 9/76	Full	1.52 m (5 ft.)	System integration and testing at 4 and 6 knots

---

* Simulated oil is floating granular material: polyethelene beads approx. diameter = 0.30 cm (0.125 in.) specific gravity = 0.96.

** OHMSETT is the abbreviation for the U.S. Environmental Protection Agency's Oil and Hazardous Materials Simulated Environmental Test Tank located in Leonardo, N.J.

Based on the results of these small scale tests, a full-scale 1.2 m (4 feet) wide model was constructed using the best bow design and a preliminary sump design. Tests in a Coast Guard flow channel in Richardson, Texas were used to refine bow and sump designs in tests with real and simulated oil (see note for Table 1). An improved model was then constructed and tested at the Lockheed Towing Basin. The model was mounted to a force balance to determine lift, drag, moments and performance under calm water and periodic wave conditions was measured at tow speeds up to 3.0 m/sec (6 knots).

The results of all these tests were then combined into a full-scale 1.5 m (5 feet) wide model for testing of OHMSETT. The model was attached to a 10.3 m (34 feet) catamaran and tow tested at 1.5 and 3.0 m/sec (3 and 6 knots). Thruput efficiencies as high as 86.5 percent at 1.5 m/sec (3 knots) and 72.0 percent at 3.0 m/sec (6 knots) were achieved under optimum conditions. These tests also identified a hydrostatic instability due to the interaction of the weight of water contained in the sump and the catamaran flotation. For testing purposes, this instability was counteracted by continuously manually adjusting the flowrate out of the sump. However, this manual method only achieved a semblance of stability with large oscillations in sump depth, freeboard and other operational parmameters. A stability control system was clearly required.

The less than perfect thruput efficiency at 3.0 m/sec (6 knots) prompted a series of full-scale sump development tests. Since the strealined oil boom is essentially a two-dimentional device, a full-scale (except for width) sump model was constructed to test several sump design options. The sump width was chosen as 8.9 cm (3.5 inches), the width of a "2X4" to produce a channel with flow requirements within the capacity of available pumps.

The stability control problem was attacked both analytically and experimentally. A stability analysis using nonlinear control system analytical techniques was used to select a promising system which was optimized through 1/3-scale tow tests in Newport Harbor.

The results of subsystem development in each of these areas were combined into a full-scale 1.5 m (5 feet) wide streamlined oil boom section for a final three week test series at OHMSETT. The purpose of these tests was to determine the overall system performance in retaining and recovering oil slicks at speeds up to 3.0 m/sec (6 knots) and with wave conditions typical of inland waterways. Overall the system performed well at both 2.0 and 3.0 (4 and 6 knots) testing speeds under calm water conditions with thruput efficiencies as high as 99+ and 87 percent at 2.0 m/sec (4 knots) and 3.0 m/sec (6 knots) respectively. In wave tests using a 0.30 m (1.0 foot) harbor chop, performance degraded significantly. This was expected since in this wave condition 10 percent of the waves are higher than 0.30 m (12 inches) trough to crest and the streamlined oil boom was designed to accommodate only 0.15 m (6 inches) free surface variation.

This report describes the development and design of the bow, sump and stability control systems. The details of the final design and testing at OHMSETT are also discussed.

SECTION 2

CONCLUSIONS

(1) The streamlined oil boom/skimmer was developed as an essentially two-dimentional device so that sections of arbitrary width could be close coupled to span a wide area.

(2) The final bow design was capable of operating at up to 3.0 m/sec (6 knots) skimming a 3.8 cm (1.5 inch) layer of oil and water into the sump in a smooth unbroken layer.

(3) The final sump design dissipated 99 percent of the incident flow's kinetic energy utilizing any of four energy dissipation mechanisms without breaking the oil slick into small droplets.

(4) An automatic stability control system was developed to adjust flow out of the sump to equal flow into the sump and reduce flotation requirements by an order of magnitude.

(5) The OHMSETT tests measured the performance of the device deployed as a high speed skimming craft with a 1.5 m (5 feet) wide section suspended between the hulls of a catamaran work platform.

(6) Results of oil slick recovery tests at OHMSETT indicated that the device is a feasible means of retaining and recovering oil slicks under calm surface conditions. Thruput efficiencies in the range of 77 to 99+ percent were measured at 2.0 m/sec (4 knots) and 53 to 87 percent were measured at 3.0 m/sec (6 knots) respectively over a range of slick thicknesses and with a 150 centistoke lube oil and a simulated number two fuel oil.

(7) In similar tests with a one foot harbor chop wave condition, thruput efficiencies degraded to the range of 0 to 21 percent. This wave condition with a 30 cm (1.0 foot) average one-tenth highest wave height was a severe test and the test results indicate that the device as developed is only effective under calm surface conditions such as those found in small harbors, lakes, smooth flowing streams and other inland waterways.

(8) The streamlined oil boom was also tested with a conventional oil boom deployed at slight angles to the tow direction to divert a 3.6 m (12 feet) wide oil slick into the 1.5 m (5 feet) working section at 3.0 m/sec (6 knots). Although the boom successfully diverted the slick into the working section, turbulent bow waves were produced entraining oil beneath the surface and lowering thruput efficiencies to the range of 18 to 41 percent.

(9) Force measurements confirmed that the streamlined design lowers drag. The drag coefficient based on frontal area was calculated to be 0.39 at 3.0 m/sec (6 knots). This compares to a drag coefficient for conventional oil boom of approximately 1.50.

SECTION 3

RECOMMENDATIONS

Based on the excellent high-speed calm surface results obtained in the OHMSETT tests it is recommended that the streamlined oil boom be further developed as a practical deployable system for high current inland applications. Both deployment options, high speed skimming craft and high current boom are feasible and should be pursued. However, less effort will be required for the high speed skimming craft application.

The following are specific recommendations:

Deployment as a High Speed Skimmer

(1) The 1.5 m (5 feet) wide section tested at OHMSETT combined with the supporting work platform are essentially a high-speed skimming craft. However, the work platform is several times larger than actually required to support the streamlined oil boom section and is unsuitable for transport to an actual spill site. A flotation/work platform should be designed and constructed specifically for the streamlined oil boom so that tests on real world spills may be conducted.

(2) The streamlined oil boom section tested at OHMSETT was designed and constructed as a research model and is not suitable for long-term service in the marine environment. Alternative materials and methods of construction should be investigated to produce a light weight, rigid and corrosion resistant structure.

(3) The overall operation of a high speed skimmer system should also be investigated. An effective oil recovery pumping and storage system should be designed to interface with the basic streamlined oil boom unit. The problem of debris should be addressed and other aspects such as cleaning, deployment and transportation should also be considered.

Deployment as a High Current Boom

(1) If the device is to be deployed as a boom, each section must be equipped with its own integral flotation system which maintains the bow at the proper vertical position to skim a thin layer of oil and water into the sump. Ideally, the flotation system would be self-adjusting so that sections spanning a variable current stream could each operate at design point.

(2) The problem of oil slick diversion should also be addressed. If the sections are close coupled, the integral flotation systems must divert oil into the active sections. An alternate method of deployment would utilize streamlined oil boom sections a substantial distance apart with a diversionary device or boom directing the oil slick into the active section. The poor performance demonstrated with diversionary boom at OHMSETT points to the need for additional work in this area.

(3) Coupling and deploying the sections in a high current environment are key problems. The section widths should be optimized for good performance in recovering oil slicks and for easy handling and deployment. Couplings should allow the sections to operate somewhat independently and yet withstand drag forces. In addition they must be easily field assembled and disassembled.

(4) An oil recovery system for combining the recovered oil from each section must also be developed. One possiblity would involve inducing a cross flow in the sump to sweep the collected oil to one end of the streamlined boom for recovery over a weir or other device. Another possibility would maifold the outputs of each section into a common pumping section.

SECTION 4

BOW DESIGN

The primary function of the streamlined oil boom bow is to direct a layer of oil and water into the sump for further processing. Ideally the bow shape should skim a thin layer into the sump at high speed with little or no turbulence so that all of the oil approaching the boom is smoothly swept into the sump.

The Phase I tests at the Lockheed Towing Basin demonstrated that streamlined hydrofoil shapes could skim most of the oil into the sump and operate with low drag but did not develop a definitive relationship between hydrofoil shape, tow velocity, freeboard and bow wave turbulence characteristics. Consequently, the Phase II bow design work focused on determining the following data:

- The important bow wave scaling parameters
- The relationship between freeboard and flow over the hydrofoil
- The parameters causing transition from turbulent to smooth bow waves
- The bow shape producing optimum flow characteristics for the streamlined oil boom

A reveiw of hydrofoil literature revealed that while substantial work had been done on deeply submerged high speed and planing applications, little was known about the "in between" area where velocities and submergence are small and the bow wave is near transition from turbulent to smooth.

The bow wave on a slightly submerged hydrofoil is a complex phenomenon. The flow conditions are determined by a balance of inertial, gravity, viscous and surface tension forces and are too complicated to calculate exactly particularly where the bow wave is turbulent or breaking. In order to obtain design data and a basic understanding of bow wave flow, a simplified phenonenological theory was developed. The results of this theory identified scaling parameters and predicted flowrates passing over a hydrofoil as functions of operating conditions. The transition from turbulent to smooth bow waves and the influence of specific hydrofoil contours could not be determined from the theory so experiments were conducted to determine these factors and develop an optimum streamlined oil boom bow.

BOW WAVE HYDRODYNAMICS AND PHENOMENOLOGICAL CORRELATION

As a hydrofoil is lowered into a swiftly moving current, the following flow regimes occur as shown in Figure 3. At very high freeboard,* no flow passes over the hydrofoil and a turbulent bow wave forms. This bow wave is characterized by a turbulent recirculating roller much like a breaking wave or a hydraulic jump. The stagnation streamline** is identical to the free surface upstream, intersects the hydrofoil near the bow and is identical to the hydrofoil's ventral contour downstream. As the hydrofoil is lowered flow begins to pass over top and the stagnation streamline descends beneath the free surface upstream and switches to the hydrofoil's dorsal side downstream. The bow wave is turbulent as before. As the hydrofoil is lowered further, the amount of flow passing over the hydrofoil increases and eventually the turbulent bow wave is swept over the hydrofoil leaving a smooth bow wave without surface turbulence, air entrainment or recirculation. Further lowering the hydrofoil increases the flowrate passing over the hydrofoil and reduces the disturbance to the free surface until at very deep submergence there is no noticeable free surface disturbance.

Ideally the streamlined oil boom bow should skim a thin layer of fluid into the sump with a smooth bow wave at all speeds up to 3.0 m/sec (6 knots). This type of operation can be described hydrodynamically as low speed and near the free surface. In terms relative to the size of the hydrofoil, low speeds means that the Froude number is small. The Froude number is a dimensionless parameter expressing the square root of the ratio of inertial to gravity forces.

$$F = \frac{V_1}{\sqrt{gL}}$$

where:

F = Froude number

V_1 = Free stream velocity

g = Acceleration of gravity

L = A characteristic length

---

* Freeboard is the hieght of the hydrofoil's uppermost point above the undisturbed free surface.

** Stagnation streamline is that streamline which divides flow over from flow under the hydrofoil. Fluid along this streamline is stagnated (brought to rest) at the hydrofoil bow.

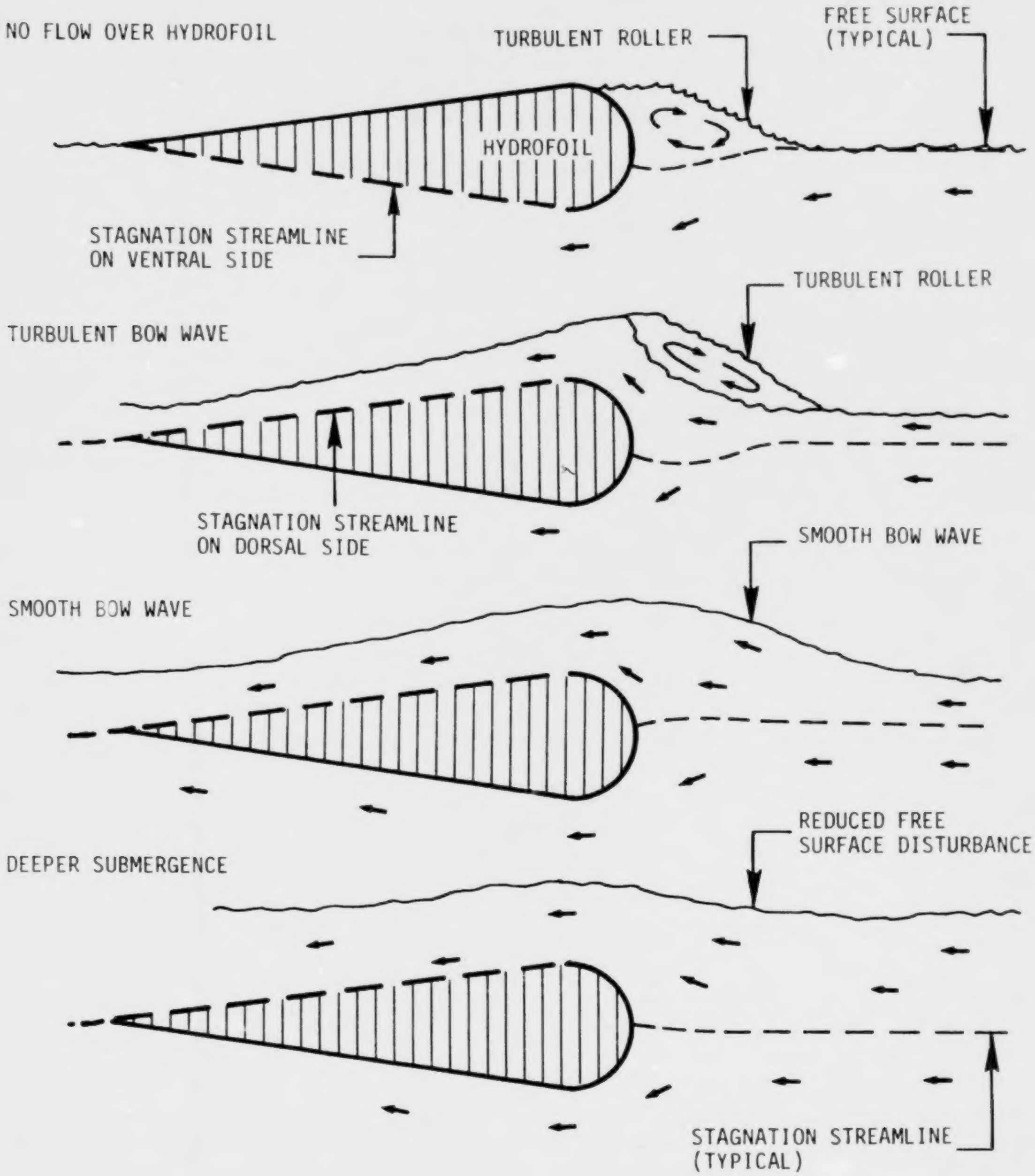
NO FLOW OVER HYDROFOIL
TURBULENT ROLLER
FREE SURFACE (TYPICAL)
HYDROFOIL
STAGNATION STREAMLINE ON VENTRAL SIDE
TURBULENT ROLLER
TURBULENT BOW WAVE
STAGNATION STREAMLINE ON DORSAL SIDE
SMOOTH BOW WAVE
SMOOTH BOW WAVE
REDUCED FREE SURFACE DISTURBANCE
DEEPER SUBMERGENCE
STAGNATION STREAMLINE (TYPICAL)

Figure 3. Typical flow over a streamlined shape at shallow submergence.

The characteristic length used here is the maximum thickness of the hydrofoil and low speed operation means that the Froude number is small, less than approximately 2.0. Following these definitions, a hydrofoil 30 cm (1.0 foot) thick would operate at low speed up to 3.5 m/sec (6.7 knots). In this low speed range both gravity and inertial forces are important but the pressure effects due to curvature of the streamlines are small.

Operation near the free surface means that the thickness of the water layer passing over they hydrofoil is the same order of magnitude as the thickness of the hydrofoil itself. Thus the flow above the hydrofoil is effectively separated from the flow beneath and the two flows behave independently.

A phenomenological theory was developed to identify scaling parameters, predict the flowrate over the hydrofoil and correlate experimental results for hydrofoils operating at low Froude numbers and near the free surface. The analysis applied the classical open channel flow equations to the flow passing over a frictionless impermeable contour consisting of the stagnation streamline upstream of the hydrofoil and the dorsal surface of the hydrofoil. The details of the analysis and results are discussed in Appendix A.

The analysis identified the reciprocal of the Froude number squared based on freestream velocity (V_1) and free board (B):

$$G = \frac{gB}{V_1^2}$$

as the important independent scaling parameter and expressed the resulting flow conditions in similar form:

$$G_1 = \frac{gY_1}{V_1^2}$$

$$G_3 = \frac{gY_3}{V_1^2}$$

where Y_1 and Y_3 are the flow depths to the stagnation streamline measured far upstream and over the hydrofoil's highest point respectively. Based on this analysis the bow wave characteristics are independent of the hydrofoil size and shape and the flowrate over the hydrofoil may be calculated given the freeboard and velocity.

Experiments were conducted over a range of hydrofoil shapes and sizes to obtain a measure of the correlation's validity. Initially small open channel flow facilities of the type normally used to model flow in rivers and streams were used to obtain small scale data on hydrofoils ranging in thickness from 1.0 to 6.0 cm (0.4 to 2.4 inches) and later larger scale experiments extended the range to 15 cm (6 inch) thickness.

The majority of the small scale experiments were conducted in an open flow channel at the California State University at Fullerton. This channel has a maximum flowrare of 12.5 l/sec (200 gallons/minute), a width of 11 cm (4.5 inches) and could be operated with subscritical flow at flow velocities up to 80 cm/sec (2.6 feet/second).* Velocity profiles measured with a pitot probe and micromanometer showed uniformity within 5 percent up to within 2.5 cm (1 inch) of the side walls. Tests were conducted by suspending two-dimensional hydrofoil models in the channel spanning the entire width and measuring the flow parameters. The free surface locus was measured with a precision height gauge and the position of the stagnation streamline was observed with dye injection.

Figure 4 shows the small scale hydrofoil shapes tested. The circular cylinders of various size were used to measure scale effects and the other models were used to determine shape effects. The large-scale hydrofoil was a NACA 4424 shape not shown in Figure 4.

The experimental results are shown in Figure 5, a plot of the flow depth passing over the highest point on the hydrofoil against freeboard normalized by the acceleration of gravity and freestream velocity expressed in Froude number form. The theoretical correlations developed from the bow wave theory (See Appendix A) are also shown. It is remarkable that the data and theory correlate so well particularly considering the range of sizes and shapes tested.

The transition from a turbulent to a smooth bow wave as a function of operating conditions can be described on a flow map. Figure 6 is the flow-map where G_B is plotted against the hydrofoil Froude number squared F^2 based on the hydrofoil thickness T. Data points representing transition from one type of bow wave to another can be plotted on this flow map to give a visual indication of hydrofoil performance. The upper most line represents the maximum freeboard for which flow passes over the hydrofoil. Along this line, all of the approaching surface layer's kinetic energy is converted into potential energy to lift the fluid to the hydrofoil's top. Slightly lowering the hydrofoil causes flow to proceed with a turbulent bow wave. For Froude number squared greater than 2.0, the maximum freeboard is limited by the hydrofoil thickness since the flow has more than enough kinetic energy to pass over the hydrofoil at any submergence.

---

* At higher velocities the channel Froude number approached 1.0 and the surface became wavy and unsuitable for hydrofoil experiments.

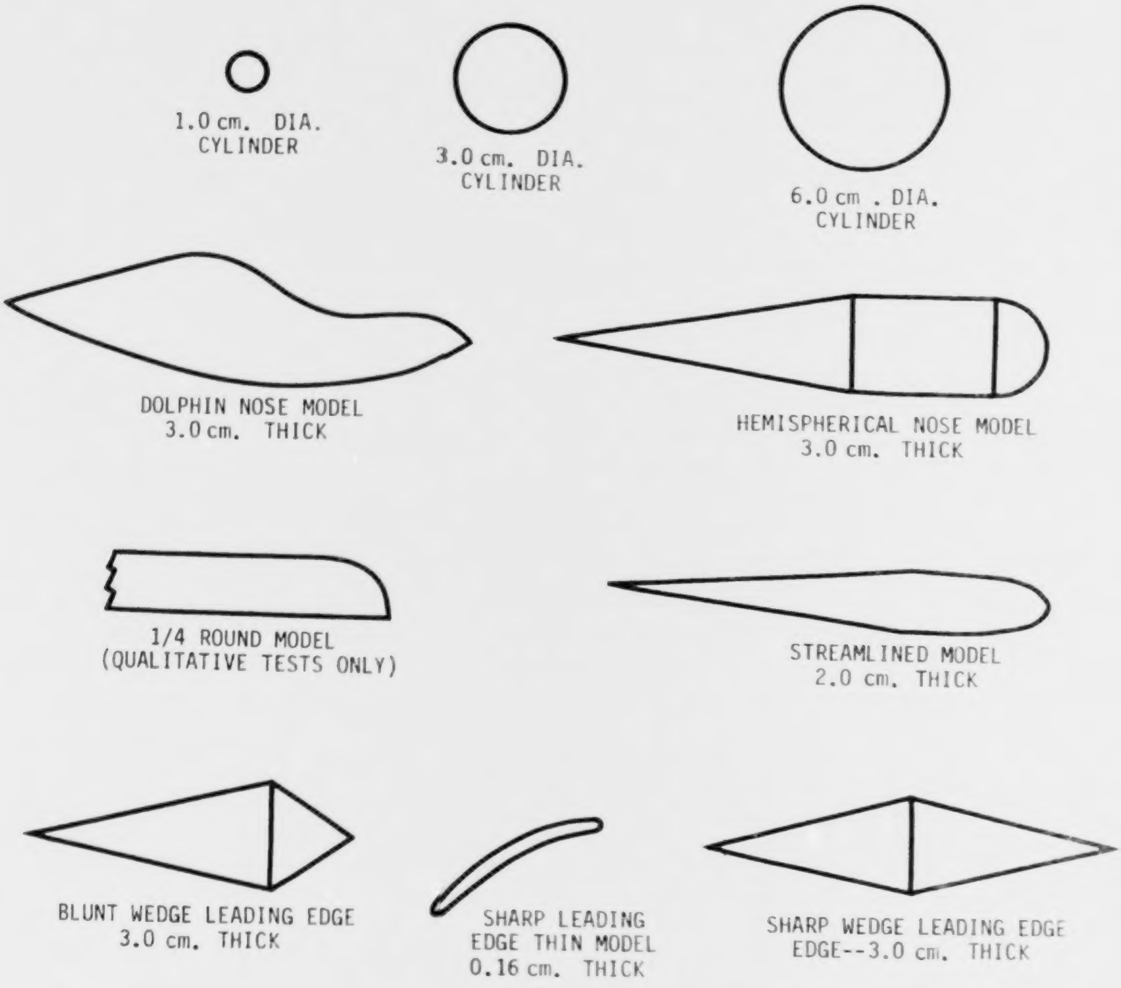
1.0 cm. DIA.
CYLINDER
3.0 cm. DIA.
CYLINDER
6.0 cm . DIA.
CYLINDER
DOLPHIN NOSE MODEL
3.0 cm. THICK
HEMISPHERICAL NOSE MODEL
3.0 cm. THICK
1/4 ROUND MODEL
(QUALITATIVE TESTS ONLY)
STREAMLINED MODEL
2.0 cm. THICK
BLUNT WEDGE LEADING EDGE
3.0 cm. THICK
SHARP LEADING
EDGE THIN MODEL
0.16 cm. THICK
SHARP WEDGE LEADING EDGE
EDGE--3.0 cm. THICK

Figure 4. Small scale models for bow wave tests.

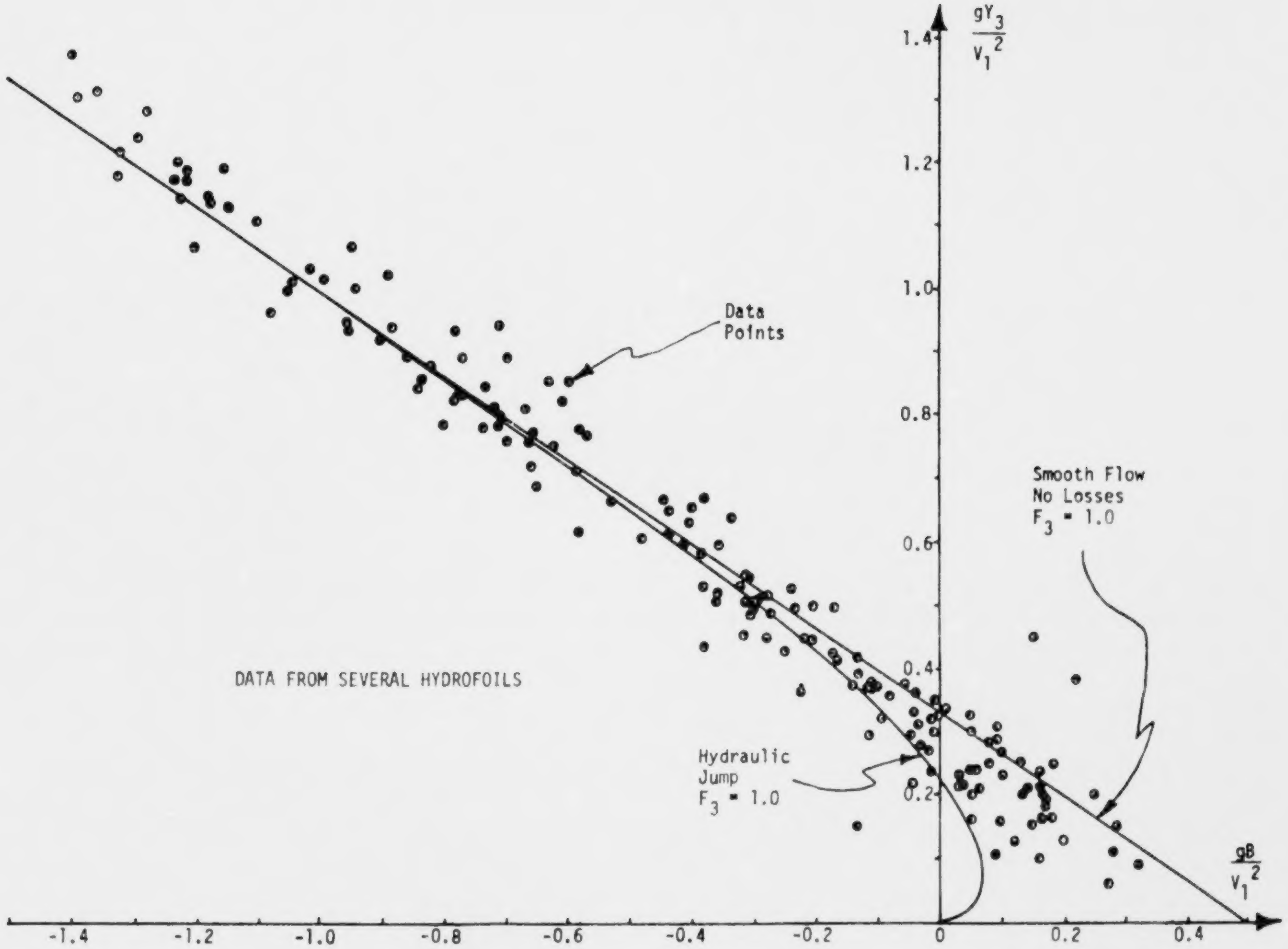

Figure 5. Emperical bow wave correlation verification.

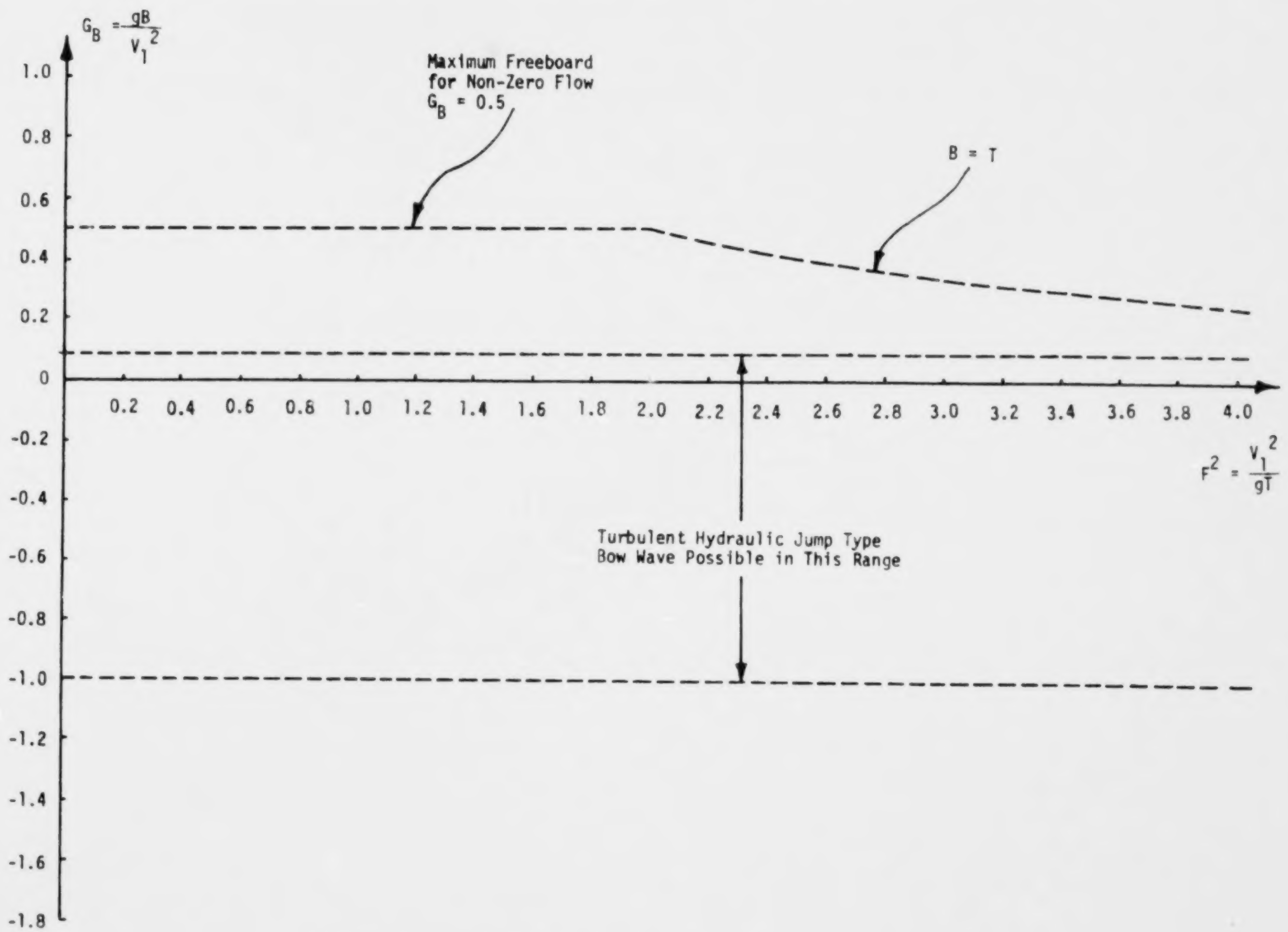

Figure 6. Dimensionless bow wave flow map.

The phenomenological theory identified the range $-1.0 < G_B < +0.07$ (also shown in Figure 6) as the range where a turbulent hydraulic jump type bow wave is possible. The transition line from smooth to turbulent bow waves should occur somehwere in this range.

Figure 7 is a flowmap showing a compilation of data from all solid hydrofoils tested. The maximum freeboard for non-zero flow data follows the theoretically predicted correlation well except for very low values of Froude number squared. These data points correspond to low velocities where the dynamic head is of the same order of magnitude as the miniscus height and surface tension effects are important.

The transition from a turbulent to a smooth bow wave is gradual and was estimated by observing the flow conditions at which paper chips deposited upon the surface upstream slow nearly to rest when passing over the hydrofoil. Dye injection was also used to qualitatively observe the bow wave turbulence. The apparent data scatter in Figure 7 is partially due to differences in the performance of various hydrofoils. In the range $0.5 < F^2 < 4$ where the streamlined oil boom bow operates, transition occurs in the range $-0.8 < G_B < 0.0$.

Data from the flowmap combined with the phenomenological correlation allow calculation of the minimum flowrate for smooth flow over a hydrofoil. Minimum flowrate corresponds to maximum G_B and from Figure 7, $G_B = 0$ appears to be a conservative value. Applying $G_B = 0$ to the phenomenological correlation equations for smooth flow (Appendix A) gives in the following equation for minimum flowrate:

$$Q = \frac{V_1^{\,3}}{3^{3/2} g}$$

where Q is the minimum flowrate per unit width. The minimum flowrate is independent of hydrofoil size and increases as the cube of the velocity reaching 550 l/sec per meter of hydrofoil width (2,700 gpm per foot of bow width) at 6 knots.

Similarly, the minimum layer skimmed can be calculated to be:

$$Y_1 = \frac{V_1^{\,2}}{3^{3/2} g}$$

and at 3.0 m/sec (6 knots) this corresponds to 18.2 cm (7.2 inches).

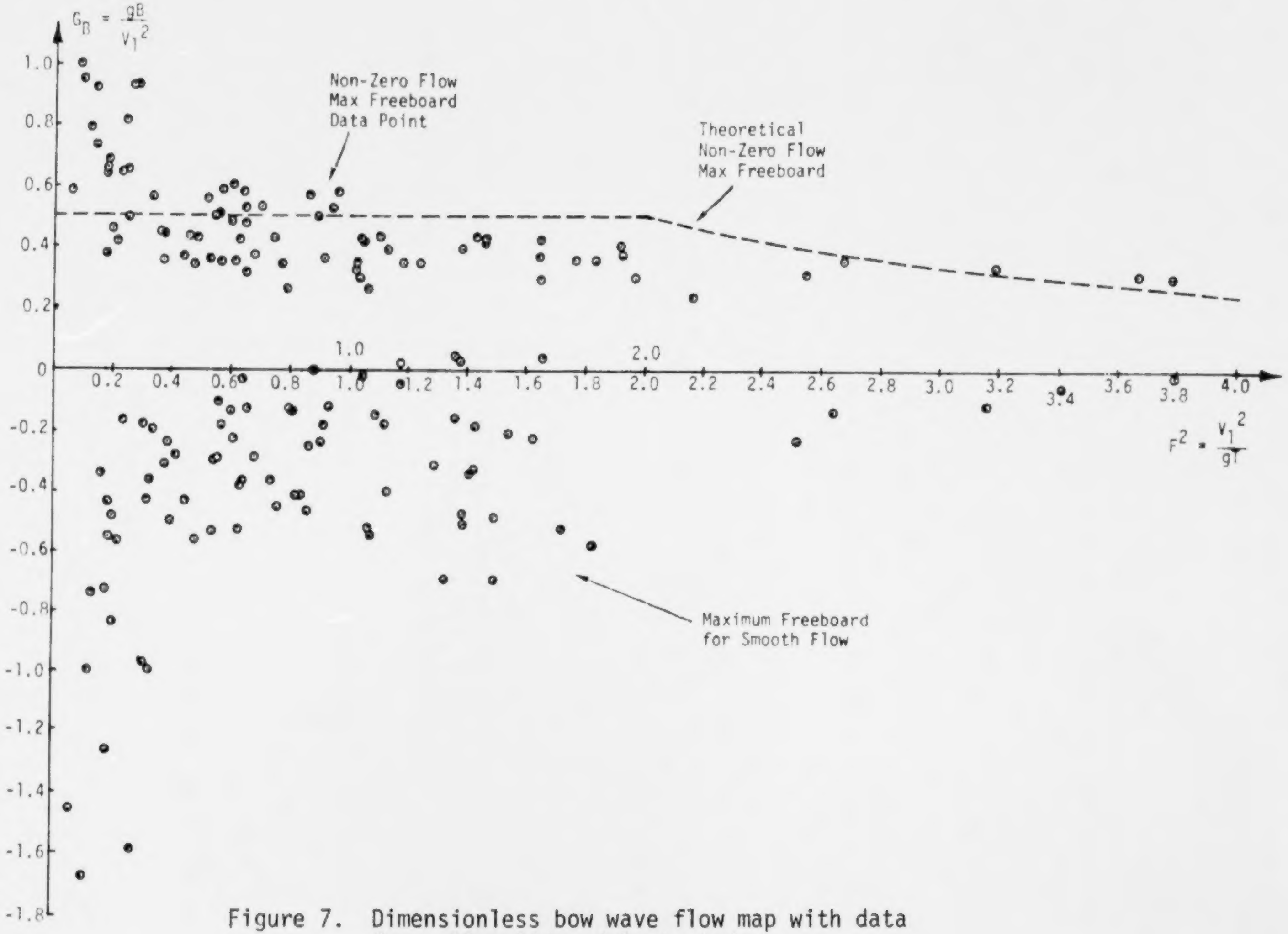

Figure 7. Dimensionless bow wave flow map with data from all solid models tested.

SLOTTED BOW DESIGNS

The empirical correlation verification in the last section demonstrates that the minimum flowrate for a smooth bow wave on streamlined hydrofoils increased as the cube of the velocity reaching quite high values at high speeds and the thickness of the layer skimmed into the sump increases as the square of the velocity. Since the thickness of the oil slicks to be recovered by the streamlined oil boom are in the range of 1 to 3 mm, the smooth flow requirement means that the vast majority of the flow into the sump will be water and as a result the sump must function as a high flowrate oil/water separator recovering dilute oil in water mixtures. A reduction of the flowrate into the sump is clearly desirable.

Flow into the sump can be reduced with slotted hydrofoils. The hydrofoil is operated deep enough to achieve a smooth bow wave and some of the flow is drawn from the hydrofoil's dorsal side to the ventral side through a slot leaving a much smaller flowrate to enter the sump. The slot width, location and contours play important roles in determining the amount of flow sucked through the slot and the characteristics of the secondary bow wave on the rear edge of the slot. For a very narrow slot width, the slot acts as a channel with flow drawn through primarily due to the pressure difference between the dorsal and ventral sides of the hydrofoil. For a very wide slot width the front and rear sections operate independently each with its own bow wave. For slot widths between these extremes flow is a complex combination of the two phenomena.

Before any special models were constructed, an existing model was modified to allow preliminary testing of the slotted model concept. Figure 8 is a scale drawing of this model showing one approximate operating condition and the two stagnation streamlines. The lower one, ending on the bow, separates flow over from flow under the bow. The upperstagnation streamline, ending at the rear edge of the slot separates flow through the slot from flow over the rear of the model. The drawing shows the flow conditions observed when the model was near the surface. The sharp slot edges caused ventilation (air entrainment) greatly reducing the effective slot open area. A separated region on the lower side of the model was also produced. When the slot was closed by tape, the free surface was only slightly changed (as shown), but the separated region was greatly reduced. Thus the flow through the slot was responsible for the majority of the flow separation. As the model was lowered further beneath the free surface, the flow through the slot diminished and the two stagnation streamlines merged. This behavior was expected since the model was symmetric.

These brief tests confirmed that flow over the bow could be reduced with a slotted hydrofoil and demonstrated that the slot should be carefully designed to eliminate sharp edges. This would increase the effective slot area and flow through the slot and reduce separation under the model. A cambered profile is another desirable modification to provide an increased pressure differential across the slot.

The two new slotted hydrofoils shown in Figure 9 were constructed incorporating these improvements. Both were based on standard NACA profiles with slots added to divert a portion of the flow above the hydrofoil to the

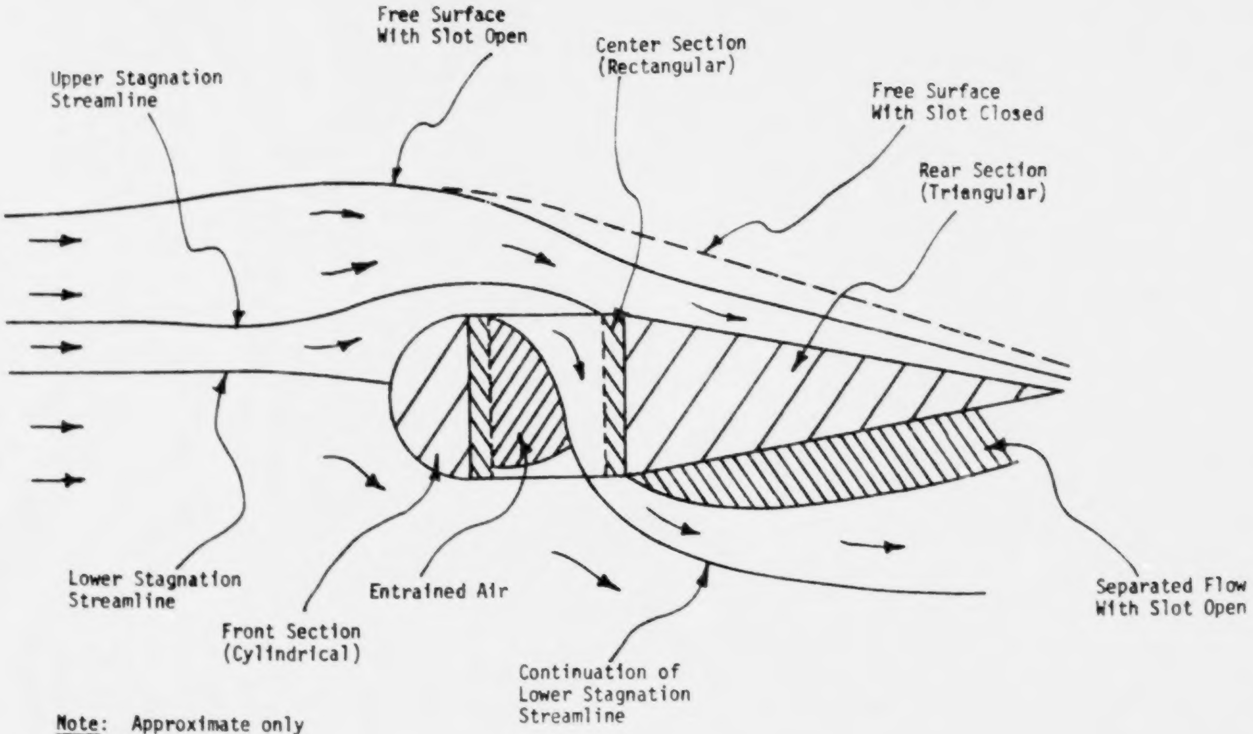
Free Surface
With Slot Open
Center Section
(Rectangular)
Upper Stagnation
Streamline
Free Surface
With Slot Closed
Rear Section
(Triangular)
Lower Stagnation
Streamline
Entrained Air
Front Section
(Cylindrical)
Separated Flow
With Slot Open
Continuation of
Lower Stagnation
Streamline

Note: Approximate only
Velocity = 90 cm/sec
(Scales to 5 ft/sec on
3 in. thick hydrofoil)

Figure 8. Preliminary slotted model tests

Full Scale
Chord = 13.3 cm
Thickness = 2.0 cm

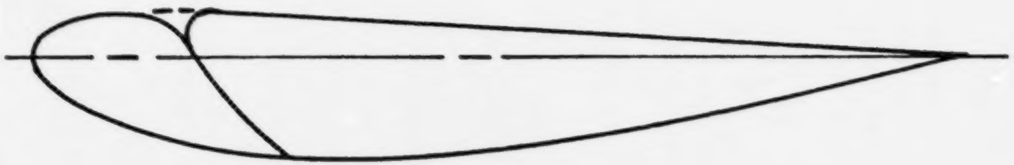

NACA 4415 Profile Model With 1 Slot
(Slot Width is Adjustable)

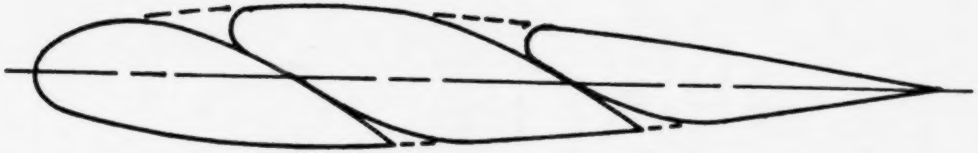

NACA 0015 Profile Model With 2 Slots
(Slot Widths are Adjustable)

Figure 9. Slotted models.

ventral side. The NACA 4415 model was operated with the cambered side down and the slot was located with the exit end in the region of lowest pressure. The slot could be adjusted from closed to more than 5 cm wide by sliding the two sections. The NACA 0015 model was noncambered but was equipped with two adjustable slots with more streamlined contours.

Figure 10 shows typical flows observed with the NACA 4415 model at slots widths of 1.0 and 3.0 cm (at zero angle of attack). These experiments were conducted at nearly the same velocity and freeboard and demonstrate the effects of variable slot width. When the slot width was reduced the amount of flow through the slot was also reduced and the upper stagnation streamline approached and, at zero slot opening, merged with the lower stagnation streamline. Figure 10 shows that, although the flowrates over the bow were approximately the same for each slot width, a larger portion of the flow passed through the wider slot. The regions of separated flow were caused by the small radius of curvature of the slot walls and viscous effects.

Typical flow over the NACA 0015 model is shown in Figure 11. Since there are three model sections, there are three stagnation streamlines. In these experiments the velocity, freeboard and sum of the slot widths were maintained constant and the widths of the front and rear slots were varied. Although the relative magnitudes of the flowrates through the slots varied, the total was essentially constant leaving nearly the same flowrate over the rear portion. However, when the front slot was closed, a turbulent bow wave formed.

Although the phenomenological theory developed for solid bodies as no provision for slot effects, the data for the front portion of the model can still be expressed on the same coordinates. Figure 12 shows the data for the experiments on the NACA 4415 and NACA 0015 slotted models. Both the depth of the stagnation streamline data and the depth of the flow over the model data follow the correlation lines closely.

Although the phenonenological theory cannot predict the flowrates through the slots, it can be extended to predict the locus of the stagnation streamlines on a point by point basis from measured free surface data. Figure 13 shows the results of applying this "no energy loss analysis" to calculate the stagnation streamlines on the NACA 0015 model in one experiment. The agreement between measured and calculated streamlines is excellent except in the vicinity of the bow of each section where the analysis assumptions are invalid because of pressure effects.

Based on the favorable results obtained with the NACA 0015 model, the front two sections of the model were incorporated into a complete streamlined oil boom model including a preliminary sump as shown in Figure 14. This design also performed well but produced a turbulent bow wave on the rear edge of the slot under some conditions.

The next bow design iteration is shown in Figure 15. Since the slot width used in previous designs was the same order of magnitude as the hydrofoil thickness, the forward portion was designed as a separate NACA 4424

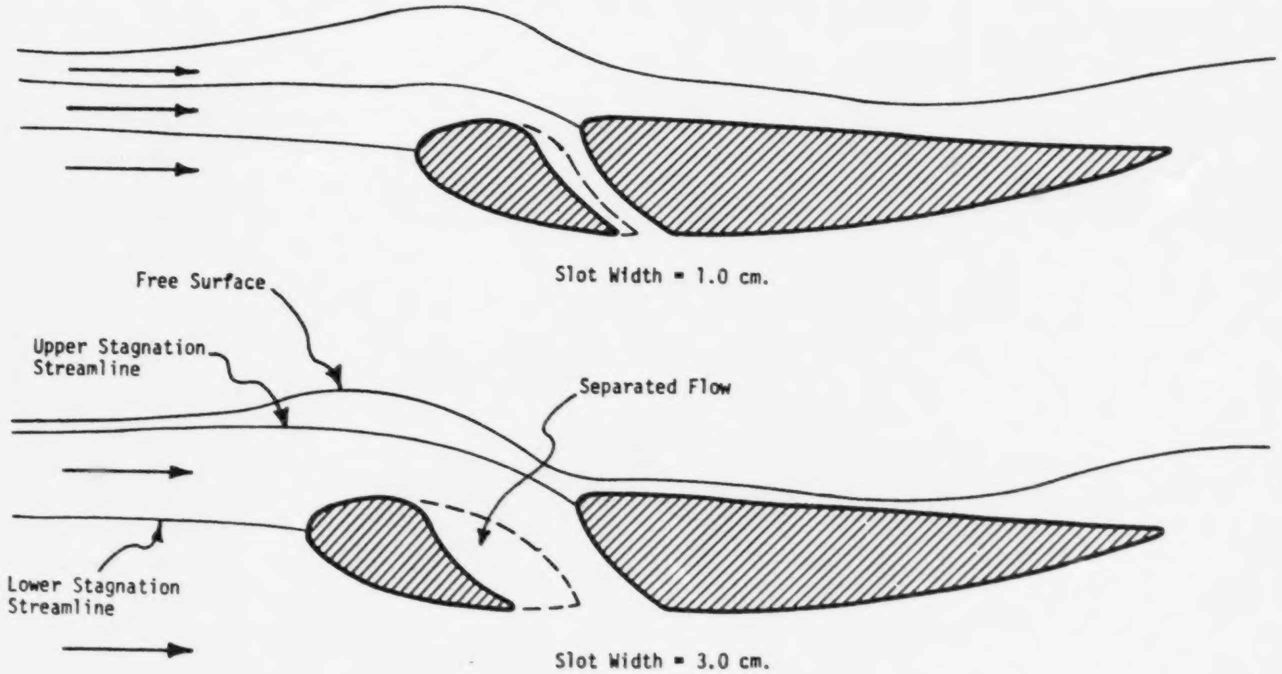
Slot Width = 1.0 cm.
Free Surface
Upper Stagnation Streamline
Separated Flow
Lower Stagnation Streamline
Slot Width = 3.0 cm.

Figure 10. Typical flow - NACA 4415 model.
(Same velocity, freeboard, and angle of attack - variable slot width)

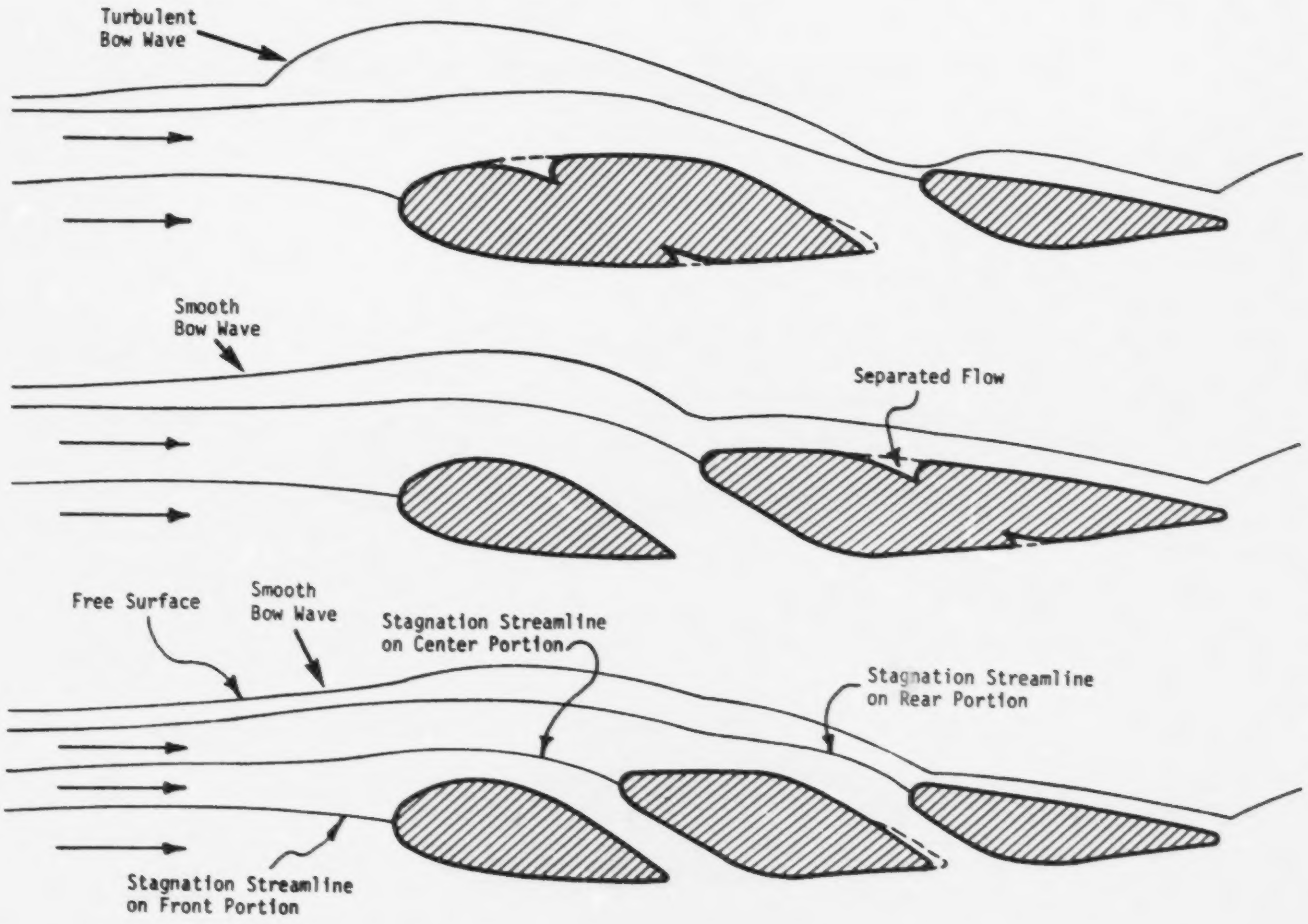
Turbulent Bow Wave
Smooth Bow Wave
Separated Flow
Free Surface
Smooth Bow Wave
Stagnation Streamline on Center Portion
Stagnation Streamline on Rear Portion
Stagnation Streamline on Front Portion

Figure 11. Typical flow - NACA 0015 model.
(same Velocity, Freeboard and angle of attack - variable slotwidths)

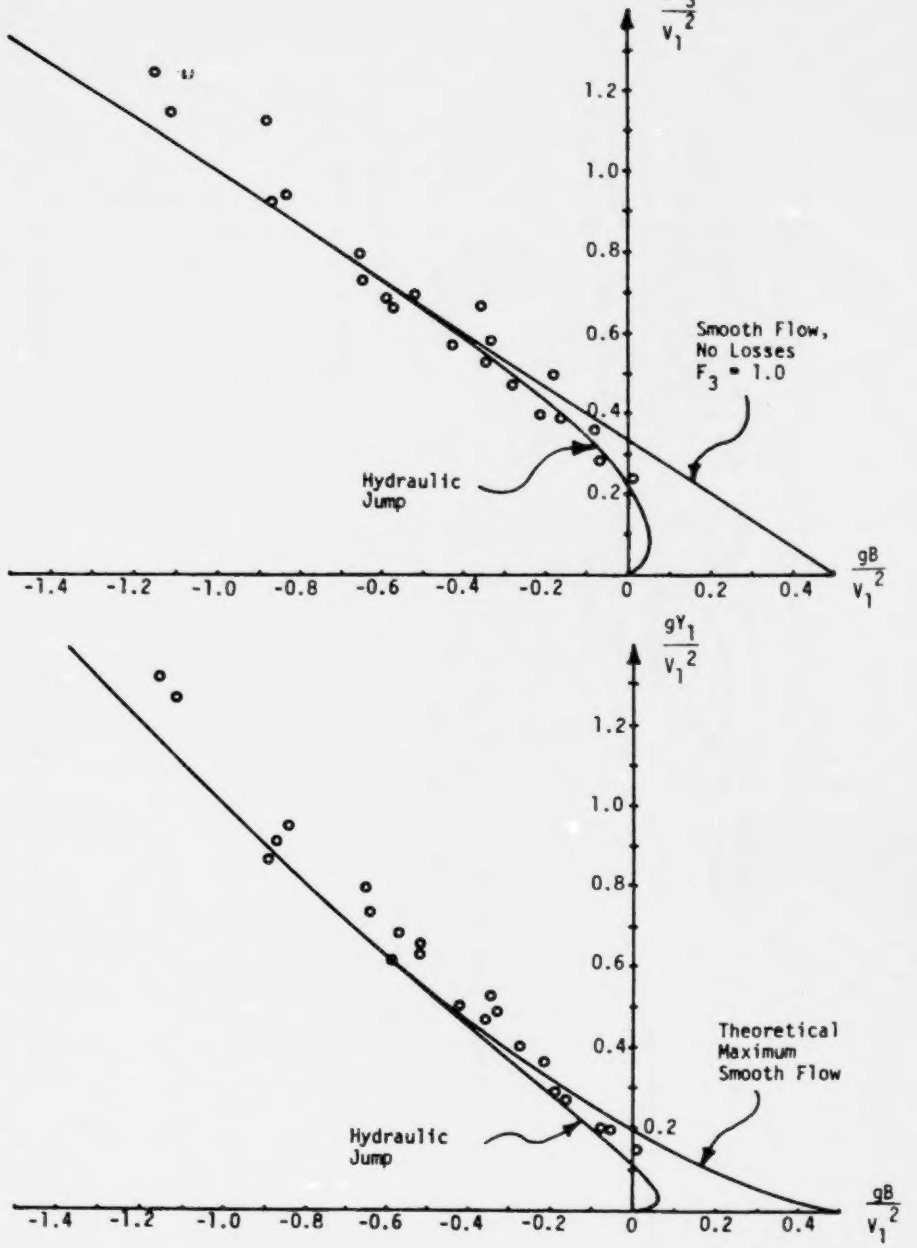

Figure 12. Correlations for bows of slotted models - NACA 4415 and NACA 0015.

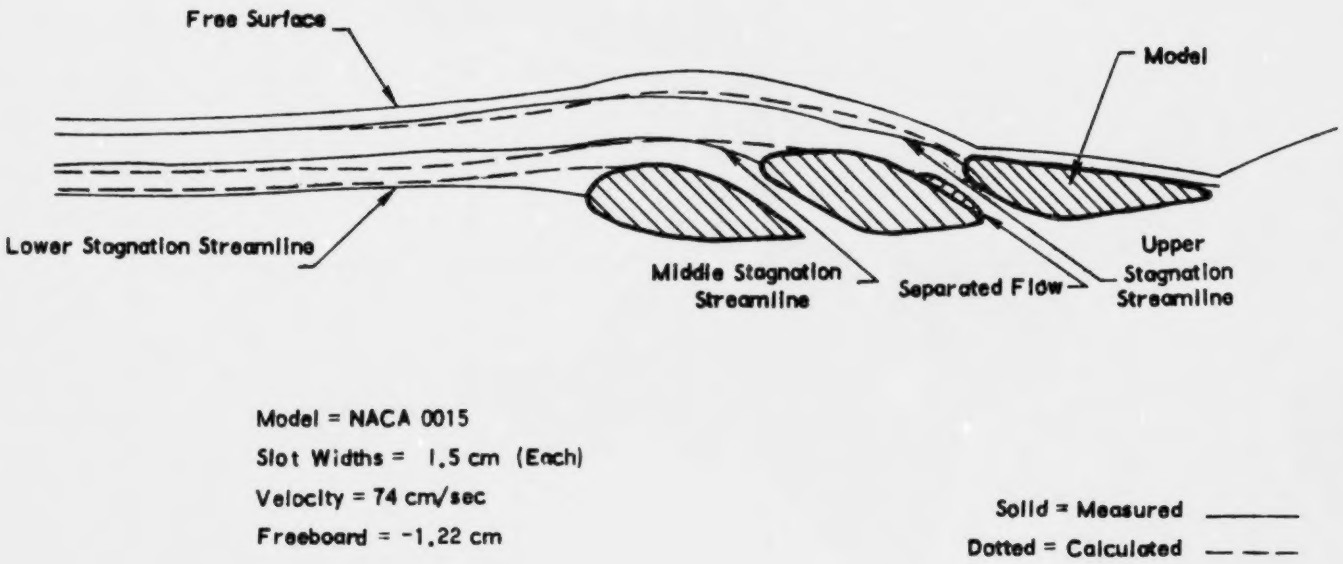
Free Surface
Model
Lower Stagnation Streamline
Middle Stagnation Streamline
Separated Flow
Upper Stagnation Streamline
Model = NACA 0015
Slot Widths = 1.5 cm (Each)
Velocity = 74 cm/sec
Freeboard = -1.22 cm
Solid = Measured
Dotted = Calculated

Figure 13. Comparison of measured and calculated stagnation streamlines.

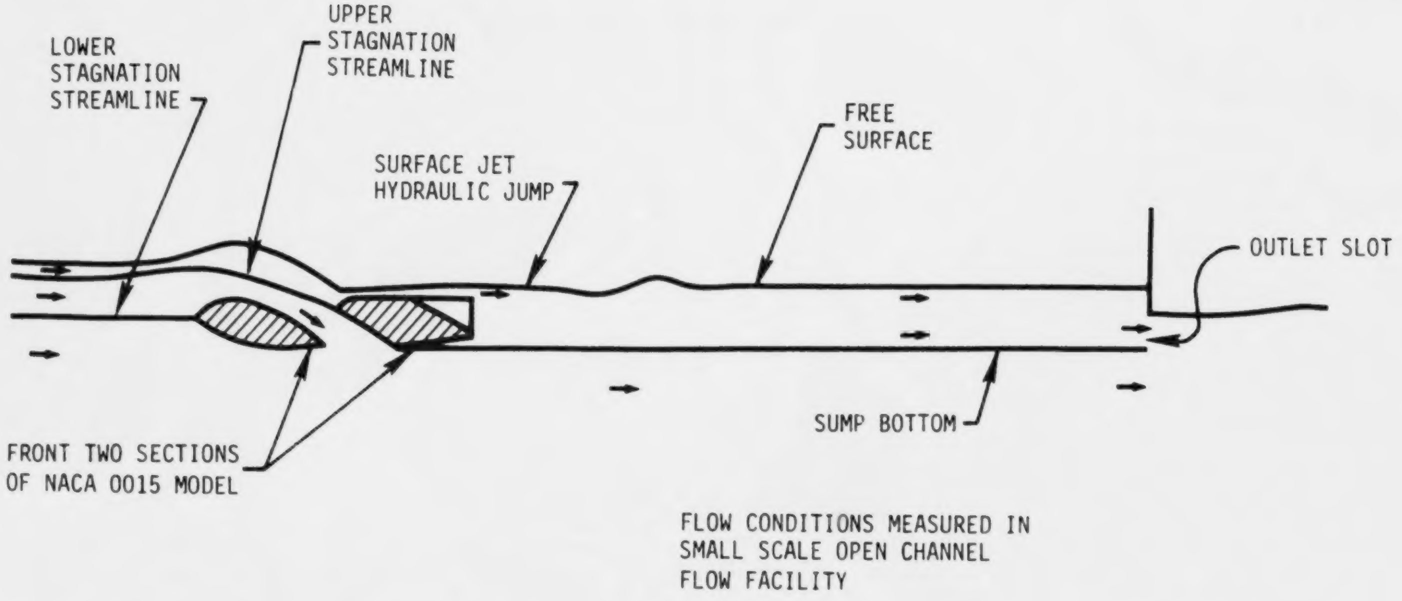
LOWER
STAGNATION
STREAMLINE
UPPER
STAGNATION
STREAMLINE
SURFACE JET
HYDRAULIC JUMP
FREE
SURFACE
OUTLET SLOT
SUMP BOTTOM
FRONT TWO SECTIONS
OF NACA 0015 MODEL
FLOW CONDITIONS MEASURED IN
SMALL SCALE OPEN CHANNEL
FLOW FACILITY

Figure 14. Preliminary streamlined oil boom model using NACA 0015 bow sections.

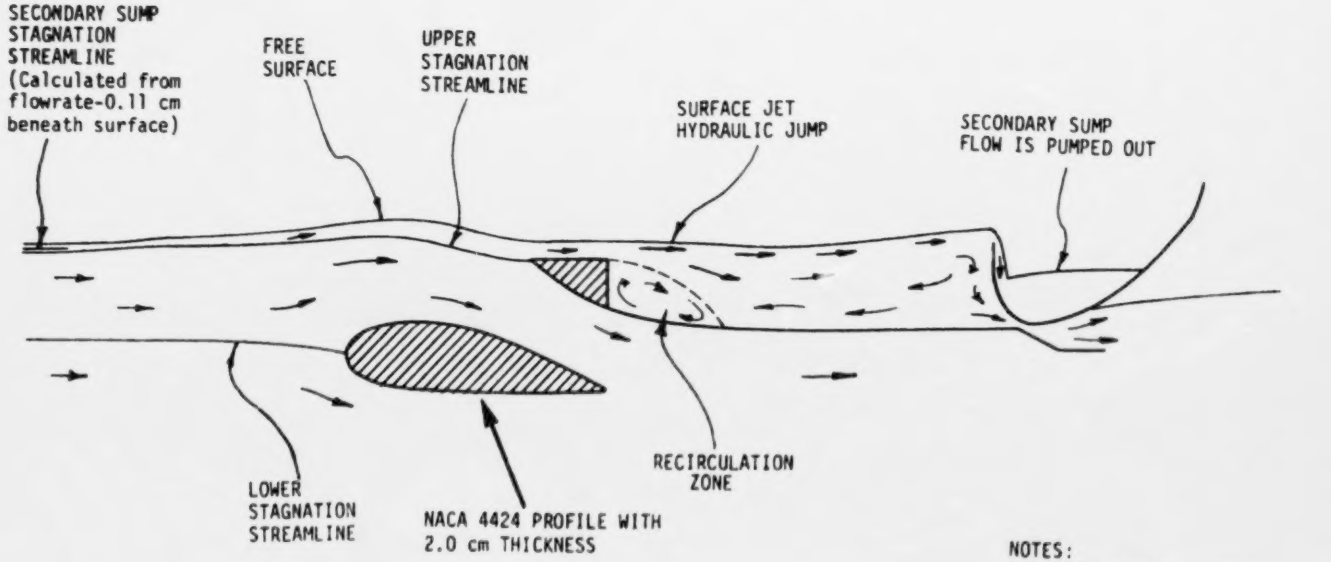
SECONDARY SUMP
STAGNATION
STREAMLINE
(Calculated from
flowrate-0.11 cm
beneath surface)
FREE
SURFACE
UPPER
STAGNATION
STREAMLINE
SURFACE JET
HYDRAULIC JUMP
SECONDARY SUMP
FLOW IS PUMPED OUT
LOWER
STAGNATION
STREAMLINE
NACA 4424 PROFILE WITH
2.0 cm THICKNESS
RECIRCULATION
ZONE

NOTES:
VELOCITY = 65.81 cm/Sec
FREEBOARD = -2.30 CM
FLOWRATE OUT OF
SECONDARY SUMP = 0.054 ℓ/Sec

Figure 15. Preliminary slotted bow design.

airfoil and operated beneath the transition from smooth to turbulent flow. The rear portion was designed with a relatively sharp leading edge to skim a thinner layer into the sump and the slot contours were arranged to produce gradually accelerating flow. This design performed very well allowing thin layers to be skimmed at high as well as low speeds without aeration or a turbulent bow wave. As a result of these tests an identical large-scale model was constructed and tested at the Coast Guard Flow Channel in Texas (see Table 1). In these tests, the bow design performed well and only minor modifications were made in subsequent revisions.

The final bow design tested in both OHMSETT test series is shown in Figure 16. Modifications include small changes to the sump inlet contours to achieve thinner layers skimmed into the sump and changes to the aft portion to accommodate a different sump design.

The OHMSETT tests demonstrated that this final design can operate with a smooth bow wave at 3.0 m/sec skimming 77 l/sec per meter or a 2.5 cm layer (6 knots skimming 374 gpm per foot width or a 1.0 inch layer). However, a 3.8 cm (1.5 inch) layer skimmed was chosen as the nominal operating point to better accommodate waves. Tests at this operating point under calm conditions demonstrated that all surface material passes into the sump smoothly. Under low wave conditions, some wave energy is reflected so that waves up to 10 cm (4.0 inches) through to crest can be tolerated with the entire free surface still entering the sump smoothly. As wave heights increase further, portions of the wave troughs pass under the bow and some surface material is lost. A buoyant flotation system moving in response to the waves or an operating point skimming a thicker layer would improve performance in larger waves.

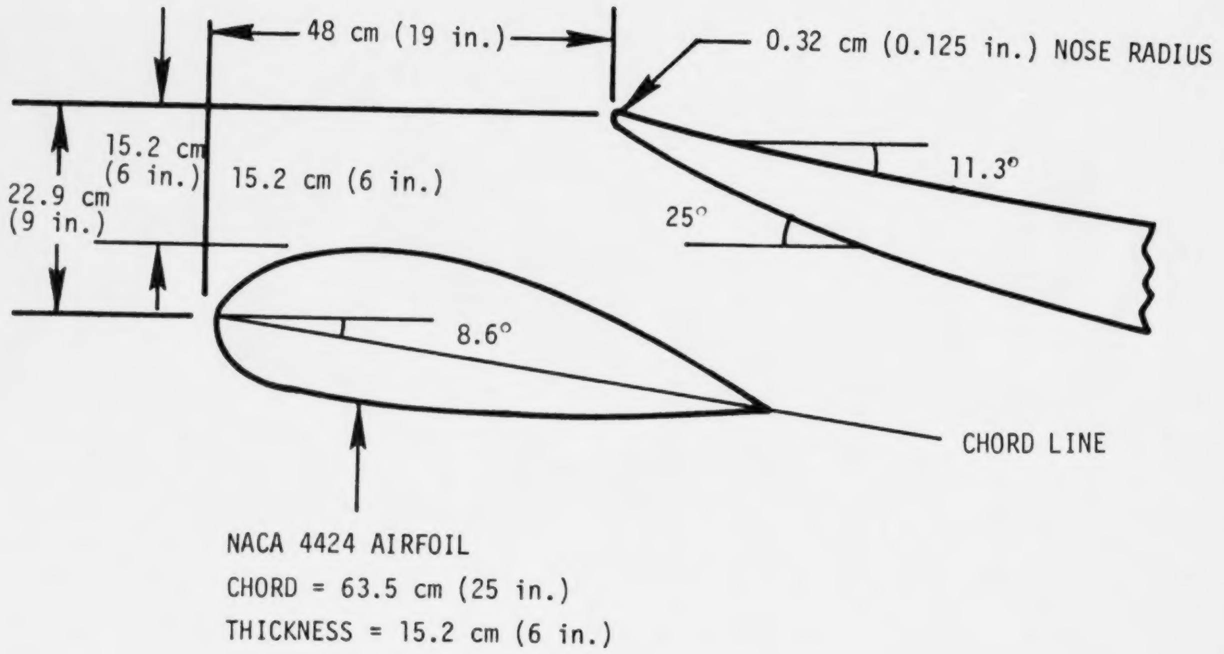
48 cm (19 in.)
0.32 cm (0.125 in.) NOSE RADIUS
15.2 cm (6 in.)
15.2 cm (6 in.)
22.9 cm (9 in.)
11.3°
25°
8.6°
CHORD LINE
NACA 4424 AIRFOIL
CHORD = 63.5 cm (25 in.)
THICKNESS = 15.2 cm (6 in.)

Figure 16. Final bow design.

SECTION 5

SUMP DESIGN

During the Phase I development, little work was done on sump design. For the full-scale tests at the Lockheed Towing Basin a flexible plastic membrane was installed in the sump and all material exiting the sump was recovered in this plastic "bag." The original plan was to either separate the oil from the excess water in the sump or to recover the entire flowrate passing over the bow for subsequent shore based separation. However, the large flowrate required for a smooth bow wave makes subsequent shore based separation impractical. Based on the 3.0 m/sec (6 knots) final bow design operating point skimming a 3.8 cm (1.5 inch) layer into the sump, a 30 m (100 feet) wide streamlined oil boom would collect 212,400 l/min (56,100 gpm) enough to fill a 30 m (100 feet) diameter tank at 29 cm (0.95 feet) per minute. This gigantic flowrate is clearly impractical for a portable or even a permanent oil/water separation system. Consequently the Phase II sump development work focused on developing a design which incorporated oil/water separation within the sump discarding the excess water (the bulk of the flow) and retaining and recovering the oil.

Figure 17 shows the basic sump design concept operating at 3.0 m/sec (6 knots) retaining and recovering an oil slick. A 3.8 cm (1.5 inch) layer of oil and water enters the sump at essentially freestream velocity and flows down a 1/5 incline. Since the flow is moving at high speed its Froude number is greater than 1.0 and a hydraulic jump forms as shown. The position of the jump is stabilized by the tailwater level which in turn is regulated by the width of the exit slot in the sump's aft portion. The hydraulic jump, one of several possible energy dissipation mechanisms, slows the flow to roughly 0.3 m/sec (0.6 knots). Some of the oil slick remains on the surface downstream of the jump while the remainder is broken into droplets in the turbulent eddies and mixed with the water. Since the flow downstream of the hydraulic jump is slow moving and relatively quiescent, many of these droplets rise to the surface to form a reconstituted oil slick in the aft portion of the sump. The excess water and any droplets not rising to the surface exit through the slot.

The aft end of the sump forms a barrier retaining the reconstituted oil slick much as a conventional oil boom since the sump velocity is slow enough to preclude the usual boom failure mechanisms. The aft end of the sump is adjustable and acts as a weir to removing the oil once enough has accumulated in a surface slick. The amount of excess water recovered with the oil depends upon the recovery pumping rate, the thickness of the oil slick in the

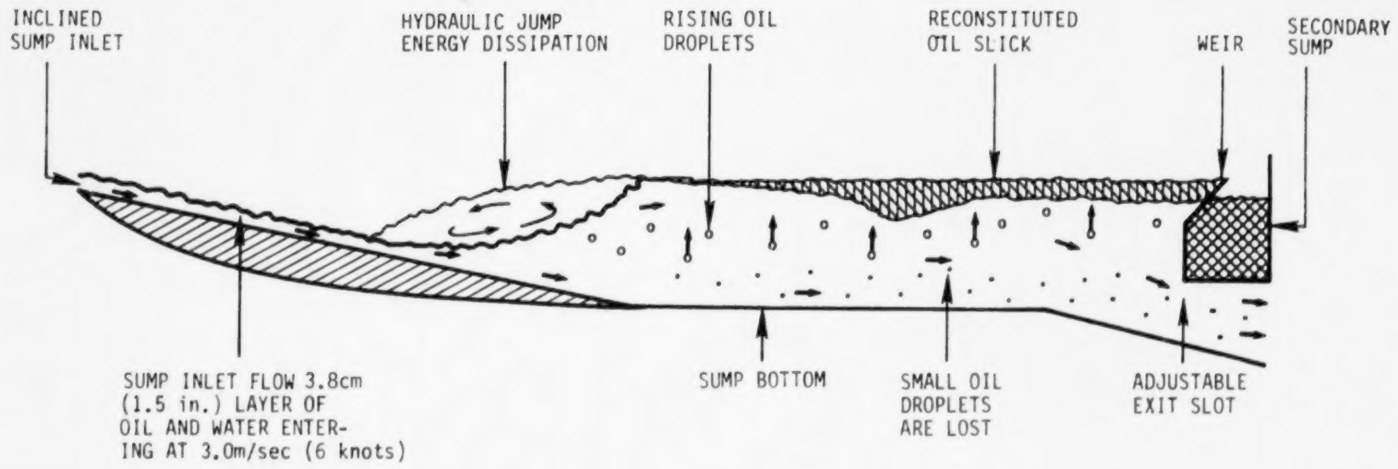
INCLINED SUMP INLET
HYDRAULIC JUMP ENERGY DISSIPATION
RISING OIL DROPLETS
RECONSTITUTED OIL SLICK
WEIR
SECONDARY SUMP
SUMP INLET FLOW 3.8cm (1.5 in.) LAYER OF OIL AND WATER ENTERING AT 3.0m/sec (6 knots)
SUMP BOTTOM
SMALL OIL DROPLETS ARE LOST
ADJUSTABLE EXIT SLOT

Figure 17. Sump design concept - schematic drawing.

sump, and specific weir geometry.

In the special case where the fluid entering the sump contains a high percentage of oil, oil/water separation in the sump is not necessary. The exit slot is closed and all the flow entering the sump is recovered over the weir. However, such conditions are improbable for inland applications. If the fluid entering the sump were 50 percent oil, the oil slick would be 1.9 cm (0.75 inches) thick corresponding to an oil flowrate of 3,500 l/min per meter (280 gpm per foot) at 3.0 m/sec (6 knots). More probably, oil slicks in the range of 1.0 to 3.0 mm would be encountered corresponding to 3 to 8 percent of the total sump flow.

The inclusion of oil/water separation into the sump design makes the characteristics of the energy dissipation process critically important. If the oil is broken into fine droplets or emulsified, the sump residence time will not be long enough to allow the droplets to rise to the surface. The oil/water separation process can also be hampered by high turbulence levels and nonuniform velocity profiles produced by energy dissipation. Since inertial, gravitational, viscous and surface tension forces are all important and the process is sensitive to oil properties, experiments must be conducted at full-scale.

The sump must perform several interrelated functions simultaneously:

- Receive all flow passing over the bow
- Dissipate kinetic energy
- Separate oil from excess water
- Discard excess water
- Retain oil in sump
- Recover oil from sump
- Interface with the stability control system

The requirements for each of these functions and the sump's basic operational parameters can be deduced from the bow design and normal operating point. Based on a 3.8 cm (1.5 inch) layer skimmed into the sump at 3.0 m/sec (6 knots), the flowrate into the sump is 116 l/sec per meter width (561 gpm per foot width). A 3 mm oil slick would enter the sump at 9.2 l/sec per meter width (44 gpm per foot width) representing 7.9 percent of the total. If the oil is to be retained in the sump under conditions similar to a conventional oil boom, the sump velocity must be no more than 0.30 m/sec (1.0 feet/second). For this sump velocity continuity requires that the flow depth must increase to 38 cm (15.0 inches), assuming no width change, and since the kinetic energy is proportional to the square of the velocity, 99 percent of the total flow's incident kinetic energy and 100 percent of the oil's kinetic energy must be dissipated. Assuming an effective sump length of 3.0 m (10 feet), if the oil is not recovered it will build up in the sump at a rate of 18.0 cm/min (7.1 inches/minute). If the oil is recovered as it is encountered, the equilibrium sump oil layer thickness will be 3.0 cm (1.2 inches.)

ENERGY DISSIPATION

Early in the sump design process it was recognized that energy dissipation was the most critical function. If in the process of energy dissipation, the oil slick is broken into very fine droplets, there is little hope of recovering a substantial portion in a compact sump. A gravity separator with a capacity of 2.100 l/min (560 gpm) (equivalent to a 0.3 m$_3$(1 foot) width of streamlined oil boom) would require approximately 5.3 m^3 (1,400 ft^3) of space and weighs 7.0 metric tons (6.9 tons) dry.* This is clearly impractical for a streamlined oil boom section even a few feet wide.

Ideally, the energy dissipation mechanism should be simple, nonclogging, insensitive to flowrate and oil properties, and avoid breaking the oil slick into fine droplets. Since energy dissipation through turbulence generation and decay meets all of these requirements except for its unknown performance on oil slicks, a majority of the sump development focused on iteratively testing with oil, various sump designs employing this priciple and measuring the subsequent separation of oil and water.

Experiments were conducted in the sump test flow channel, shown schematically in Figure 18. This flow channel was constructed to be a full-scale internal model of the sump in all dimensions except width. Full-scale allowed meaningful experiments to be conducted with oil without scaling problems and the high costs of tow testing a complete streamlined oil boom model merely to obtain sump design data. Since the streamlined oil boom is essentially two-dimentional, a specific width is not important for accurate testing. A width of 8.9 cm (3.5 inches) was chosen to produce a 3.8 cm (1.5 inch) layer of water at 3.0 m/sec (6 knots) entering the sump with the available pumps and equipment. The channel bottom had a series of 1.9 cm (0.75 inch) holes joining a plenum beneath to simulate a porous sump bottom. The holes could be individually plugged or left open to model any flow exit configuration. Water passed through the porous bottom into the plenum, a manifold system and into two pumps which supplied water to the head tank. Water from the head tank entered the channel (or sump) in a thin layer at high speed (supercritical flow) and flowed down the incline. The flow's kinetic energy was dissipated through a hydraulic jump or other dissipation mechanism, flowed through the porous bottom and the cycle repeated. The channel was designed to model sumps up to 7.3 m (24 feet) long and the aft portion could be blocked off to simulate shorter sumps.

A light lubricating oil was used for the majority of the tests. It was deposited on the surface of the high speed flow immediately downstream from the head tank and recovered from the surface in the aft portion of the simulated sump with a small self-priming recovery pump. The channel was thoroughly cleaned after each test so that the volumes of oil deposited and recovered would provide and accurate measure of sump performance.

---

* Dimensions are based on a model 14.6 gravity separator with a capacity of 500 gpm manufactured by Hyde Products, Inc., Cleveland, Ohio.

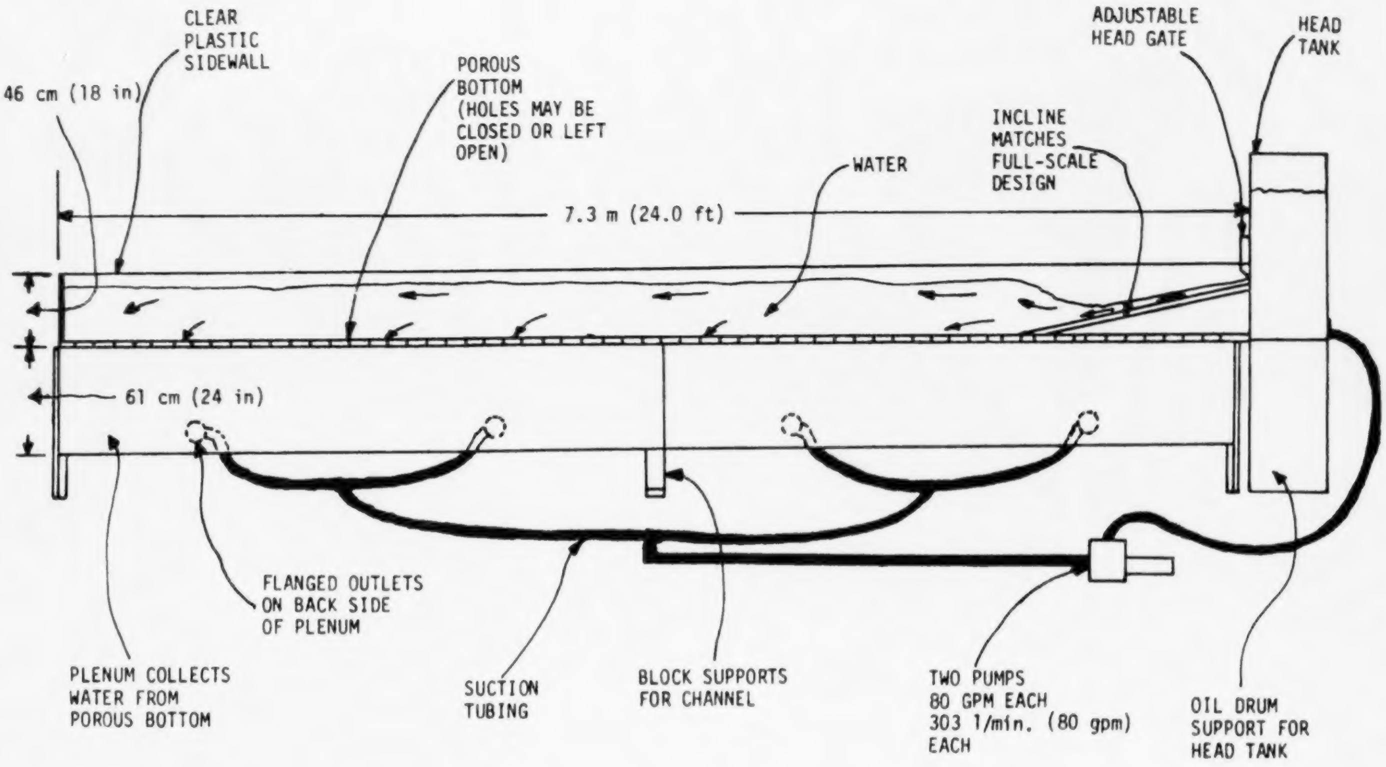
CLEAR PLASTIC SIDEWALL
46 cm (18 in)
POROUS BOTTOM (HOLES MAY BE CLOSED OR LEFT OPEN)
WATER
INCLINE MATCHES FULL-SCALE DESIGN
ADJUSTABLE HEAD GATE
HEAD TANK
7.3 m (24.0 ft)
61 cm (24 in)
FLANGED OUTLETS ON BACK SIDE OF PLENUM
PLENUM COLLECTS WATER FROM POROUS BOTTOM
SUCTION TUBING
BLOCK SUPPORTS FOR CHANNEL
TWO PUMPS 80 GPM EACH 303 l/min. (80 gpm) EACH
OIL DRUM SUPPORT FOR HEAD TANK

Figure 18. Sump test flow channel.

Several energy dissipation mechanisms were investigated analytically and those found suitable for the streamlined oil boom were iteratively tested in the sump test flow channel with oil. Out of the many designs tested the four shown in Figure 19 performed the best. The important characteristics of each device along with the results of the oil tests in the sump test flow channel are shown in Table 2.

The normal hydraulic jump is the simplest design and has no obstructions to cause clogging. Flow enters the sump at essentially freestream velocity and accelerates down the incline where a turbulent roller forms dissipating energy. The hydraulic jump automatically positions itself in response to the tailwater level producing a relatively uniform downstream velocity profile. The scale of the turbulent eddies produced is of the same order as the roller dimensions and these eddies decay downstream. The normal hydraulic jump sump design was tested full-scale in the first OHMSETT test series (see Table 1) at 1.5 and 3.0 m/sec (3 and 6 knots). Good results were obrained at 1.5 m/sec (3 knots) with the majority of the oil slick appearing on the surface immediately downstream of the roller and thruput efficiencies as high as 86.5 percent were achieved. At 3.0 m/sec (6 knots) however, the amount of energy dissipated in the jump was four times as great producing large violent eddies and breaking the oil slick into much smaller droplets. Efficient oil/water separation was impossible with these small droplets and the high sump turbulence level and as a result thruput efficiency dropped to near zero. The experiments in the sump test flow channel confirmed this performance and a maximum thruput efficiency of 25 percent was obtained with a sump length twice as long as that used for the other options. Because of the desire to develop a system with good 3.0 m/sec (6 knot) performance most of the development work focused on the other energy dissipation mechanisms. However, the freedom from clogging, simplicity and good 1.5 m/sec (3.0 knot) performance make the hydradulic jump an excellent candidate for a lower speed design.

The array of surface piercing rods dissipates energy through the hydrodynamic drag on each rod. Since the rods are surface piercing energy is dissipated uniformly throughout the flow depth without the formation of a roller or other flow separation. The equations of motion for flow through an array of surface piercing rods can be developed by assurming a drag coefficient for each rod and modifying the usual equations for open channel flow to account for the energy loss. The final equations after some manipulation are identical to the equations of two dimensional open channel flow with the surface friction terms replaced by terms involving the rod drag coefficient.

The hydrodynamic drag coefficient for cylindrical rods normal to the flow (based on frontal area) is approximately 100 times as great as the drag coefficient for a flat plate such as the sump bottom (based on the plate area). Consequently a relatively close packed array where the frontal area of the rods is approximately the same as the sump bottom area can provide energy dissipation in approximately 1 percent of the space required for flat plate friction. Furthermore since the energy dissipation is proportional to the square of the velocity, the array of surface piercing rods

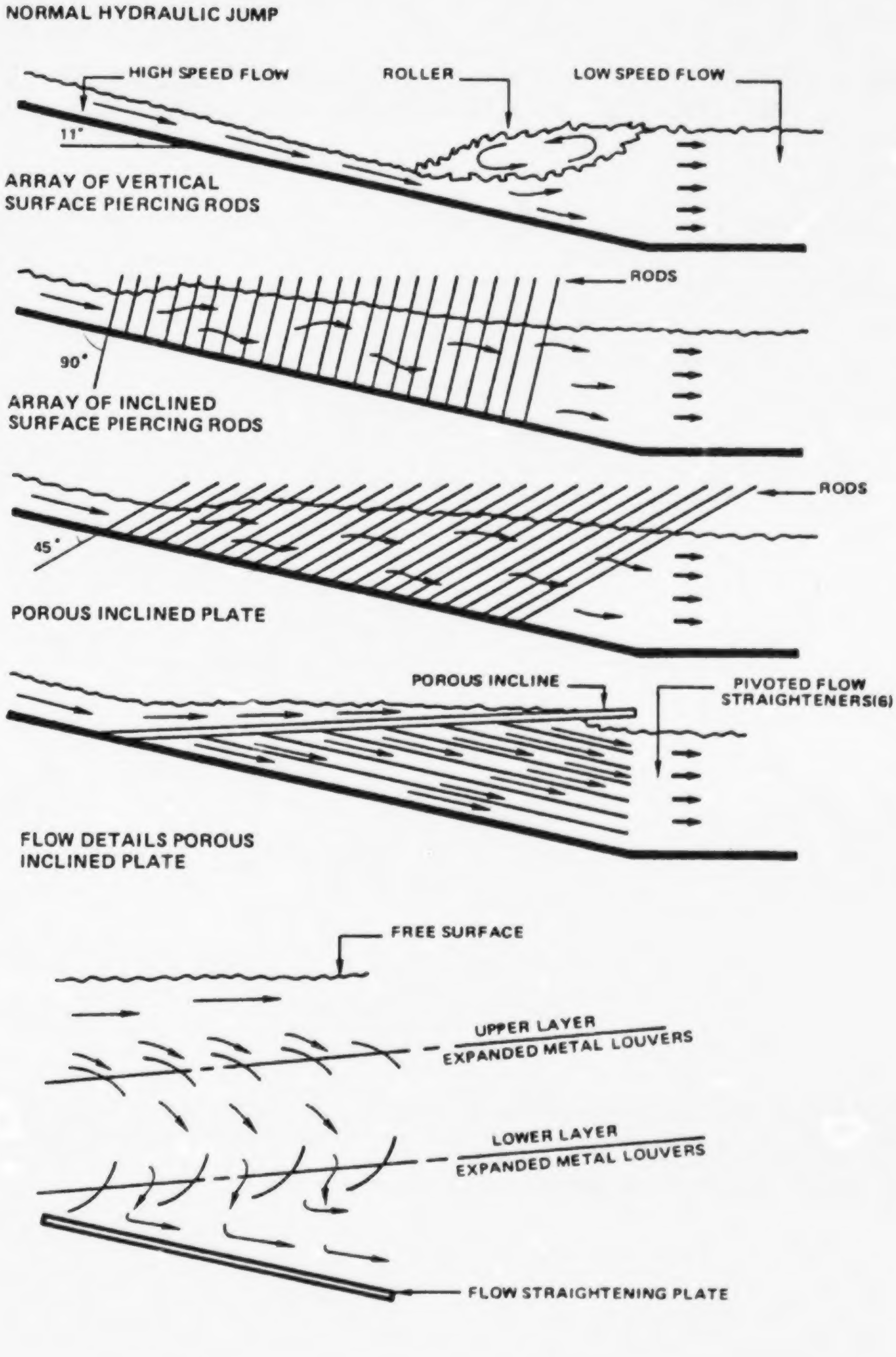
NORMAL HYDRAULIC JUMP
HIGH SPEED FLOW
ROLLER
LOW SPEED FLOW
11°
ARRAY OF VERTICAL SURFACE PIERCING RODS
RODS
90°
ARRAY OF INCLINED SURFACE PIERCING RODS
RODS
45°
POROUS INCLINED PLATE
POROUS INCLINE
PIVOTED FLOW STRAIGHTENERS(6)
FLOW DETAILS POROUS INCLINED PLATE
FREE SURFACE
UPPER LAYER
EXPANDED METAL LOUVERS
LOWER LAYER
EXPANDED METAL LOUVERS
FLOW STRAIGHTENING PLATE

Figure 19. Energy dissipation mechanisms.

TABLE 2. ENERGY DISSIPATION DEVICES: IMPORTANT CHARACTERISTICS AND RESULTS OF TESTS IN SUMP TEST FLOW CHANNEL

Energy Dissipation Device	Construction Details	Thruput* Efficiency	Clogging Rating** (1=Best)
Hydraulic Jump	Incline Slope = 1/5	25	1
Array of vertical surface piercing rods	Rod diameter = 0.64 cm (1/4 in) Rod density = 0.088/cm^2(0.57/in^2) Array geometry = staggered rows spaced 2.5 cm (1.0 in) in flow direction	71-77	4
Array of inclined surface piercing rods	Incline angle = 45° in flow direction Rod diameter = 0.64 cm (1/4 in) Rod density = 0.12/cm^2 (0.76/in^2) Array geometry = staggered rows spaced 1.3 cm (0.5 in) in flow direction with every third row empty	75-81	3
Inclined expanded metal	Double layer of expanded metal louvers inclining in direction of flow Incline angle = 1.9° Upper layer: Louvers declining in flow direction Hole spacing: in flow direction 1.97/cm (5.0/in); normal to flow direction = 0.98 cm (2.50/in) Lower layer: Louvers inclining in flow direction Hole spacing: in flow direction 1.57/cm (4.0/in); normal to flow direction = 0.52/cm (1.33/in) Layer spacing = 1.90 cm (0.75 in)	78	2

* Measured in sump test flow channel with 3.0 m/sec (6 knots) inlet velocity with 30 wt. detergent motor oil (except hydraulic jump — vegetable oil).

** Clogging rating is a qualitative judgement of estimated performance with small debris.

tends to smooth out velocity profile irregularities and produce a uniform velocity profile downstream. The scale of the turbulent eddies is roughly the same size as the rod diameter, much smaller than the eddies produced by the hydraulic jump, and consequently the eddies decay faster producing a more quiescent flow downstream. Several geometries were tested to optimize rod diameter and spacing. Best results were achieved with 0.63 cm (0.25 inch) diameter rods speced 0.088/cm^2 (0.57/in^2) and thruput efficiencies in the range of 71 to 77 percent were obtained in the sump test flow channel experiments with a 3.0 m/sec (6 knot) inlet velocity.

One obvious disadvantage of the surface piercing rods is their tendency to catch debris, particularly long stringy debris such as weeds, rags, sticks, etc. Inclining the rods at a 45° angle reduces the clogging problems. With inclined rods, the fluid has a velocity component parallel as well as perpendicular to the rods and debris is carried upward to the free surface level. Occasionally lowering the array so the rod tips are beneath the surface would wash away any debris collected. Since the velocity component perpendicular to the rods is smaller, the drag on each rod is also smaller and the rod spacing must be decreased to achieve the same energy dissipation. As expected, best results were achieved with the same rod diameter as the vertical array and a spacing of 0.12/cm^2 (0.76/in^2). Thruput efficiencies in the range of 75 to 81 percent were obtained in the sump test flow channel experiments with a 3.0 m/sec (6 knots) inlet velocity. This is comparable to the performance of the vertical rods considering experimental errors.

The energy dissipation devices discussed above are similar in that all of the fluid entering the sump, both oil and water, passes through the turbulent area simultaneously and as a result when the oil slick is broken into droplets, the droplets mix with the entire flow. The porous inclined plate energy dissipation mechanism remedies this problem by allowing the oil slick to pass through the turbulent zone last so that any oil droplets are mixed with only the uppermost layer of water. The porous inclined plate is a double layer of expanded metal louvers slightly inclined to the flow direction so that the flow moves nearly parallel to the incline.

The upper layer acts as a cascade or blade row directing fluid downward with little energy loss. The lower layer is coarser, inclined in the opposite direction and acts as a stalled cascade with high drag and energy dissipation. Flat plates hinged to the incline's bottom side redirect flow in the downstream direction, smooth turbulent eddies and pivot in response to the local static pressure to maintain a uniform downstream velocity profile. Experiments in the sump test flow channel gave a thruput efficiency of 78 percent with a 3.0 m/sec (6 knot) inlet velocity, comparable to the arrays of surface piercing rods. The porous incline is expected to offer less clogging problems than the arrays of surface piercing rods. Debris larger than the holes in the expanded metal is carried up the metal surface by the flow and may be manually moved as required. Small debris may tend to accumulate on the expanded metal surface. However backflushing or brushing the surface should remove most materials.

OIL/WATER SEPARATION

Downstream of the energy dissipation device, the mixture of oil and water enters the oil/water separation area where the buoyant oil droplets rise to the surface to form a reconstituted oil slick. The slick is retained against the aft end of the sump and recovered as required while excess water is discarded. This portion of the sump is essentially a gravity oil/water separator operating with a very high flowrate.

Gravity oil/water separators have been the subject of considerable research. The principles of operation, scaling parameters and design details for efficient operation are all well known and units of varying capacity are available from many commercial sources. The American Petroleum Institute (API) recommends* designing oil/water separators to remove oil droplets as small as 0.015 cm (0.006 inch) and to have a maximum flow velocity of 1.52 cm/sec (0.6 in/sec or 0.03 knots). Applying these specifications to the streamlined oil boom sump operating point gives a minimum sump depth of 7.6m (25 feet), impractical for a streamlined oil boom skimming only 3.8 cm (1.5 inch). Furthermore, the minimum size droplets to be recovered is the minimum size droplet produced in the energy dissipation process which may be either smaller or larger than 0.015 cm (0.006 inch).

This portion of the streamlined oil boom sump was designed to separate as small a droplet size as was feasible within reasonable sump size constraints. Experiments were conducted in the sump test flow channel testing various sump geometries, lengths and flow outlet configurations in conjunction with alternative energy dissipation devices to optimize performance. The final streamlined oil boom design is shown in Figure 20. The sump is essentially a rectangular chamber with a porous bottom over a triangular plenum with a pivoting weir skimmer at the aft end. After passing through the energy dissipation device, the mixture of water and oil droplets enters the chamber and begins to separate by gravity. As the flow proceeds through the sump, the excess water (and some oil) is withdrawn through the porous bottom into the triangular plenum. The fluid progressively withdrawn is the cleanest (freeist from oil droplets) because it is nearest the bottom. Since the sump's horizontal velocity component decreases monotonically to zero at the aft end, the effective sump residence time for oil droplets is increased.

The rising oil droplets migrate to the surface where they form a reconsituted oil slick. Since the sump's horizontal velocity drops to zero at the aft end, the slick is effectively retained without the usual high current oil boom failure mechanisms such as drainage and droplet entrainment.**

---

* Manual on Disposal of Refinery Wastes, "Chapter 5 - Oil-Water Separator Process Design," American Petroleum Institute, 1969.

** However, if the oil is allowed to accumulate until the slick thickness approaches a large portion of the sump depth, these failure mechanisms may occur causing some losses.

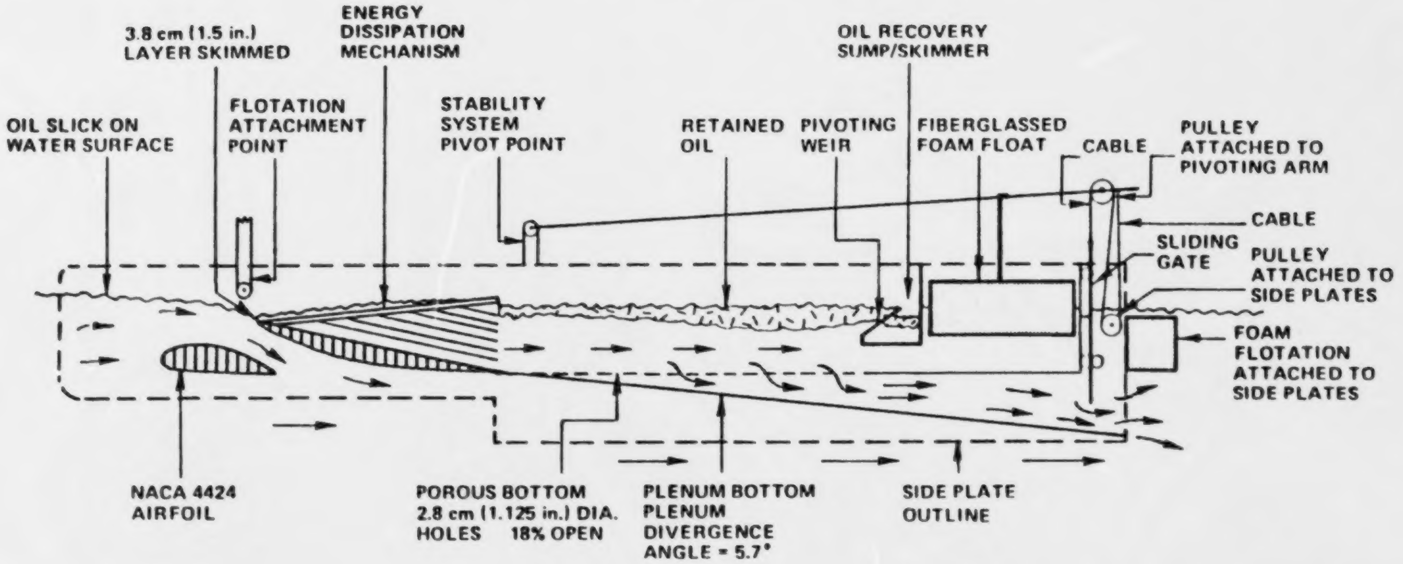
3.8 cm (1.5 in.) LAYER SKIMMED
ENERGY DISSIPATION MECHANISM
OIL RECOVERY SUMP/SKIMMER
OIL SLICK ON WATER SURFACE
FLOTATION ATTACHMENT POINT
STABILITY SYSTEM PIVOT POINT
RETAINED OIL
PIVOTING WEIR
FIBERGLASSED FOAM FLOAT
CABLE
PULLEY ATTACHED TO PIVOTING ARM
CABLE
SLIDING GATE
PULLEY ATTACHED TO SIDE PLATES
FOAM FLOTATION ATTACHED TO SIDE PLATES
NACA 4424 AIRFOIL
POROUS BOTTOM 2.8 cm (1.125 in.) DIA. HOLES 18% OPEN
PLENUM BOTTOM PLENUM DIVERGENCE ANGLE = 5.7°
SIDE PLATE OUTLINE

BOW DESIGN DETAILS

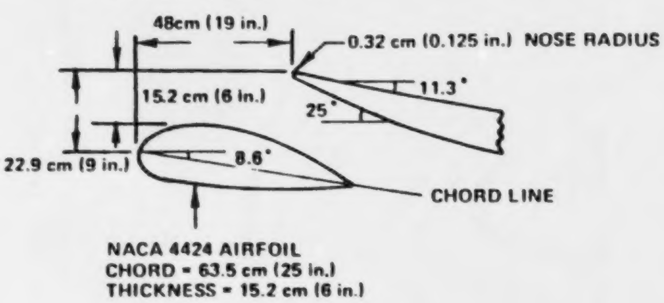
48cm (19 in.)
0.32 cm (0.125 in.) NOSE RADIUS
15.2 cm (6 in.)
11.3°
25°
22.9 cm (9 in.)
8.6°
CHORD LINE
NACA 4424 AIRFOIL
CHORD = 63.5 cm (25 in.)
THICKNESS = 15.2 cm (6 in.)

NOTES:

1. Any of the Energy Dissipation Mechanisms Shown in Figure 19 Can Be Used.
2. Oil is Recovered from Sump/Skimmer with Hose and Pump System (Not Shown).
3. Dimentions: Overall Length = 6.7m(22 ft.)
   Side Plate Hieght = 1.0m (40 in.)
4. Cable System Amplifies Gate Motion by Factor of 3.

Figure 20. Final streamlined oil boom/skimmer design.

The performance of this sump design in separating oil droplets can be estimated following the procedures for conventional oil/water separation neglecting turbulence, short circuiting and the interaction of oil droplets one with another. Under these conditions it can be shown that all oil droplets with a terminal rising velocity greater than

$$V_R = \frac{Q_0}{L\ W}$$

where:

Q_0 = sump flowrate

L = sump length

W = sump width

V_R = terminal rising velocity

will rise to the surface to form a reconstituted oil slick regardless of their initial depth in the sump. For droplets with slower terminal rising velocities the initial depth is important and all droplets initially a distance Y_0 above the bottom rise to the surface:

$$Y_0 = D \left(1 - \frac{V_R\ L\ W}{Q_0}\right) \qquad \text{where} \qquad D = \text{sump depth}$$

These relationsips can be applied to determine the minimum droplet size collected by the streamlined oil boom sump. This calculation was performed using the bow design point with a 3.8 cm (1.5 inch) layer entering the sump, the geometry shown in Figure 20 and an oil with a specific gravity of 0.875. Figure 21 shows the calculated minimum droplet size completely recovered as a function of the current velocity. At the 3.0 m/sec (6 knots) design point, all droplets greater than 0.12 cm (0.047 inch) are recovered. While this is a relatively small droplet, it is eight times the recommended API design point.

WATER REMOVAL AND OIL RECOVERY

The porous bottom and plenum beneath it were designed to withdraw fluid uniformly across the entire sump bottom. This produces a linearly decreasing horizontal sump velocity as the fluid moves aft and a vertical velocity proportional to the distance from the free surface. It can be shown that these conditions approximate potential flow* and thus minimize the formation of vortices which might entrain oil.

---

* Potential flow is incompressible flow with zero or constant vorticity; it is not influenced by viscous effects.

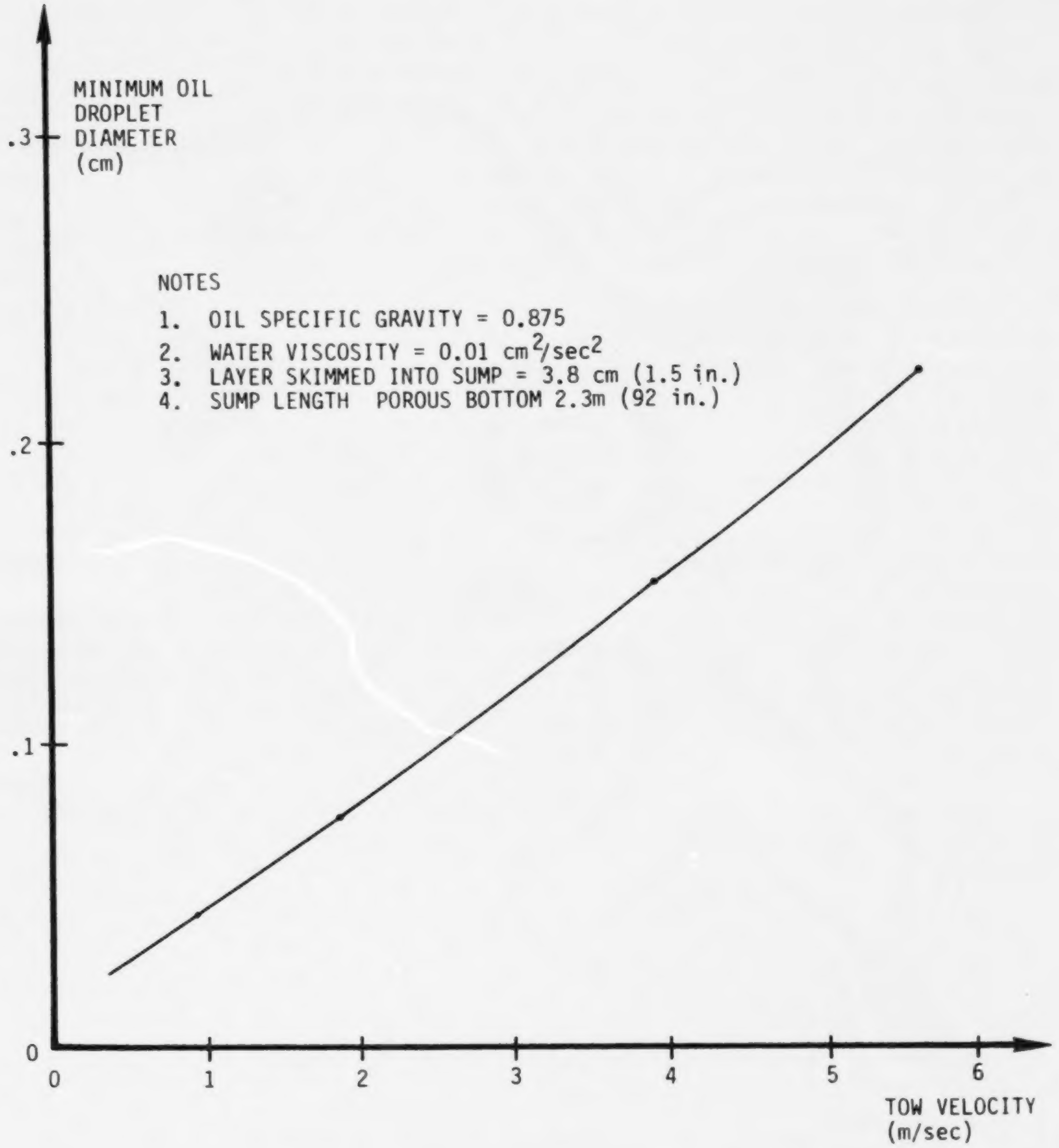

NOTES

1. OIL SPECIFIC GRAVITY = 0.875
2. WATER VISCOSITY = 0.01 cm^2/sec^2
3. LAYER SKIMMED INTO SUMP = 3.8 cm (1.5 in.)
4. SUMP LENGTH POROUS BOTTOM 2.3m (92 in.)

Figure 21. Minimum oil droplet size completely removed from final sump design as a function of tow velocity.

The plenum has a constant included angle of 5.7° producing a cross-section area increasing linearly in the downstream direction. The angle was chosen as a balance between a substantial passage width and minimum pressure drag on the flow passing beneath. The porous bottom is an array of 2.86 cm (1.125 inch) diameter holes arranged to produce a porous plate approximately 18 percent open. The holes are slightly closer together (greater percentage open) in the front portion to allow for pressure losses in the plenum. The pressure loss across the porous bottom is approximately 0.58 cm (0.23 inch) of water at the 3.0 m/sec (6 knot) design point. This small loss is insignificant compared to the free stream dynamic pressure of 47 cm (1.55 feet) and leaves ample pressure differential to control flow out of the plenum with a downstream restriction.

Figure 22 shows the operation of the oil removal device. It is a self-adjusting pivoting weir which automatically adjusts to variations in the sump water level. The weir edge is pivoted about a horizontal axis and supported by a float in the secondary sump. As fluid is pumped from the secondary sump, the fluid level drops and the weir pivots allowing a thin layer to be skimmed. In this manner the weir follows the secondary sump fluid level maintaining a small differential between the levels in the main and secondary sumps. The size of the float determines the difference in levels and the thickness of the layer skimmed measured at the weir edge. For a small float, the difference in levels is small and the weir edge pivots substantially allowing a thick layer to be skimmed. For large floats, the difference in levels is larger and the thickness of the layer skimmed decreases. The minimum thickness is achieved when fluid passes over the weir as a free overfall. Under these conditions a 1 mm oil slick entering the sump at 3.0 m/sec (6 knots) would pass over the weir as a 0.98 cm (0.39 inche) oil slick.* The weir edge was serrated to reduce flow variations over the weir width.

This weir oil recovery device is only one of several possible devices to remove oil once it has accumulated in the sump. Other possiblities include:

- Conventional floating skimmer head mounted in the sump
- Rotating disc or drum skimmer
- Sorbent skimming system

---

* This calculation assumes that the Froude number based on local velocity and flow depth at the weir is unity.

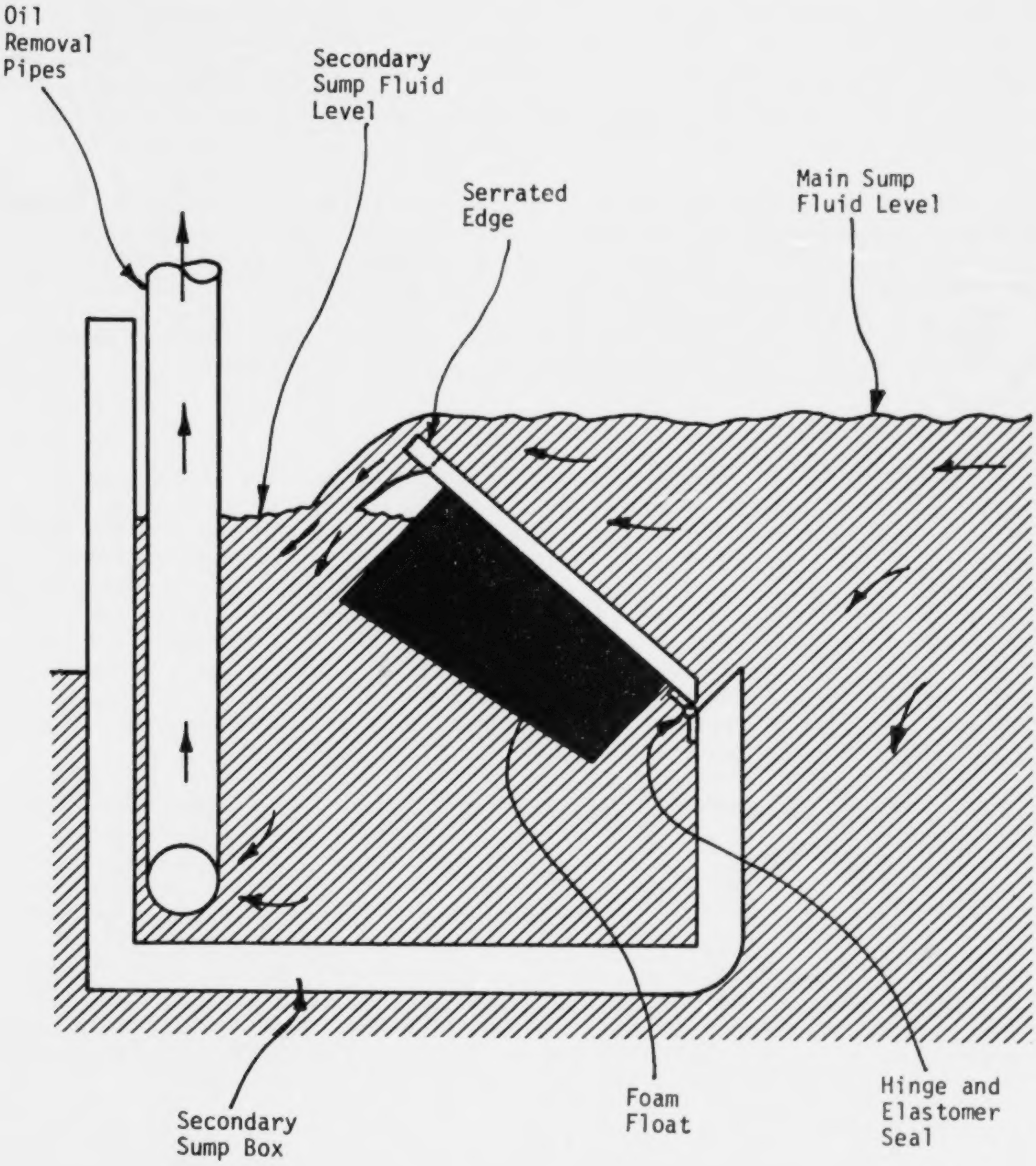
Oil Removal Pipes
Secondary Sump Fluid Level
Serrated Edge
Main Sump Fluid Level
Secondary Sump Box
Foam Float
Hinge and Elastomer Seal

Figure 22. Self-adjusting weir and secondary sump.

SECTION 6

FORCES AND STABILITY

The forces exerted by the flow on the streamlined oil boom and its response to those forces are important considerations. If it is deployed as a boom spanning a wide high current area, an integral flotation system must be provided to counteract any vertical loads without porpoising or other instabilities and a cable system must be provided to oppose the drag. If it is deployed as a high speed skimming craft, the lift and drag must be considered in designing hulls and determing powering requirements.

FORCE MEASUREMENT

Vertical forces on the boom are complex combinations of hydrodynamic and hydrostatic forces. Hydrodynamic forces are produced by changes in velocity and direction of fluid passing over, around, and through the boom, and viscous shear stresses. Hydrostatic forces are caused by the difference in water level inside and outside the sump. If the level inside the sump is higher than outside, there is a net force downward due to the weight of the excess water contained in the sump and vice versa. Although hydrostatic forces can be estimated from expected water levels, hydrodynamic forces generally defy analysis where the flow is complex and adjacent to a free surface. The horizontal force or drag on the boom is entirely hydrodynamic and increases as the square of the tow velocity (approximately).*

The forces on the streamlined oil boom were measured during the Phase II series at the Lockheed Towing Basin in San Diego. In these tests a 0.6 m (2 feet) wide full-scale model was rigidly attached to a carriage and towed at speeds up to 3.0 m/sec (6 knots) over a range of operating parameters as forces and water levels were measured. Figure 23 shows the design of the model used in these tests.** Six load cells were used to measure forces. Four of these (two forward and two aft) measured lift forces, and the other two (in series with the forward lift load cells) measured drag. Two water level transducers were also used, one over the sump inlet and the other just upstream of the weir. Data from these transducers allowed the relationships between operating parameters and lift and drag to be determined.

---

* Force measurements during the Phase I Lockheed tests showed pronounced dips in the drag versus velocity curve as the bow wave passed through various flow regimes,

** Since this model was not the final design the numberical values of the forces measured are not the same as the final design, but the general behavior is similar.

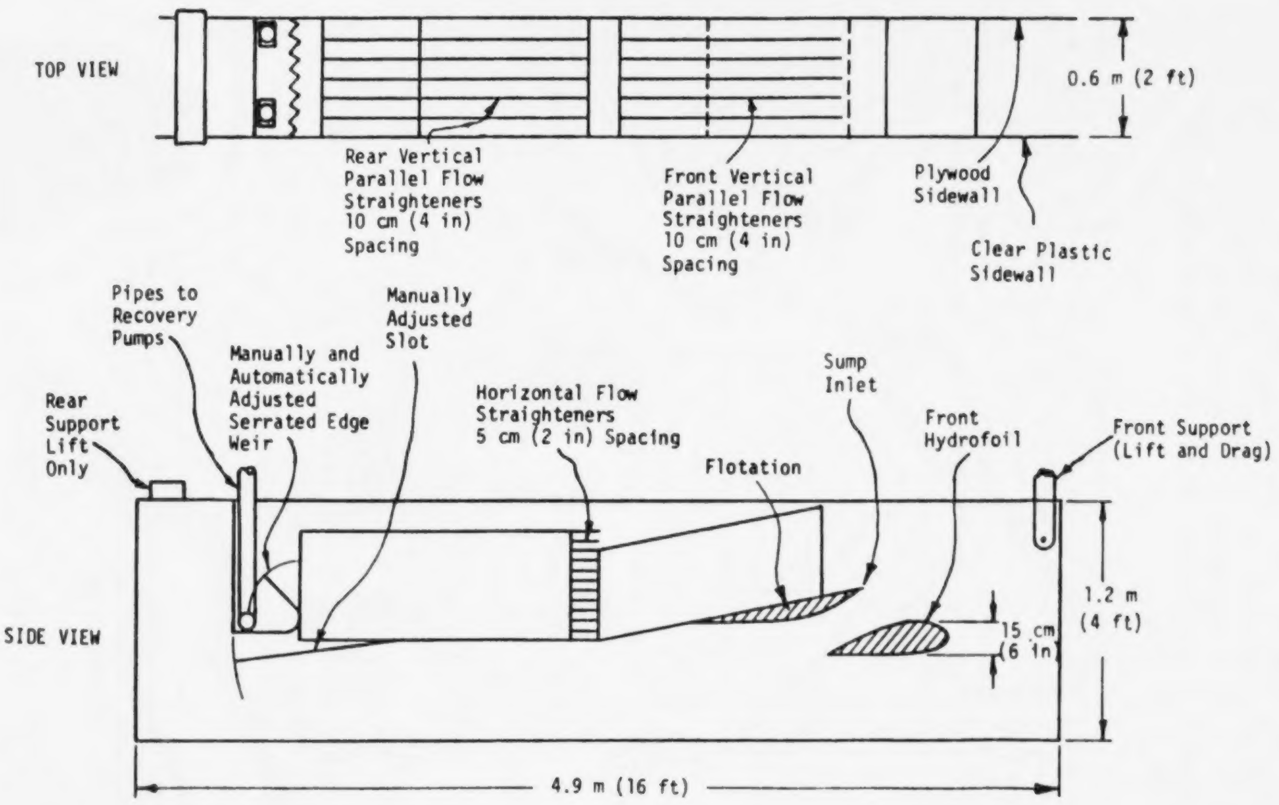
TOP VIEW
0.6 m (2 ft)
Rear Vertical Parallel Flow Straighteners 10 cm (4 in) Spacing
Front Vertical Parallel Flow Straighteners 10 cm (4 in) Spacing
Plywood Sidewall
Clear Plastic Sidewall
Pipes to Recovery Pumps
Manually Adjusted Slot
Manually and Automatically Adjusted Serrated Edge Weir
Rear Support Lift Only
Horizontal Flow Straighteners 5 cm (2 in) Spacing
Sump Inlet
Front Hydrofoil
Flotation
Front Support (Lift and Drag)
15 cm (6 in)
1.2 m (4 ft)
SIDE VIEW
4.9 m (16 ft)

Figure 23. Model for Lockheed tests.

Perhaps the most important result of these force measurements is that hydrodynamic forces were found to be small compared to hydrostatic forces. This is shown in Figure 24, a plot of total vertical force against difference in free surface level ϵ (inside sump minus outside sump). If only hydrostatic forces were important, the data would show vertical forces directly proportional to ϵ. The data exhibit this general trend but with some data scatter due to hydrodynamic forces which vary with other parameters not held constant.*

This implies that flotation requirements could be significantly reduced by maintaining the level of water inside the sump nearly the same as the level outside the sump. From Figure 24 it can be seen that in all cases where the absolute value of ϵ was less than 0.5 cm (0.2 inch), the total vertical force was less than 89 N (20 pounds). This corresponds to a flotation requirement of 146 N per meter of boom width (10 pounds per foot of boom width). These small forces imply relatively small buoyancy requirements.

The water level in the sump (and hence ϵ) is a function of the difference in flowrate into and out of the sump. If the flowrate into the sump is greater than the flowrate out, excess fluid builds up in the sump and the water level increases and vice versa. Since the streamlined oil boom processes a large flowrate, even small percentage flowrate differences cause large sump weight changes. For example, if the streamlined oil boom is operating at the 3.0 m/sec (6 knot) design point with 116 l/sec per meter width (561 gpm per foot width) entering the sump, and the flowrate leaving the sump is only 10 percent less, excess fluid will build up in the sump at the rate of 119 N/sec per meter width (490 pounds/minute per foot width). This large weight change coupled with the characteristics of a flotation system can lead to dynamic instabilities.

HYDRODYNAMIC INSTABILITY

Consider the operation of the streamlined oil boom supported by a buoyant flotation system as shown in Figure 25. The exit slot-width is adjusted so that at equilibrium the flowrate entering the sump equals the flowrate leaving the sump and the weight of excess water in the sump is balanced by the flotation buoyancy. Although this operating point is an equilibrium condition it is not necessarily a stable equilibrium. If the flotation system is too compliant and for some reason the flowrate entering the sump slightly exceeds the flowrate out of the sump, excess fluid would accumulate in the sump forcing the flotation downward and further increasing the flowrate into the sump and so on until the sump swamped. Stable operation can only be achieved where the flotation system is large enough to accommodate these sump weight changes.

---

* Such as velocity, freeboard, etc.

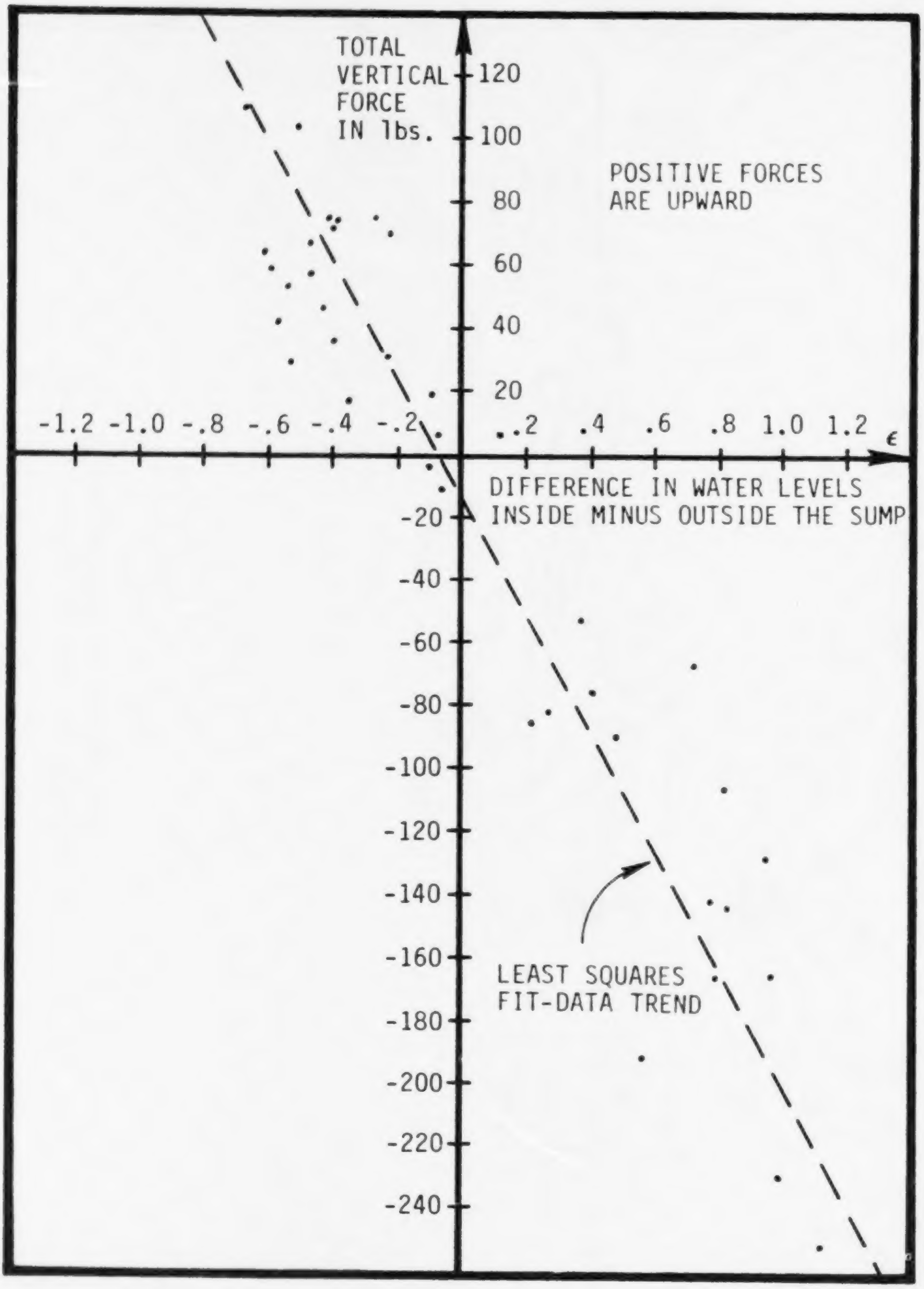

Figure 24. Total vertical force vs. difference in free surface levels (inside minus outside the sump).

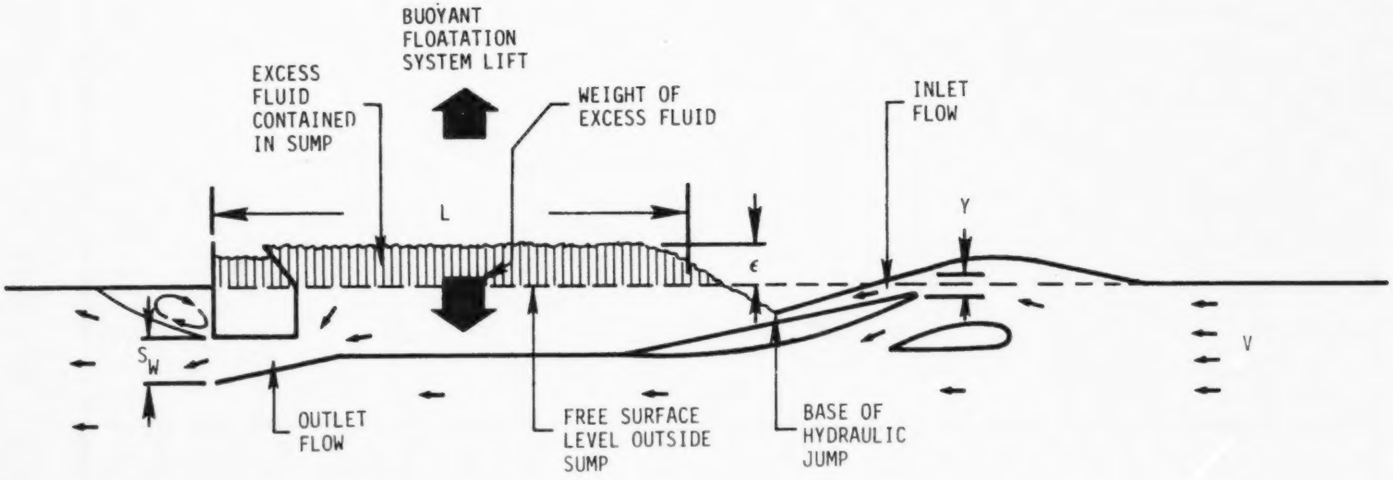
BUOYANT FLOATATION SYSTEM LIFT
EXCESS FLUID CONTAINED IN SUMP
WEIGHT OF EXCESS FLUID
INLET FLOW
L
Y
ϵ
V
S_W
OUTLET FLOW
FREE SURFACE LEVEL OUTSIDE SUMP
BASE OF HYDRAULIC JUMP

Figure 25. Schematic diagram of streamlined oil boom supported by buoyant floatation system.

This instability was observed in the 1975 OHMSETT tests when a 1.5 m (5 feet) wide full-scale model was rigidly attached to a flotation supported catamaran work platform and tow tested at 1.5 to 3.0 m/sec (3 and 6 knots). In these tests the freeboard was adjusted to vary the flowrate into the sump and a manually adjusted slot was positioned to set the flowrate out of the sump. At 1.5 m/sec (3 knots), operation was stable. As the boom was brought up to the test speed all parameters approach equilibrium asymtotically with no hunting or oscillations.

At 3.0 m/sec (6 knots), however, stable equilibrium could only be attained with a very low sump water level and a very thin layer skimmed into the sump. The streamlined oil boom could not be adjusted for stable operation at the design point. All attempts to increase the layer skimmed or sump depth by decreasing freeboard or closing the slot caused the sump to swamp by the mechanism described above. In order to obtain a "quasi" stable equilibrium for the 3.0 m/sec (6 knot) tests, the slot width was continously adjusted during the experiments in response to changes in sump water level.

A stability analysis was conducted to calculate the flotation requirements for stable operation. The slope of the force versus vertical displacement curve (as shown in Figure 26) determines stability. For a positive slope the equilibrium is unstable, and for negative slope it is stable. The borderline case of zero slope is astable, with many equilibrium states and the boom "hunts" moving up and down with no net force.

The vertical motion of the streamlined oil boom can be modeled subject to the following assumptions:

1. Vertical forces exerted on the boom are a result of the weight of the excess water in the sump and are proportional to the difference in water levels inside and outside the sump, ϵ .
2. Hydrodynamic forces are neglected.
3. Flow into the sump increases linearly with draft.
4. Flow passes out of the sump through a submerged slot of fixed width S_W.
5. Inertial forces are neglected.
6. Vertical forces are opposed by a flotation system with stiffness, S.

The first two assumptions follow from the force measurements at the Lockheed Towing Basin and the third assumption is a direct result of the bow wave analysis.* Neglecting inertial forces (the fifth assumption) confines

---

* Neglecting second order effects.

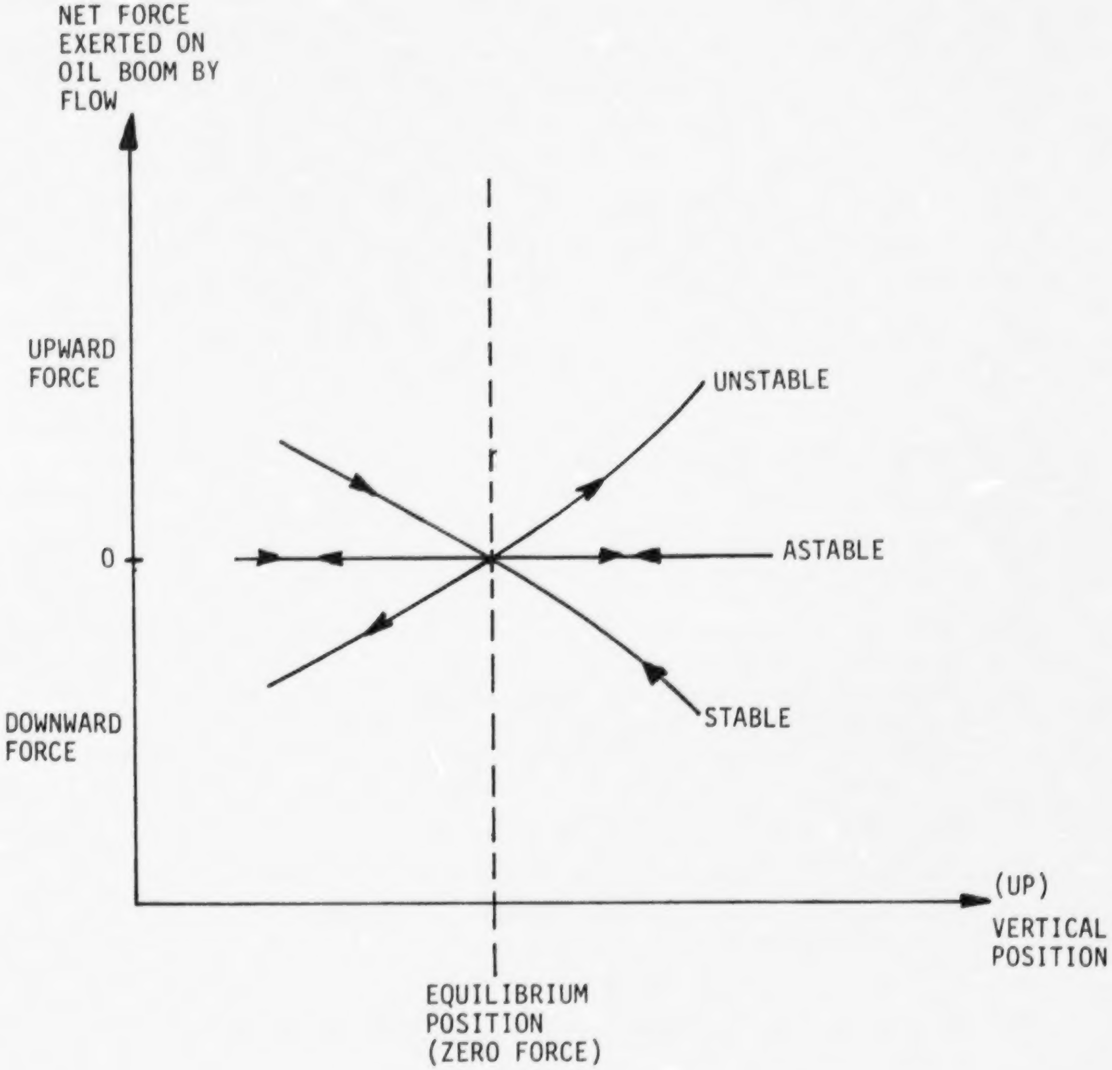
NET FORCE EXERTED ON OIL BOOM BY FLOW
UPWARD FORCE
0
DOWNWARD FORCE
UNSTABLE
ASTABLE
STABLE
(UP) VERTICAL POSITION
EQUILIBRIUM POSITION (ZERO FORCE)

Figure 26. Vertical stability as a function of net vertical force.

the analysis to vertical motion much slower than that produced by wave motion in the sump. Flotation stiffness is the ratio of increased lift to increased displacement as a flotation device is forced downward. For example, a buoyant float with a one square meter of area measured at the water line would have 98 N/cm stiffness in fresh water (a 1.0 square foot float would have 5.2 pounds/inch stiffness).

The results of the analysis define a dimensionless stability number S_N:

$$S_N = \frac{S\, S_W{}^2 g}{V_1{}^2 \; W\, L\, Y_1\, C_D \gamma}$$

where:

$S_N > 1$ Stable
$S_N = 1$ Astable
$S_N < 1$ Unstable

C_D = Sump exit slot discharge coefficient (assumed - 1.5)
γ = Fluid weight density

and the other parameters are evaluated at equilibrium.

Stability numbers for the OHMSETT tests were calculated from the emperical data and the results are shown in Figure 27. The analysis provides a good indication of stability but the dividing line between stable and unstable cases should be about (0.8) instead of 1.0. This difference is most likely due to the uncertainties in the effective sump length (not directly measured), and the layer thickness Y_1 measured only to the nearest 0.63 cm (1/4-inch) - a 25 percent uncertainty on a 2.5 cm (1.0 inch) layer.

The analysis is helpful in understanding stability for various oil boom designs over a range of test conditions. For example, it shows that increasing velocity tends to make the oil boom unstable (expected and observed at OHMSETT) and that decreasing the layer skimmed Y_1 tends to increase stability (unexpected and observed at OHMSETT).

This stability problem can be solved in two ways. Either enough flotation stiffness could be provided to achieve stability by "brute force," or the flowrate out of the sump could be adjusted to match the flowrate into the sump. While the stiff flotation method could be used, the stability analysis shows the minimum stiffness for stability at 3.0 m/sec (6 knots) to

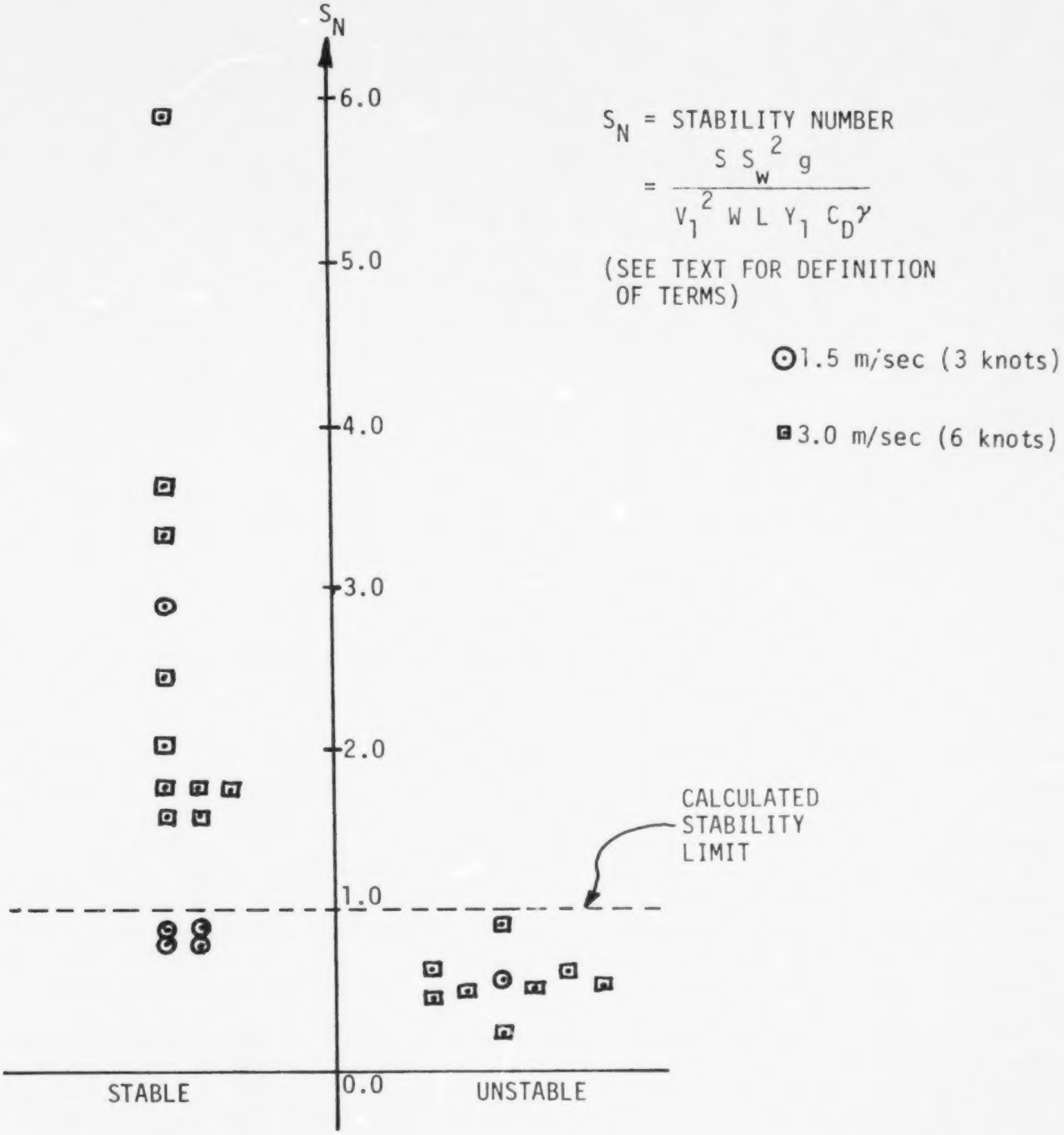

Figure 27. Comparison of stability numbers with observed stability - OHMSETT Tests 1975.

be 2,900 N/cm per meter of boom width (500 pounds/inch per foot width). This corresponds to an area several times the effective sump area and is clearly impractical. Consequently, the remaining development focused on designing an automatic stability control system to continuously adjust flow out of the sump in response to changing operation conditions.

STABILITY CONTROL SYSTEM

The streamlined oil boom support system was developed as two subsystems: a stability control system which adjusts the flowrate out of the sump to match the flowrate into the sump thus minimizing hydrostatic forces, and a flotation system to oppose the remaining forces.

There are several ways to adjust flow out of the sump but the simplest and most promising method is to regulate the width of an outlet slot in response to the weight of the sump. A stability analysis similar to that conducted for fixed slot widths was conducted on several alternative designs and the system shown in Figure 20 (page 43) was chosen for experimental optimization. In this design the streamlined oil boom is pivoted from a front flotation system with a center of buoyancy located near the sump inlet. The after portion of the boom is free to move in response to the vertical hydrodynamic and hydrostatic forces. Flowrate into the sump is determined primarily by the freeboard at the sump inlet* and flowrate out of the sump is regulated by a sliding gate moving in response to the float in the sump. If the flowrate leaving the sump is too small the rising sump fluid level will raise the gate until the flowrates are equated, and the sump weight is counteracted by the small block of flotation in the aft end.

This sytem allows adjustment of four key control system parameters:

- operating point
- gain
- damping
- feedback

The operating point (equilibrium sump depth) may be adjusted by varying the length of the vertical link, the gain (ratio of change in flowrate to change in float position) may be adjusted by changing the linkage geometry and the damping (float response time) may be adjusted by restricting the passage connecting the main sump and float chamber. Feedback is the relationship between flowrate into the sump and the operation of the stability control system and may be adjusted by changing the flotation pivot point. If the pivot point is at the sump inlet, the stability control system motion will not affect the flowrate into the sump - zero feedback. If the pivot point is moved aft, a downward motion of the sump's aft portion will raise the sump inlet reducing the flowrate into the sump - negative feedback.

---

* Angle of attack changes produce only small flowrate changes.

The operation of this stability control system is a complex nonlinear problem. Although the simplified stability analysis indicated that stable operation could be achieved, it did not model the system with enough accuracy to permit analytical optimization. Experiments were required.

Since the stability control system responds primarily to gravity and inertial forces, Froude number modeling can be used to conduct experiments on small scale. Proper scaling requires velocity to be scaled as the square of physical dimensions. One-third scale was chosen for the experiments since it produced a convenient model size roughly 2.2 m. (7.3 feet) long, and 3.0 m/sec (6 knots) full-scale tow velocities scale to 1.76 m/sec(3.4 knots), well within the speed capability of a small boat powered with a small outboard motor.

A 1/3-scale model of the entire oil boom was constructed from fiberglassed foam and resin coated plywood using construction techniques similar to those employed in the full-scale model. It incorporated an array of vertical rods in the sump as the energy dissipating mechanism and a stability control system with wide ranges of adjustment. The model was attached to a force balance and suspended between the hulls of a 4.8 m (16 feet) catamaran powered by a 7.5 hp outboard motor for tow testing in Newport Harbor.

Since the apparatus could operate at test speed for long periods, both starting transients and equilibrium operation could be observed. Four test series were run to observe the control system operation as the control system parameters were varied. Those combinations of adjustments found to be unstable were eliminated and the remaining experiments concentrated on measuring performance under stabe conditions as freeboard was varied.

Overall the stability control system was found to operate simply and reliably and could be adjusted to give stable operation with the model pivoted at the sump inlet and at the middle of the sump incline. Some damping was beneficial and reduced oscillations under certain conditions. However, with more damping the time lag between sump water level changes and float position changes was too great causing an out of phase feedback instability with large oscillations and porpoising.

When the model was pivoted at the bottom of the incline, stable operation could not be achieved. Large slot width and sump depth oscillations were observed with a frequency of approximately 1.0 Hertz. Damping and aft buoyancy improved performance but stable operation could not be achieved with any combination tested.

Pivot point location is an important variable. When the model is pivoted at the sump inlet, the stability control system balances the weight of excess water in the sump and consequently minimizes vertical forces on the front flotation. However, since the freeboard at the sump inlet and hence the layer skimmed are determined directly by the flotation system, its parameters are critical to proper operation. As the pivot point is moved aft of the sump inlet, the amount of sump weight supported by the front flotation increases but the negative feedback helps to adjust the sump inlet position minimizing the requirement for accurately setting flotation system parameters.

The force balance measured lift and drag at each operating point, and the results can be extrapolated to full-scale values through Froude number modeling. At the full-scale 3.0 m/sec (6 knot) design point with the boom pivoted at the sump inlet, the rate of change of vertical force with vertical pivot point position is 161 N/cm per meter of boom width (28 poinds/inch per foot of boom width). The front flotation system must have at least this amount of stiffness for stable operation. This compares with a flotation stiffness requirement of 2,900 N/cm per meter width (500 pounds/inch per foot width) without a stability control system. Stiffness requirements increased as the pivot point was moved aft as expected. The full-scale hydrodynamic drag was 14.6 per meter width (86 pounds per foot width) or a drag coefficient based on frontal area of 0.39. As a comparison, a conventional oil boom has a drag coefficient of about 1.50.

SECTION 7

SYSTEM INTEGRATION TESTS

The previously developed bow, sump and stability control system were combined in a full-scale 1.5 m (5 feet) wide streamlined oil boom preprototype model for a three-week system integration test series at OHMSETT. The objectives of these tests were to tune the system for optimum operation and determine the overall system performance in retaining and recovering oil slicks at speeds up to 3.0 m/sec (6 knots) and conditions typical of inland waterways.

MODEL CONSTRUCTION AND TEST RIGGING

Figure 28 is a photograph of the completed model and Figure 20 (page 43) is a side view drawing. The model was constructed as a two-dimentional 1.5 m (5 feet) wide section held together with vertical side plates. The materials of construction were chosen for low cost and ease of fabrication rather than desirability for long term immersion in a marine environment. The front hydrofoil and sump inlet were constructed of fiberglassed foam, similar to surfboards, and the remainder of the model was primarily 1.9 cm (0.75 inch) thick exterior and marine grade plywood coated with resin. One of the side plates was made of transparent acrylic plastic in the aft sump area to permit observation of oil movement with underwater video.

The inclining sump inlet was designed for operation with a hydraulic jump as the basic energy dissipation mechanism and the other mechanism (arrays of vertical and inclined rods and the porous plate assembly) were constructed as bolt-on modifications.

The stability control system utilized a cable and pulley system to control gate position allowing the gain to be adjusted in three increments (1.2/1, 2.5/1 and 2.8/1) and the gate position to be remotely adjusted during testing. The float was a fiberglassed polyurethane foam module with approximately 2,670 N (600 pounds) buoyancy and 91 N/cm (52 poinds/inch) stiffness. It was made intentionally oversize to reduce hysteresis due to friction in the cable mechanism at the highest gain setting.

The model was supported from a free floating catamaran work platform and pivoted above the sump inlet.* The catamaran work platform was constructed from two 34-feet Sea and Air Products, Inc. Flattop Catamaran Hulls

---

* Provision was made for pivoting 76 cm (30 inches) aft of the sump inlet as well, but this arrangement was not tested.

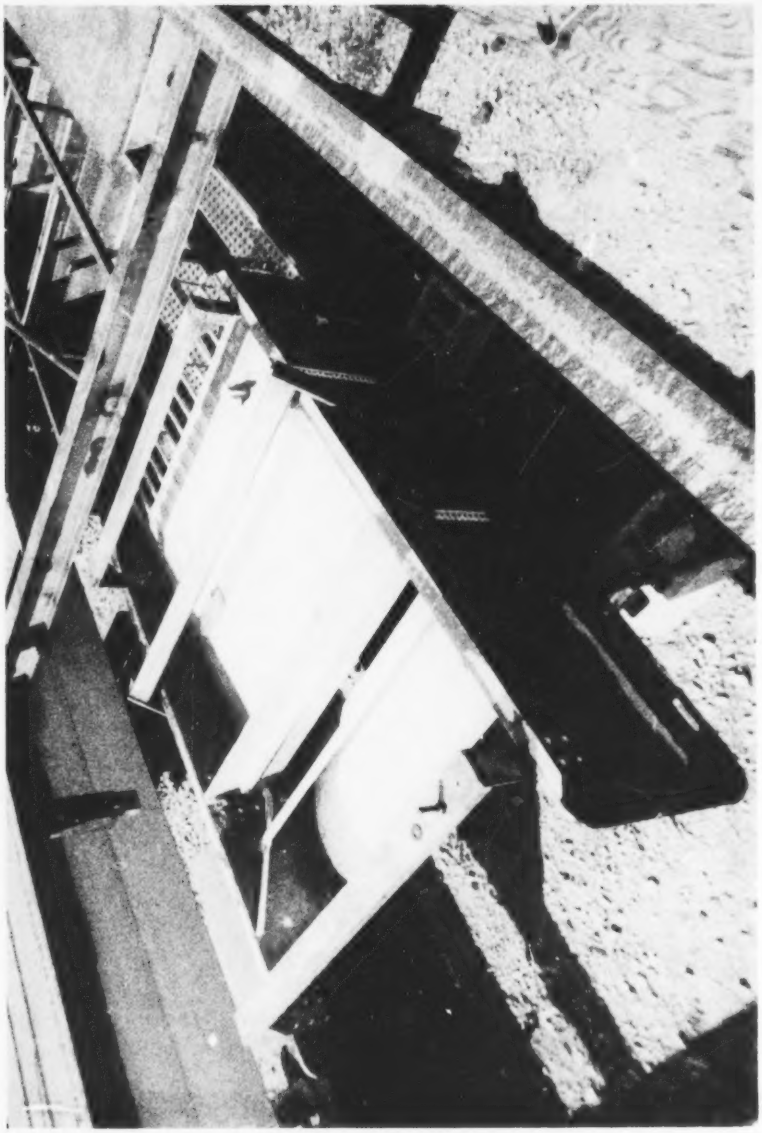

Figure 28. Streamlined oil boom model for System Integration Tests.

connected together with four wide flange steel beams and decked with 1.9 cm (0.75 inch) thick plywood to form a U-shaped 6.1 m (20 feet) wide working platform. The two hulls provided ample buoyancy and 1,300 N/cm (750 pounds/inch) flotation stiffness. Since the minimum required for a 1.5 m (5 feet) wide streamlined oil boom module was calculated to be 242 N/cm (140 pounds/inch), these hulls provide a factor of safety greater than 5.

The streamlined oil boom module and catamaran work platform together form a high-speed skimming craft. Figures 29 and 30 show how it was rigged for testing in the OHMSETT channel. The catamaran was towed between the main bridge and truss near one side of the channel with the video truss in the center so oil flow in the sump could be observed through the clear plastic sideplate. Oil was distributed approximately 15 m (50 feet) ahead of the model through a distribution manifold suspended 0.6 m (2 feet) above the water surface and cascaded onto the surface over an inclined plywood sheet. For the majority of tests the oil slick was constrained by trailing ropes into a 1.2 m (4 feet) wide surface slick thus ensuring essentially 100 percent encounter efficiency.* On two tests the ropes were removed and replaced by diversionary boom stretched from the oil distribution manifold to the streamlined oil boom side plates. The diversionary booms were of the conventional type with a 30 cm (1 foot) draft and were inclined at 6 degree angles to the tow direction to divert a 3.7 m (12 feet) wide oil slick into the streamlined oil boom working section.

Oil was recovered from the secondary sump through two 7.5 cm (3 inch) hoses feeding two air operated double diaphragm pumps mounted on the catamaran. The pump discharges were manifolded together and pumped through a 10 cm (4 inch) discharge hose to a series of 378 l (100 gallon) recovery barrels on the rear truss.

TEST PROCEDURES

Three types of tests were run over a range of operating conditions to adjust hydrodynamic parameters and measure the system's performance in retaining and recovering oil:

- Stability tests
- Holding tests
- System tests

The following is a brief description of the purposes and procedures used for these tests. The detailed test procedures are shown in Appendix B.

---

* Encounter efficiency is the ratio of the oil volume encountering the streamlined oil boom active section to the oil volume distributed upstream.

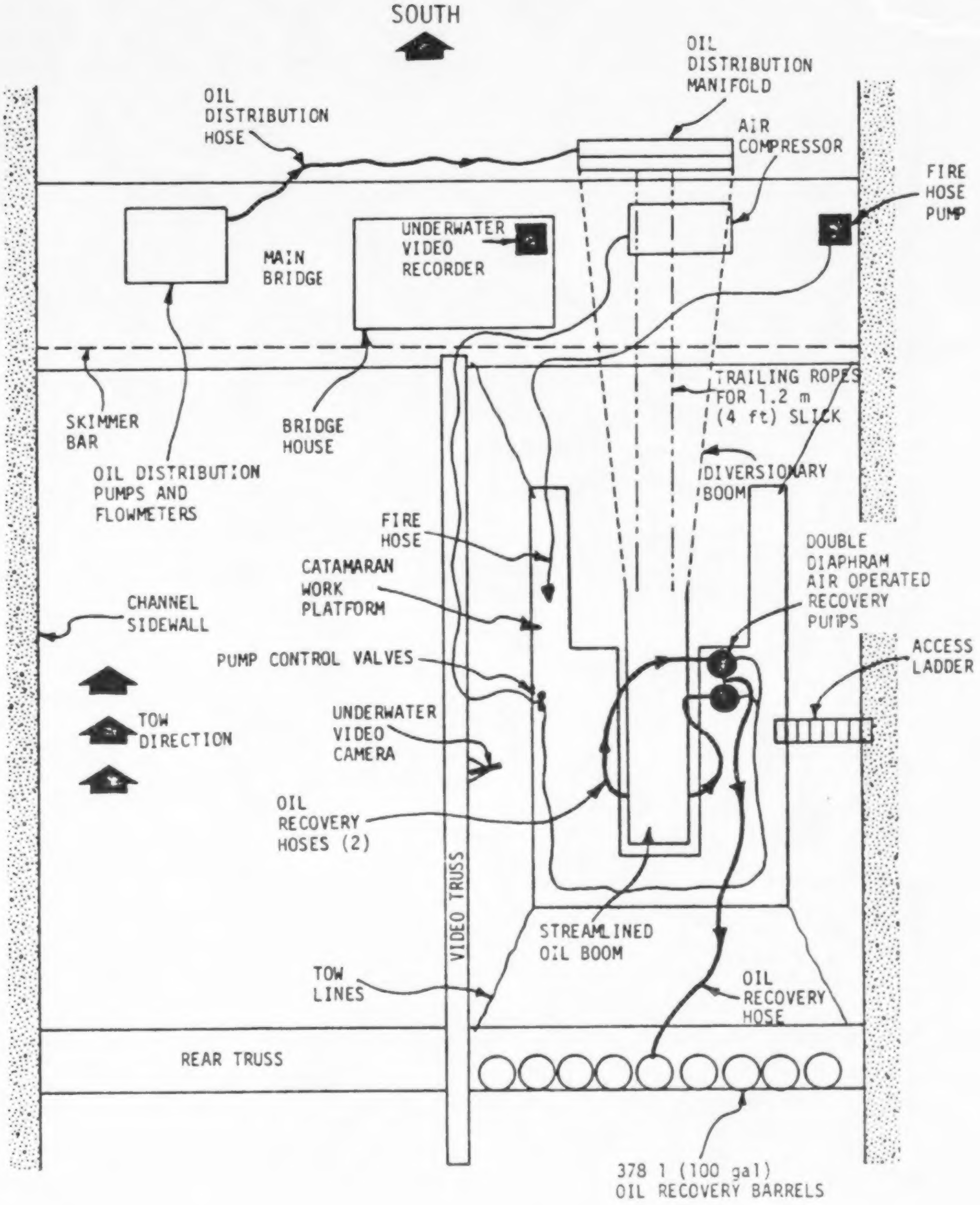
SOUTH
OIL DISTRIBUTION MANIFOLD
OIL DISTRIBUTION HOSE
AIR COMPRESSOR
FIRE HOSE PUMP
UNDERWATER VIDEO RECORDER
MAIN BRIDGE
SKIMMER BAR
BRIDGE HOUSE
OIL DISTRIBUTION PUMPS AND FLOWMETERS
TRAILING ROPES FOR 1.2 m (4 ft) SLICK
DIVERSIONARY BOOM
FIRE HOSE
CATAMARAN WORK PLATFORM
DOUBLE DIAPHRAM AIR OPERATED RECOVERY PUMPS
CHANNEL SIDEWALL
ACCESS LADDER
PUMP CONTROL VALVES
TOW DIRECTION
UNDERWATER VIDEO CAMERA
OIL RECOVERY HOSES (2)
VIDEO TRUSS
STREAMLINED OIL BOOM
TOW LINES
OIL RECOVERY HOSE
REAR TRUSS
378 l (100 gal) OIL RECOVERY BARRELS

Figure 29. Plan view of OHMSETT testing arrangement - 1976.

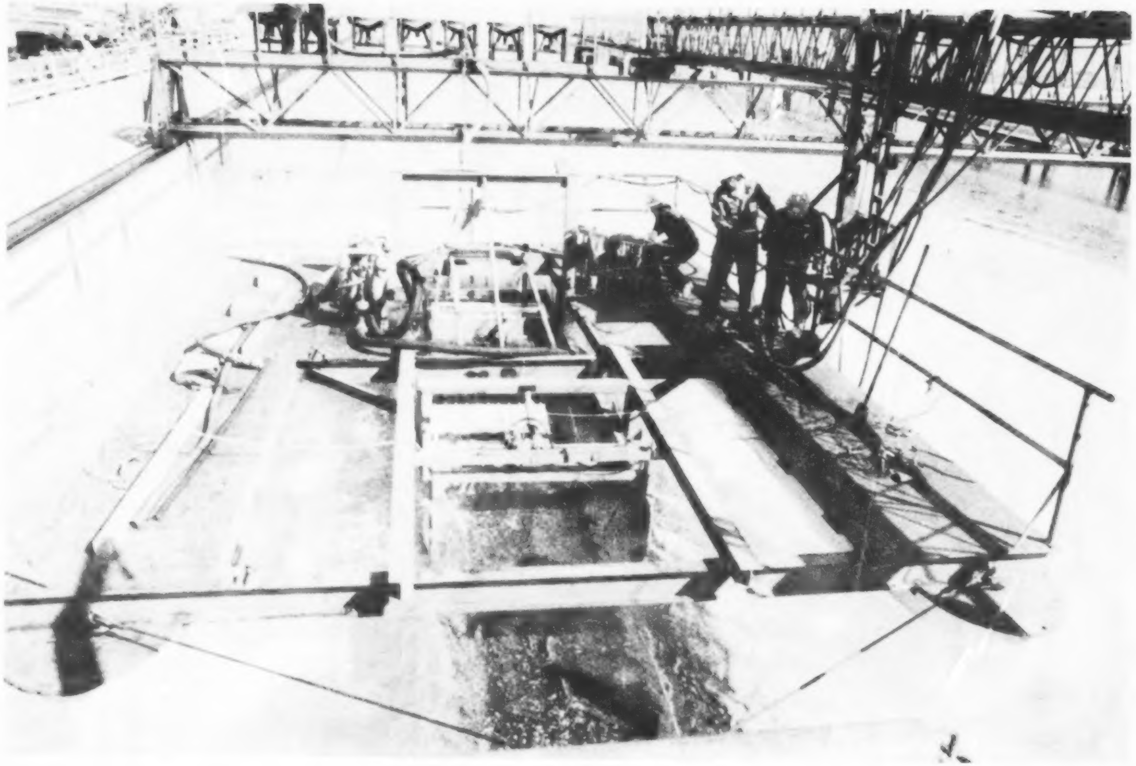

Figure 30. Streamlined oil boom in system test at OHMSETT.

Stability Tests

Stability tests were run without oil to monitor the operation of the stability control system and adjust control system variables for optimum stability. Although the stability control system had been previously tested on 1/3-scale, additional full-scale tests were required to tune operation to the OHMSETT test conditions and provide full-scale stability data. The variables adjusted included:

- Freeboard at sump inlet
- Gate position
- Gain
- Damping
- Aft buoyancy

The freeboard at the sump inlet and sump depth were remotely adjustable during the tests. The freeboard was fixed by the position of an electrically powered linear actuator controlled by a catamaran mounted switch. The sump depth was controlled by the position of the sliding gate regulating flow out of the plenum. The lenth of the cable controlling the gate motion was adjustable through a winch mechanism mounted on the catamaran deck. These two remote adjustments greatly simplified the stability testing procedure since the proper adjustments could be made during the tests rather than setting the adjustments and conducting a series of tests by trial and error. The gain, damping and aft buoyancy were not remotely adjustable and were set at the desired values prior to each test.

The stability test procedure allowed the operation of the stability control system to be observed and the hydrodynamic parameters to be measured under static and dynamic conditions. The control system variables were first adjusted to the desired values under static conditions and the water levels at various stations on the model were recorded. The catamaran was then accelerated to test speed and the operation of the control system was observed. The freeboard and sump depths were adjusted as required and when a stable equilibrium was achieved the water levels, model trim and velocities in the sump and plenum exit were recorded. The model was then decelerated to a stop and returned to its initial position.

Comparison of static and dynamic measurement data allowed the effects of each variable to be determined and the system to be adjusted for optimum operation. Twenty-nine stability tests were run and best results were achieved with the following adjustments:

- Freeboard at sump inlet - adjusted to achieve a 3.8 cm (1.5 inch) layer entering the sump
- Gate position - adjusted to achieve a 38 cm (15 inch) sump depth
- Gain - 3.8/1.0
- Damping - none
- Aft Buoyancy - 1,600 N (360 pounds)

The freeboard and gate position for optimum operation were found to be functions of test speed. The adjustments for best results are shown in Table 3. The highest available gain setting 3.8/1 and zero damping allowed rapid changes in gate position in response to changing sump depth. The sump depth was maintained constant in most tests within ±2.5 cm (±1.0 inch) of the desired value with the gate making exursions of approximately ±10 cm (±4.0 inches).

Aft buoyancy was used to improve the model's trim. At 3.0 m/sec (6 knots), the surface disturbances produced by the streamlined oil boom bow have primary wavelenghts approximately equal to the model's length. This causes the aft portion of the model to ride in a trough and gives the model a positive angle of attack. Adding flotation to the aft portion of the model partially counteracts this trim change.

Oil Tests

The oil tests measured the streamlined oil boom's performance in retaining and recovering oil slicks. Figure 31 shows how oil flows through the streamlined oil boom and identifies the oil loss mechanisms. A portion of an oil slick approaching the streamlined oil boom could be lost around the sideplates. This loss mechanism was reduced essentially to zero in the OHMSETT calm water tests by directing the oil slick between the side plates with trailing ropes. A portion of the oil slick passing between the side plates could also be lost under the sump inlet. Underwater observation at OHMSETT and previous test series confirmed that this loss mechanism was essentially zero under calm water conditions with free surface variations less than 10 cm (4 inches) trough to crest.

The oil and water entering the sump passes through an energy dissipation mechanism where the flow is slowed to 10 percent of its initial velocity. In the process, a portion of the oil slick is mixed with the water in the form of droplets. In the gravity oil/water separation portion of the sump many of these droplets rise to form a reconstituted oil slick which is retained in the sump. Those droplets not rising into the reconstituted slick are lost out the porous bottom. A portion of the surface oil slick may also be lost prior to its recovery by the weir skimmer.

TABLE 3. FREEBOARD AND GATE POSITION ADJUSTMENTS FOR OPTIMUM PERFORMANCE*

	Test Velocity	
Variable	2.0 m/sec (4 knots)	3.0 m/sec (6 Knots)
Freeboard at sump inlet	+1.3 cm (+0.5 in.)	+2.5 cm (+1.0 in.)
Sump depth** for zero slot width	38 cm (15 in.)	43 cm (17 in.)

* These adjustments give approximately 3.8 cm (1.5 in.) layer skimmed into the sump measured at the sump inlet and 38 cm (15 in.) sump depth measured at the weir skimmer.

** Sump depth measured at center of stability control system float.

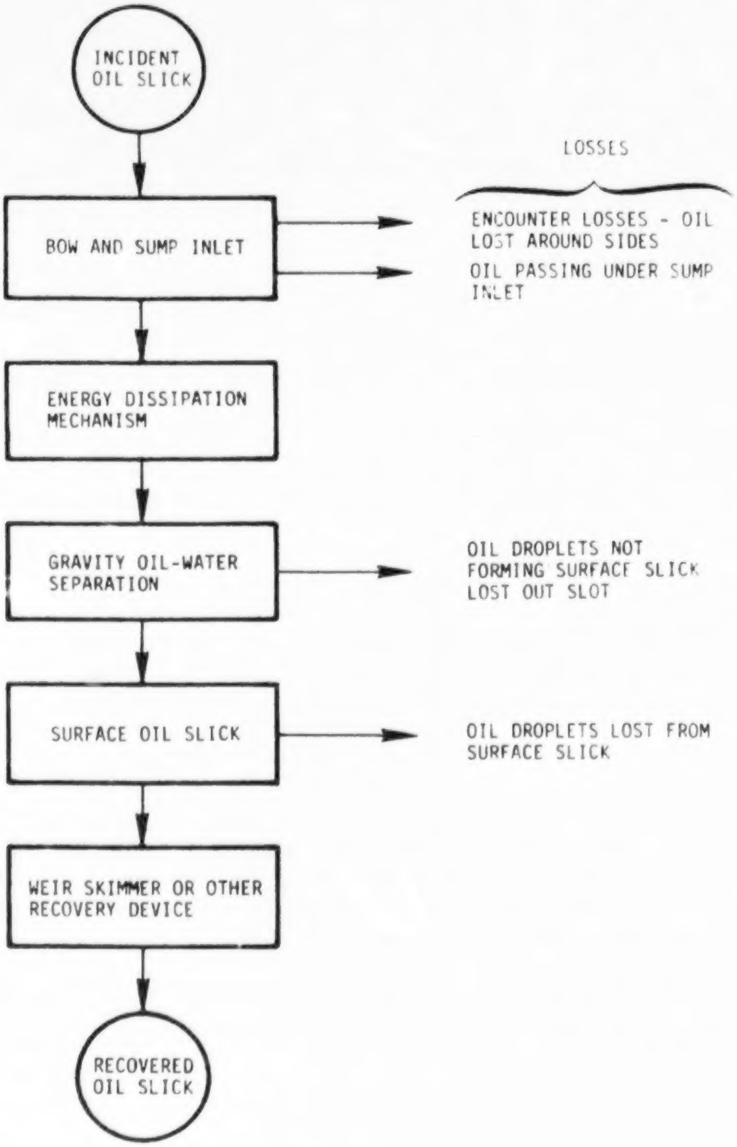
INCIDENT OIL SLICK
LOSSES
BOW AND SUMP INLET
ENCOUNTER LOSSES - OIL LOST AROUND SIDES
OIL PASSING UNDER SUMP INLET
ENERGY DISSIPATION MECHANISM
GRAVITY OIL-WATER SEPARATION
OIL DROPLETS NOT FORMING SURFACE SLICK LOST OUT SLOT
SURFACE OIL SLICK
OIL DROPLETS LOST FROM SURFACE SLICK
WEIR SKIMMER OR OTHER RECOVERY DEVICE
RECOVERED OIL SLICK

Figure 31. Oil flow through streamlined oil boom system.

Losses from the oil slick in the sump were measured in the holding tests. A measured volume of oil was deposited directly into the sump with the model stationary. The model was then accelerated to test speed, towed the length of the channel and decelerated to a stop. The recovery pumps were then started and the oil retained in the sump (and some water) was pumped into recovery barrels. The volume of the recovered oil was measured, corrected for water content and compared to the initial preload to determine the magnitude of the losses.

Systems tests measured the performance of all portions of the streamlined oil boom operating as a system recovering oil slicks at high speed. To reduce starting transients and simulate equilibrium conditions the sump was preloaded with oil similar to the holding tests. The model was accelerated to test speed. Then an oil slick was distributed ahead of the model and the recovery pumps were operated simultaneously. Oil was distributed for a predetermined time period corresponding to an oil slick approximately 100 m (325 feet) long and the recovery pumps were operated until the last of the oil slick entered the sump. The model was then decelerated to a stop. The total volume of oil and water pumped into the recovery barrels during the test was measured and divided by the recovery pump operation time to determine the recovery flowrate. Next any oil remaining in the weir box, hoses and pumps was flushed into the recoery barrels. The volume of the recovered oil was measured and corrected for water content. The recovery efficiency was calculated as the ratio of the oil volume recovered to the total oil and water volume pumped into the recovery barrels during the run. The oil volume retained in the sump was also measured as in the holding tests to complete the oil inventory. Tests where the initial and final sump oil volumes were essentially equal were considered to be equilibrium.

TEST RESULTS

Test Conditions

Following a series of stability tests where the system was adjusted for optimum hydrodynamic performance 23 oil tests were run with two test oil, calm and random wave conditions and at two tow speeds.

The test oil characteristics are listed in Table 4. The lube oil was used for the majority of the tests and was similar to a 30 wt non-detergent lubricating oil with viscosity similar to number two fuel oil and interfacial surface tension modified with a surfactant to approximate number two fuel oil.

Tests were conducted in both calm and "1 foot harbor chop" surface conditions. During the calm water tests the OHMSETT wave generator was not operated and the only surface disturbances were those caused by wind. Under some conditions, these waves approached 5 cm (2 inches) trough to crest.* The 1 foot harbor chop is a standard wave pattern used to test oil spill control equipment at OHMSETT. Waves are produced by two hydraulically powered wave flaps spanning at the south end of the tank. The flaps are pivoted at the bottom and extend well above the water line. The 1 foot harbor chop was produced by driving these flaps out of phase at 35 rpm with a 3.8 cm (1.5 inch) stroke. The wave generator was operated for 10 minutes prior to the test to allow a semi-random confused wave state to build up.

The characteristics of the 1 foot harbor chop were measured by the OHMSETT facility operator prior to the Streamlined Oil Boom Tests. A wave probe was mounted in approximately the center of the tank and the free surface oscillations were recorded on an analog tape recorder. The analog

TABLE 4. TEST OIL PROPERTIES

Parameter	Lube Oil	#2 Simulant	Units
Viscosity	144.8	32.5	centistokes @ 70°F
Specific gravity	0.871	0.850	relative to water
Surface tension	31.5	30.2	dynes/cm
Interfacial surface tension	11.8	10.3	dynes/cm
Water and sediment	0.1	0.1	percent

---

* Estimated.

tape was played back on a Precision Instrument Tape Recorder, the signal was filtered to eliminate noise and the data was processed digitally. The results of the analysis on six data runs are shown in Table 5 and show the average wave height to be approximately 15 cm (6 inches) with the average 1/3 highest and average 1/10 highest wave heights approximately 23 and 30 cm (9 and 12 inches) respectively.

During the streamlined oil boom wave tests with the 1 foot harbor chop, the characteristics of the waves were observed to vary with position in the tank. Near the north end of the tank (opposite end from the wave generator) nearly standing waves with trough to crest heights of approximately 0.6 m (2 feet) were observed with substantially smaller waves along the tank centerline a few meters from the north end. Consequently, the wave data in Table 5 should be considered only a rough indication of the 1 foot harbor chop wave environment.

Two towing speeds were used - 3.0 and 2.0 m/sec (6 and 4 knots). Three m/sec (6 knots) was the highest tow speed available at OHMSETT and was used for a majority of the tests. The 203 m (667 feet) OHMSETT tank length allowed approximately 30 seconds constant speed running time at 3.0 m/sec (6 knots) and 45 seconds constant speed running time at 2.0 m/sec (4 knots) after allowing for acceleration, deceleration and the space between the two bridges. Two m/sec (4 knots) was chosen as the slower test speed because the dynamic pressure at 2.0 m/sec (4 knots) is roughly half of the dynamic pressure at 3.0 m/sec (6 knots).

TABLE 5. AVERAGE WAVE HEIGHTS IN OHMSETT'S "1.0 FOOT HARBOR CHOP"

	Wave Heights in Inches		
Run	Average	1/3 Highest	1/10 Highest
K-18	5.691	8.828	10.959
K-19	6.613	9.659	12.059
K-22	5.129	8.195	10.626
L-25	5.977	9.598	12.345
L-28	6.659	10.562	13.091
K-40	5.807	8.904	11.359
Average	5.904	9.291	11.740
Standard Deviation	0.509	0.826	0.926

NOTE: Data from OHMSETT Facility operated - Mason and Hanger - Silas Mason Co., Inc.

Efficiency Calculations

The streamlined oil boom's performance in these oil tests may be described in terms of thruput and recovery efficiencies. Thruput efficiency is an index of the overall performances and is defined as the ratio of oil volume recovered to oil volume distributed. In the holding tests the thruput efficiency η_T is defined as:

$$\eta_T = \frac{V_F}{V_p} \quad \text{(expressed as percent)}$$

where:

V_F = final oil volume contained in sump and weir box at the end of the test

V_p = preloaded oil volume

This thruput efficiciency is a measure of the streamlined oil boom's performance in retaining oil in the sump. If η_T = 100 all of the oil initially preloaded into the sump was retained and if η_T = 0 it was all lost.

In the system's tests, the thruput efficiency must be corrected to account for changes in sump oil volume as follows:

$$\eta_T = \frac{V_R + V_F - V_P}{V_S} \quad \text{(expressed as percent)}$$

where:

V_R = volume of oil recovered over the weir during the test

V_S = volume of oil slick distributed.

If η_T = 100, no oil was lost; all was either recovered over the weir or retained in the sump. If $V_F = V_p$ the test operated essentially at equilibrium and the thruput efficiency reduces to the ratio of oil volume recovered to oil volume distributed. Thruput efficiencies less than zero are also possible in cases where the sum of the final sump oil volume and volume of oil recovered over the weir is less than the initial preload.

Recovery efficiency η_R is defined as the concentration of oil in the recovered oil/water mixture:

$$\eta_R = \frac{V_R}{V_T} \quad \text{(expressed as percent)}$$

where:

V_T = the total volume of oil and water recovered.
Recovery efficiency was calculated for the system tests only.

Appendix C discusses the oil handling procedures used in these tests and the probable experimental error associated with oil volume measurements. Based on Appendix C, the calculated values of thruput and recovery efficiencies are probably within a range of +15 to -10 percent. The range of experimental error is larger on the plus side since some losses of recovered oil before measurement were inevitable.

Test Data

The numerical results from the 23 oil tests are shown in Table 6. Overall the tests demonstrated good performance at both 2.0 and 3.0 m/sec (4 and 6 knots) testing speeds under calm water conditions. In the system tests thruput efficiencies as high as 99+ percent and 87 percent were observed at 2.0 m/sec (4 knots) and 3.0 m/sec (6 knots) repectively and losses in the holding tests were minimal. As expected, thruput efficiencies degraded in waves but in holding tests a high percentage of the initial preload was retained.

The first six tests compared the performance of three energy dissipation options under similar 3.0 m/sec (6 knots) test conditions with lube oil. A holding test with a 283 l (75 gallon) preload and a system test with a 151 l (40 gallon) preload and a 2.5 mm thick oil slick were run on each on each option.* The results shown in Table 6 demonstrate that each design performed well with thruput efficiencies for both holding and system tests in the range of 80 to 88 percent. Oil losses in the holding tests appeared to be caused by starting and stopping transients rather than losses during the constant speed portion of the test. During acceleration, the oil slick sloshed toward the aft portion of the sump with some flowing into the float chamber and some undoubtedly lost out the porous bottom. During deceleration, the oil slick sloshed forward toward the sump inlet. Although a pivoting door was deployed across the sump inlet during deceleration, at the end of each test some oil was usually observed to escape. These losses could easily total 38 to 57 l (10 to 15 gallons), and be responsible for the entire losses observed in the holding tests. If the oil lost in the holding tests is assumed to be due entirely to transient phenomena and the thruput efficiencies on the thruput tests are corrected for these losses, the thruput efficiences for system tests 4, 5 and 6 would be 96.1, 98.6 and 99.6 percent respectively. Since each energy dissipation mechanism performed equally well and since the expanded metal incline was expected to perform best in other tests and to be relatively free from clogging problems, it was used for the remainder of the tests.

Tests 6-9 are 3.0 m/sec (6 knot) calm surface systems tests with the expanded metal incline over a range of slick thicknesses with lube oil. Tests 20-22 are similar tests with simulated number two oil. The thruput and

---

* Test input parameters were maintained at approximately these values - variations were due to limitations of the testing procedure.

TABLE 6. OHMSETT SYSTEM INTEGRATION TEST RESULTS

Test Conditions					Oil Input				Oil Recovery				Efficiencies	
						Slick			During Run					
Run No.	Test[1] Type	Oil[2] Type	Tow Speed Knots	Waves[3]	Preload gal.	Thickness mm	Volume gal.	Distribution Rate gal.	Recovery Rate gpm	Oil gal.	Total gal.	Final Sump gal.	Recovery[4] %	Thruput[5] %
1	Holding[6]	Lube	6	Calm	75.0							65.3		87.1
2	Holding[7]	Lube	6	Calm	75.4							64.1		85.0
3	Holding	Lube	6	Calm	74.9							60.2		80.3
4	System[6]	Lube	6	Calm	40.0	2.8	101.1	200.8	175.4	59.1	95.0	68.4	62.2	86.5
5	System[7]	Lube	6	Calm	40.0	2.8	99.9	198.5	178.2	54.2	98.0	73.0	55.3	87.3
6	System	Lube	6	Calm	40.5	2.5	89.4	176.5	128.4	40.3	68.0	74.5	59.3	83.1
7	System	Lube	6	Calm	40.0	1.1	41.5	81.8	80.5	22.8	44.0	49.1	41.8	76.9
8	System	Lube	6	Calm	40.0	3.7	156.8	259.9	237.4	91.8	158.2	45.7	58.0	62.2
9	System	Lube	6	Calm	75.2	2.6	101.9	202.1	249.4	83.4	133.0	71.4	62.7	78.1
10	System[8]	Lube	6	Calm	40.0	0.9	36.5	72.4	97.9	21.7	54.5	24.8	39.8	17.8
11	System[8]	Lube	6	Calm	40.0	2.6	98.9	197.8	227.4	52.5	133.0	28.3	39.5	41.3
12	Holding	Lube	6	1' H.C.	74.9							51.0		68.1
13	System	Lube	6	1' H.C.	40.0	0.9	31.0	60.5	88.8	2.5	51.5	10.3	4.9	neg.
14	System	Lube	6	1' H.C.	40.0	2.8	101.3	200.6	220.3	31.3	128.5	21.7	24.4	12.8
15	Holding	Lube	4	Calm	74.9							66.0		88.1
16	System	Lube	4	Calm	40.0	1.4	46.5	69.2	91.4	41.2	71.0	46.5	58.0	99+
17	System	Lube	4	Calm	40.5	4.4	147.9	220.1	239.5	91.4	196.0	70.3	46.6	81.9
18	Holding	Lube	4	1' H.C.	74.9							52.8		70.5
19	System	Lube	4	1' H.C.	40.2	4.6	150.9	101.1	249.3	44.6	182.0	26.8	24.5	20.7
20	System	#2	6	Calm	40.0	0.9	33.0	65.6	94.2	23.6	51.0	33.9	46.3	53.0
21	System	#2	6	Calm	39.5	3.2	115.9	231.8	266.9	54.8	145.0	61.7	37.8	66.4
22	System	#2	6	Calm	74.9	5.0	188.8	375.7	294.2	91.3	153.0	90.0	59.7	56.4
23	System	#2	4	Calm	41.2	1.6	52.2	78.0	90.0	28.9	65.0	52.6	44.5	77.2

1. Inclined porous plate energy dissipation method unless otherwise stated.
2. Average oil characteristics - lube: viscosity = 145 centistoke @ 70°F, specific gravity = 0.87, simulated #2 (a lube oil with surfactant added to approximate #2 fuel oil): viscosity = 32 centistoke @ 70°F, specific gravity = 0.85.
3. Surface condition - calm no waves generated some wind induced surface chop estimated at up to 2 inch trough to crest, 1' H.C. = 1.0 feet harbor chop semi-random wave condition.
4. Recovery efficiency = oil volume recovered/total volume recovered.
5. Thruput efficiency for system tests = oil volume recovered during run plus final sump oil volume minus oil preload volume divided by oil volume distributed. Thruput efficiency for holding tests = final sump oil volume divided by oil preload volume.
6. Energy dissipation method: 45° array of rods.
7. Energy dissipation method: 90° array of rods.
8. With diversionary boom (see text).

recovery efficiencies for these tests are plotted against slick thickness in Figure 32. Thruput efficiencies with the higher viscosity lube oil were generally superior to the simulated number two oil. The higher viscosity oil offers more resistance to shearing in the turbulent energy dissipation process producing larger oil droplets which can be recovered more easily in the gravity separation portion of the sump. Thruput and recovery efficiencies were relatively insensitive to slick thickness. The limited number of tests and the probable experimental error range of +15 and -10 percent make if difficult to accurately assess the effects of slick thickness. The 1.0 to 5.0 mm oil slick thickness corresponds to 2.6 to 13.0 percent of the total sump flowrate, at most a small percentage. Losses due to oil passing under the sump inlet would not be expected under calm conditions unless this percentage were near 100 percent.

Recovery efficiencies for these tests were in the range of 37 to 63 percent. Thus the flow passing over the weir was roughly half oil and half water. Recovery efficiency should increase with the volume of oil contained in the sump (the oil layer thickness) and decrease as recovery flowrate increases. However, the range of values covered in the experiments is not large enough to demonstrate these relationships.

Tests numbers 10 and 11 were 3.0 m/sec (6 knot) calm surface system tests where a 3.7 m (12 feet) wide lube oil slick was diverted into the streamlined oil boom active section with conventional diversionary boom deployed at slight angles to the tow direction. The diversionary angle was chosen as 5.7 degrees so that the component of velocity normal to the divertionary boom was 0.3 m/sec (0.6 knots). Since conventional oil booms operate satisfactorily with normal components of velocity up to this value, the diversionary boom was expected to divert the oil slick into the streamlined oil boom without the usual droplet entrainment and drainage failure mechanisms.

The flow patterns observed in these tests are shown in Figure 33. The leading edge of each diversionary boom produced a substantial turbulent breaking bow wave. The bow waves between the booms intersected approximately midway along the boom lenth and reflected from the opposite sides about 2 m (7 feet) upstream of the bow. The resulting diamond shaped wave patterns significantly affected the oil slick. The overall result was a channeling of the slick between the streamlined oil boom sideplates with no visible losses due to diversionary boom failure. However, the breaking waves also entrained a substantial portion of the slick beneath the surface and produced a frothy turbulent flow at the sump inlet. This accounts for the significantly lower thruput efficiencies achieved in tests 10 and 11. Comparing these results to similar 3.0 m/sec (6 knot) calm surface tests where no oil diversion was involved shows that thruput efficiency dropped from 83 to 41 percent for a 2.5 mm slick and from 77 to 18 percent for a 1 mm slick.

Tests 15-17 and 23 are 2.0 m/sec (4 knot) calm surface tests and demonstrate improved performance over the 3.0 m/sec (6 knot) tests. The kinetic evergy dissipated in the sump at 2.0 m/sec (4 knots) is only half that dissipated at 3.0 m/sec (6 knot) and as a result the breakup of the oil slick into small droplets, the principle loss mechanism was significantly reduced

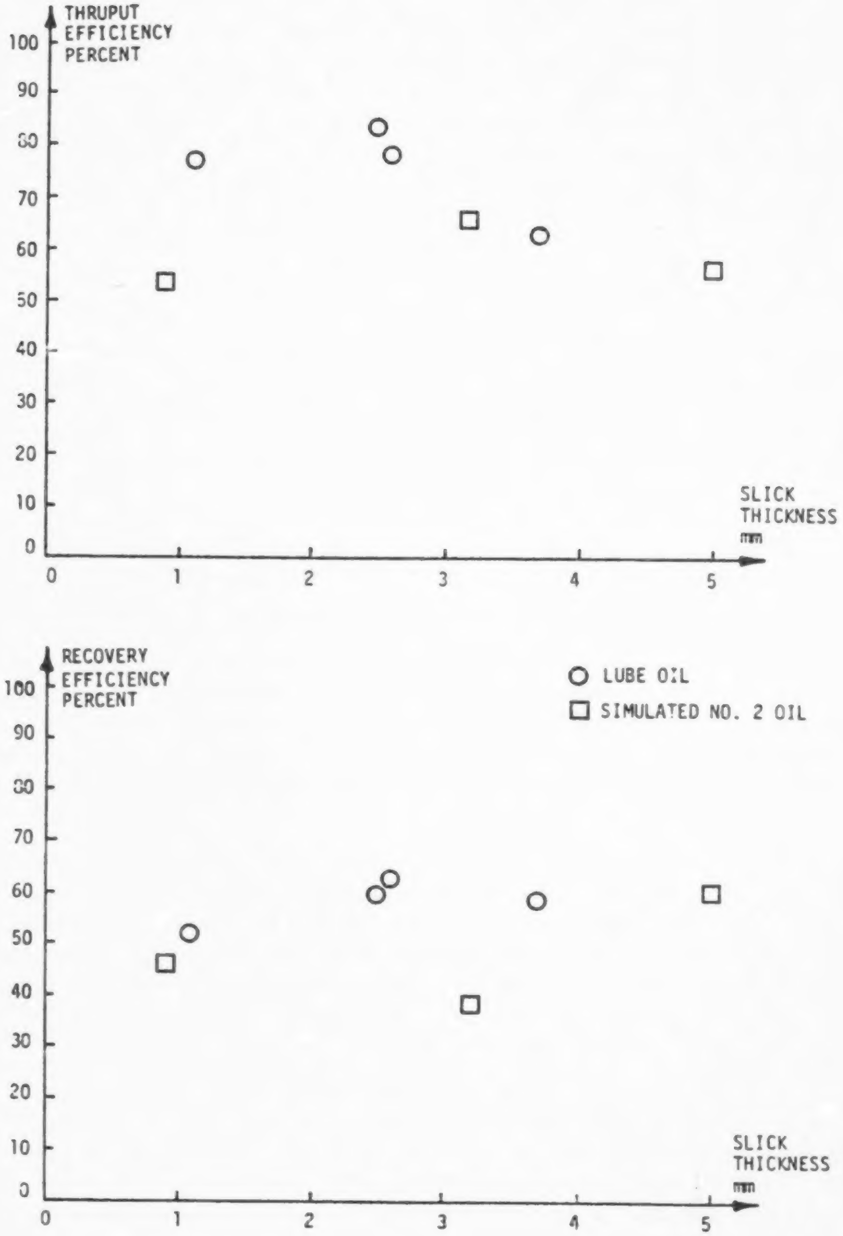

Figure 32. System Tests Results - Calm Surface at 3.0 m/sec (6 knots)

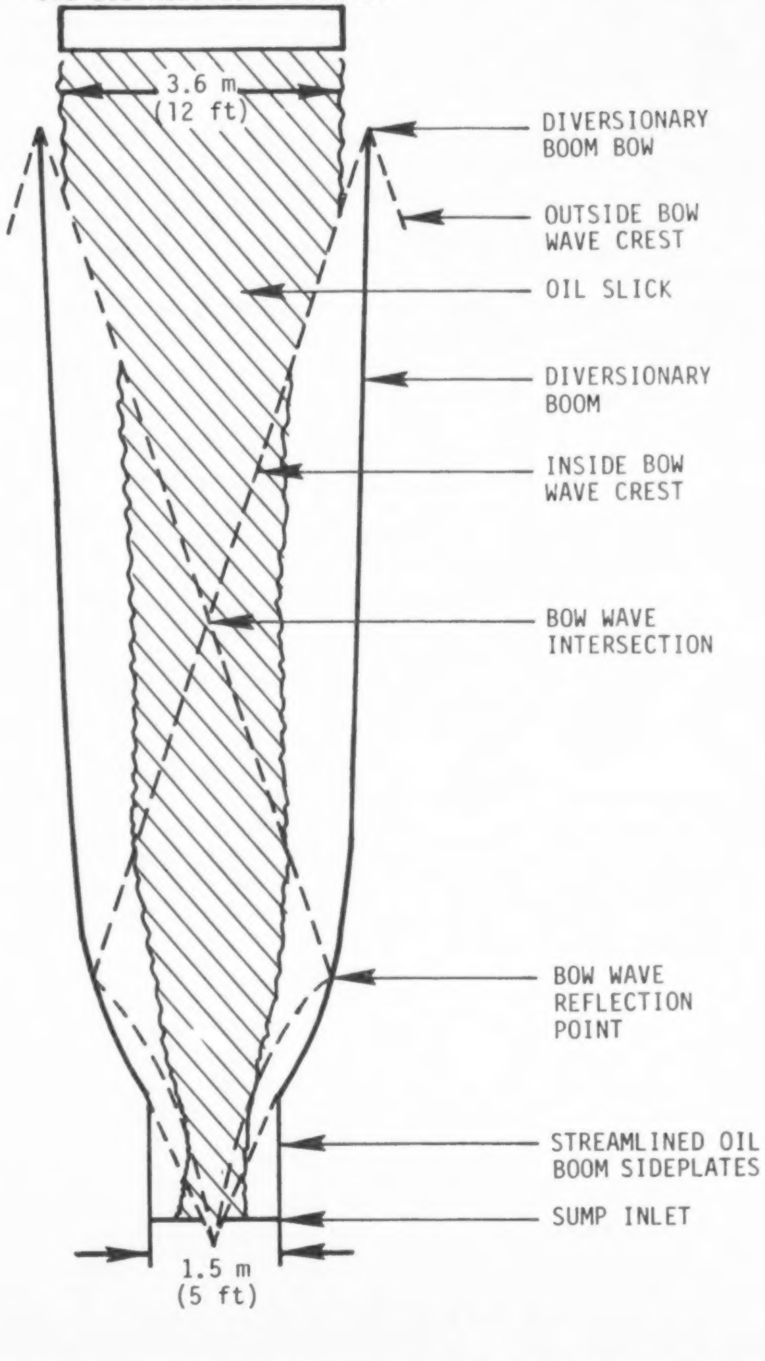
OIL DISTRIBUTION MANIFOLD
3.6 m
(12 ft)
DIVERSIONARY BOOM BOW
OUTSIDE BOW WAVE CREST
OIL SLICK
DIVERSIONARY BOOM
INSIDE BOW WAVE CREST
BOW WAVE INTERSECTION
BOW WAVE REFLECTION POINT
STREAMLINED OIL BOOM SIDEPLATES
SUMP INLET
1.5 m
(5 ft)

Figure 33. System Tests with Diversionary Boom - Flow Pattern

resulting in higher thruput efficienicies. Figure 34 shows the thruput and recovery efficiencies plotted against slick thickness and can be compared to the similar 3.0 m/sec (6 knot) plots in Figure 32. Again, there is insufficient data to determine a trend but the efficiencies at 2.0 m/sec (4 knot) thruput are clearly higher than at 3.0 m/sec (6 knots).

The streamlined oil boom was designed to operate in calm and relatively low wave conditions typical of small rivers, lakes and other inland waterways where the maximum free surface excursions do no exceed about 15 cm (6 inches) trough to crest. Ideally, the wave tests at OHMSETT should have included several wave states both below and above this threshold. Unfortunately the smallest random wave state available at OHMSETT without a lengthy calibration procedure was the 1 foot harbor chop with an average 1/10 highest wave height of 30 cm (1 foot) trough to crest. Since the streamlined oil boom relies on skimming a thin layer of oil and water into the sump, performance in this wave state was expected to be poor.

Tests 12 to 14 were the 3.0 m/sec (6 knot) wave tests and tests 18 and 19 were the 2.0 m/sec (4 knot) wave tests. Comparing these data with similar calm water data shows that thruput efficiencies were reduced from calm surface values of 60-100 percent to 0-20 percent. Some of the losses were due to oil passing around the side plates since the slick was not effectively contained by the trailing ropes. Other losses occured as the wave trough (and some oil) passed under the sump inlet and also due to wave action in the sump. The impact of the wave crests passing into the sump caused substantial splashing and agitation in the sump. In test 13 one large wave swamped the sump shortly after the test begain, causing the entire sump preload to be lost.

In summary, performance degraded significantly in the wave tests. However, this wave environment was much more severe than the maximum 15 cm (6 inch) free surface excursions for which the streamlined oil boom was designed. The reduction in performance in these tests demonstrates that the streamlined oil boom is not suitable for large harbors, bays and other areas where theses larger waves occur.

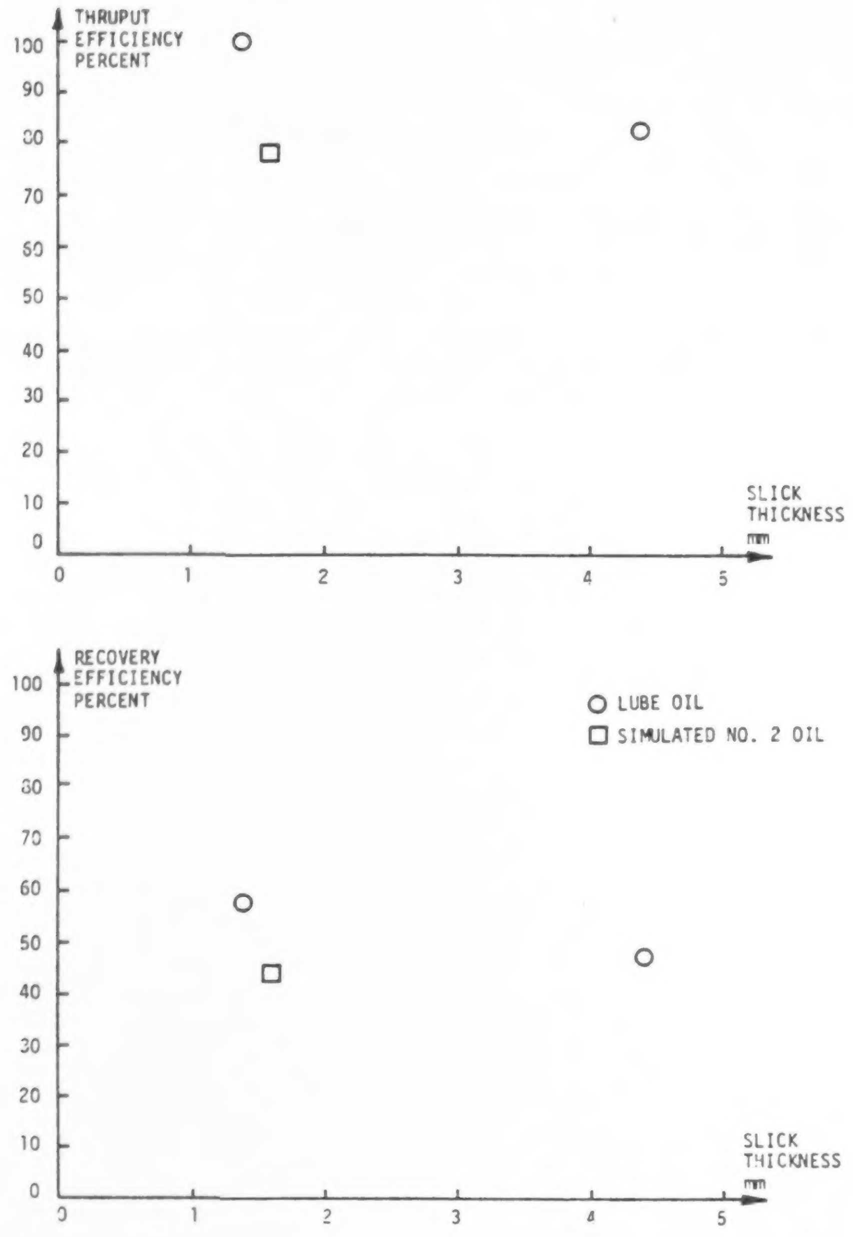

Figure 34. System Tests Results - Calm Water at 2.0 m/sec (4 knots)

REFERENCES

1. Dorrler, J. Stephen, Ray Ayers, and David C. Wooten 1975. High Current Control of Floating Oil, *1975 Conference on Prevention and Control of Oil Pollution*, March 25-27, 1975.

2. Folsom, B.A. and C. Johnson 1977. Development of a High Current Streamlined Oil Boom/Skimmer for Inland Waterways, *1977 Oil Spill Conference Proceedings*, March 5-10, 1977.

3. Wooten, David C. 1973. Mechanical Control of Oil Spills Utilizing a Streamlined Boom, *1973 Conference on Prevention and Control of Oil Spills*, March 13-15, 1973.

4. Wooten, D.C. and B.A. Folsom 1975. "Bow Wave Hydrodynamics for a Slightly Submerged Hydrofoil at Low Froude Numbers", presented at American Society of Civil Engineers, Hydraulics Division, 23rd Annual Hydraulics Division Specialty Conference, Seattle, Washington, August 6-8, 1975.

APPENDIX A

PHENOMENOLOGICAL BOW WAVE THEORY

This appendix discusses a phenomenological theory describing flow over the upper surface of a slightly submerged hydrofoil at low Froude number with smooth and turbulent bow waves where both inertial and gravity forces are important. The theory is phenomenological in that it does not predict flow conditions per se but merely assumes that the flow behaves with the same phenomena as open channel flow over a complex contour.

The flow passing over the hydrofoil was assumed to be totally separated from flow passing beneath the hydrofoil by an impermeable frictionless boundary consisting of the stagnation streamline and the upper surface of the hydrofoil. Flow over the contour was assumed to meet the requirements of frictionless open channel flow and the equation of continuity, energy and momentum were applied to determine the location of the stagnation streamline and free surface at several well defined stations.

The following assumptions were made to simplify the analysis:

- Two-dimensional flow
- Neglect surface tension forces
- Neglect viscous forces
- Assume the velocity to be horizontal everywhere
- Assume all energy loss occurs in a hydraulic jump of infinitesimal length

The two-dimensional flow assumption requires that the hydrofoil shape be the same at every section and that the velocity of the flow approaching the hydrofoil be uniformly constant.

Neglecting surface tension effects is a reasonable assumption for the streamlined oil boom application since they are responsible for capillary waves and other small scale effects not important here.

Neglecting viscous forces is justified if the boundary layer thickness produced by these forces is small compared to the total flow depth passing over the hydrofoil. Boundary layer thickness starts at zero where the stagnation streamline intersects the hydrofoil and increases as flow moves downstream. Since the flow is accelerating up to the top of the hydrofoil, the boundary layer is thin in this region but increases in thickness downstream.

Although the velocity is clearly not horizontal everywhere, the important factors for this analysis are the reduction in dynamic pressure due to the neglected vertical velocity component and the pressures produced by curving streamlines. Since the error in dynamic pressure introduced by neglecting the vertical component is proportional to the square of the sine of the inclination of the total velocity vector from the horizontal, an 18° inclination will reduce the dynamic pressure by less than 10 percent. The pressure produced by curving streamlines is a function of the radius of curvature and is small when the radius of curvature is large compared to the thickness of flow passing over the hydrofoil.

Flow over a hydrofoil with a turbulent bow wave modeled by a hydraulic jump is shown in Figure A-1. A Froude number* based on the local flow conditions can be defined at several stations:

$$F_i = \frac{V_i}{\sqrt{gY_i}}$$

where F_i, V_i and Y_i are the local values of Froude number, velocity and flow depth respectively and g is the acceleration of gravity. Station 1 is the undisturbed flow far upstream and consequently V_1 is the freestream velocity and Y_1 is the thickness of the layer skimmed over the hydrofoil. A hydraulic jump modeling a turbulent bow wave is assumed to form over the horizontal stagnation streamline with Station 1 upstream and Station 2 downstream. The characteristics of a hydraulic jump require that the local Froude number upstream be greater than 1.0 (supercritical) and downstream be less than 1.0 (subcritical).

Downstream from Station 2 the flow accelerates continuously and this requires that the Froude number at Station 3, the highest point on the hydrofoil, be equal to 1.0 and the Froude number downstream, Station 4, be greater than 1.0 (supercritical).**

With these assumptions, the flow conditions at stations 1 through 3 can be calculated by applying the usual equations of open channel flow:

$$\text{(1) Continuity:} \quad V_1 Y_1 = V_2 Y_2 = V_3 Y_3 = Q$$

$$\text{(2) Hydraulic Jump:} \quad Y_2/Y_1 = \frac{\left[8 \frac{V_1^2}{gY_1} + 1\right]^{1/2} - 1}{2}$$

---

* Froude number is a dimensionless flow parameter expressing (the square root of) the ratio of inertial to gravity forces.

** This is equivalent to saying that the flow over the hydrofoil is not affected by the downstream conditions, observed to be true in applications skimming thin layers.

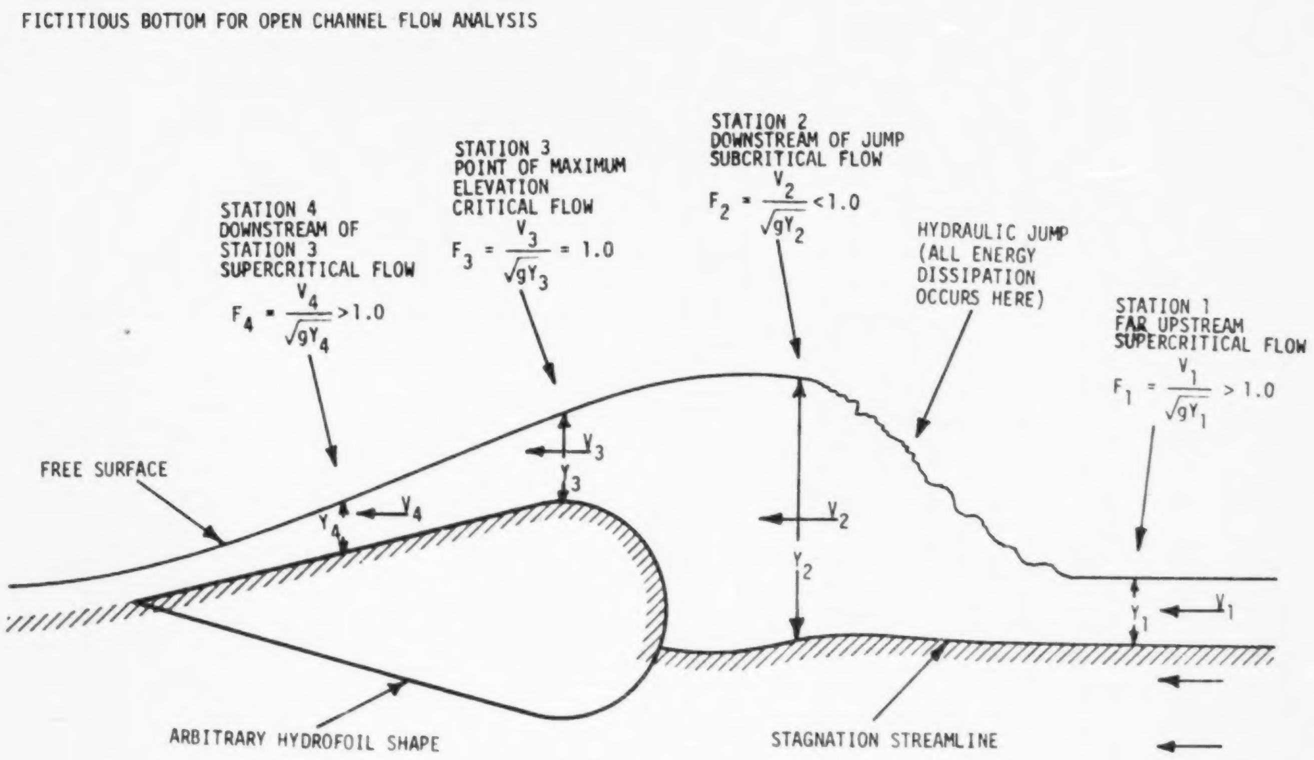
FICTITIOUS BOTTOM FOR OPEN CHANNEL FLOW ANALYSIS
STATION 4
DOWNSTREAM OF
STATION 3
SUPERCRITICAL FLOW
$F_4 = \frac{V_4}{\sqrt{gY_4}} > 1.0$
STATION 3
POINT OF MAXIMUM
ELEVATION
CRITICAL FLOW
$F_3 = \frac{V_3}{\sqrt{gY_3}} = 1.0$
STATION 2
DOWNSTREAM OF JUMP
SUBCRITICAL FLOW
$F_2 = \frac{V_2}{\sqrt{gY_2}} < 1.0$
HYDRAULIC JUMP
(ALL ENERGY
DISSIPATION
OCCURS HERE)
STATION 1
FAR UPSTREAM
SUPERCRITICAL FLOW
$F_1 = \frac{V_1}{\sqrt{gY_1}} > 1.0$
FREE SURFACE
V_3
Y_3
V_4
Y_4
V_2
Y_2
Y_1
V_1
ARBITRARY HYDROFOIL SHAPE
STAGNATION STREAMLINE

Figure A-1. Turbulent bow wave flow model.

(3) Energy: $\frac{V_2^2}{2g} + Y_2 + h_2 = \frac{V_3^2}{2g} + Y_3 + h_3$

(4) Freeboard Definition: $B = h_3 - (Y_1 + h_1)$

(5) Froude Number at Station 3: $\frac{V_3^2}{gY_3} = 1.0$

where h is the height of the stagnation streamline or top of the hydrofoil above an arbitrary horizontal datum line.

Equation 1 is the continuity equation for two-dimensional open channel flow and Q is the flowrate per unit width. Equation 2 is the relationship expressing the ratio of upstream and downstream flow depths for a hydraulic jump over a level contour and may be derived from momentum and continuity considerations. Equation 3 states that no energy is lost between stations 2 and 3 and Equation 4 defines the freeboard B as the height of the hydrofoil's highest point (at Station 3) above the undisturbed free surface. Equation 5 equates the local Froude number at Station 3 to 1.0 as discussed above.

These five equations can be solved by eliminating the unknown conditions at Station 2 and expressing the conditions at stations 1 and 3 in terms of the freestream velocity V_1 and the freeboard B. The results identify a dimensionless independent parameter:

$$G_B = \frac{gB}{V_1^2}$$

which is the reciprocal of the Froude number squared based on freestream velocity and freeboard. The reciprocal squared form is used so that positive, zero and negative values of B may be considered without resorting to complex or infinite terms. Two dimensionless dependent parameters describe the resulting flow.

$$G_1 = \frac{gY_1}{V_1^2}$$

$$G_3 = \frac{gY_3}{V_1^2}$$

These parameters are also the reciprocal of Froude number squared form. Both utilize the freestream velocity V_1 and the local values of flow depth at stations 1 and 3.

After some manipulation, the results can be expressed as follows:

$$(6)\quad G_B = \frac{2}{-\left[\left(\frac{G_1 + 8}{G_1}\right)^{1/2} - 1\right]^2} + \left[\left(\frac{G_1 + 8}{G_1}\right)^{1/2} - 1\right] G_1 - \frac{3}{2} G_1^{2/3} - G_1$$

$$(7)\quad G_3 = (G_1)^{2/3}$$

$$(8)\quad Q = \frac{G_1 V_1^{3}}{g}$$

Flow over a hydrofoil with a smooth bow wave is shown in Figure A-2. As in the turbulent flow model, this flow is analyzed by applying the equations of open channel flow to the flow above the stagnation streamline and top side of the hydrofoil. However, since there is no energy dissipation, station 2 is nonexistent and the five equations for the turbulent model reduce to:

(9) Continuity: $V_1 Y_1 = V_3 Y_3 = Q$

(10) Energy: $\frac{V_1^2}{2g} + Y_1 + h_1 = \frac{V_3^2}{2g} + Y_3 + h_3$

(11) Freeboard Definition: $B = h_3 - (Y_1 + h_1)$

(12) Froude Number at Station 3: $\frac{V_3^2}{gY_3} = 1.0$

Equation 12, equating the Froude number at station 3 to 1.0, is not a necessary requirement for smooth flow over a hydrofoil. However, it can be shown that this condition produces maximum flow over the hydrofoil and measurements of flow depth and velocity have confirmed that the Froude number is very close to 1.0 at Station 3 for shallow submergence. For very deep submergence*, Froude number is clearly not equal to 1.0 and instead the condition $Y_3 = -B$ is more appropriate.

---

* Very deep submergence means that the thickness of the flow layer passing over the hydrofoil is significantly greater than the hydrofoil thickness

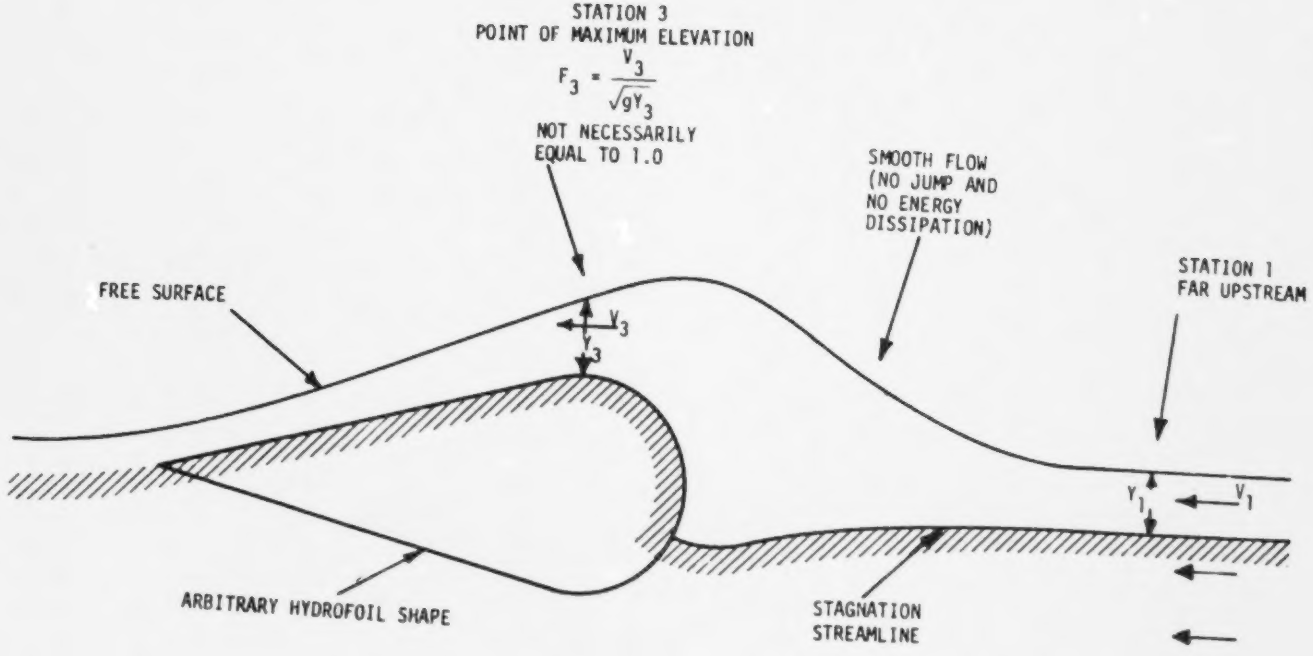
STATION 3
POINT OF MAXIMUM ELEVATION
$F_3 = \frac{V_3}{\sqrt{gY_3}}$
NOT NECESSARILY EQUAL TO 1.0
SMOOTH FLOW (NO JUMP AND NO ENERGY DISSIPATION)
STATION 1 FAR UPSTREAM
FREE SURFACE
V_3
Y_3
Y_1
V_1
ARBITRARY HYDROFOIL SHAPE
STAGNATION STREAMLINE

Figure A-2. Fictitious Bottom Contour For Open Channel Flow Analysis - Smooth Bow Wave Flow Model

Solving these equations in the same manner as the turbulent case gives the following results:

$$\left.\begin{aligned} &(13)\quad G_3 = \frac{1}{3}(1 - 2G_B) \\ &(14)\quad G_1 = (G_3)^{3/2} = \left[\frac{1}{3}(1 - 2G_B)\right]^{3/2} \end{aligned}\right\} \text{ if } \frac{V_3{}^2}{gY_3} = 1.0$$

$$(15)\quad Q = \frac{G_1 V_1{}^3}{g}$$

The results of the smooth and turbulent analysis can be displayed in graphical form. Figures A-3 and A-4 are plots of G_3 versus G_B and G_1 versus G_B respectively. These graphs may be interpreted as plots of Y_3 and Y_1 against B at constant velocity.

The hydraulic jump is only possible for the range $-1.0 < G_B < 0.07$. For $G_B > 0.07$, the flow does not contain enough energy to flow over the body through a jump, and for $G_B < -1.0$, the local Froude number upstream (at Station 1) is subcritical precluding the existence of a jump. As $G_B \rightarrow -1.0$, the jump strength becomes smaller and the turbulent bow wave curves blend into the smooth flow curves.

For smooth flow the maximum value of G_B is 0.50 and corresponds to the point at which the energy of the flow is just great enought to lift the water to the top of the body. These smooth flow curves represent solutions to the equations with the Froude number at Station 3 equal to 1.0. With Froude number at the top of the body less than 1.0, the value of G_3 will be greater than that plotted and similarly if the Froude number at the top of the hydrofoil is greater than 1.0, the value of G_3 will be less than that plotted. For very deep submergence, there will be little disturbance to the free surface, and G_3 will be approximately equal to $-G_B$. This deep submergence relationship is also shown in Figure A-3.

The phenomenological theory can be extended to include the three-dimensional effects associated with non-uniform velocity profiles. Figure A-5 shows the typical three-dimensional phenomena observed when flow with a non-uniform velocity profile approaches a two-dimensional hydrofoil. The velocity profile shown with velocity defects near the end of the hydrofoil's span is similar to that measured in the small scale experiments and was produced by hydrodynamic friction along the channel side plates. As flow passes upward over the hydrofoil some of the kinetic energy, in the form of velocity head, is converted to potential energy, in the form of the height of the water surface. If the velocity profile is uniform all of the flow passes over the model. However, if there is a boundary layer on the sidewall there will be some region in which the velocity head is not great enough for flow to pass over the top. Flow with higher velocity will then move into this area and form a vortex and the flow in the center of the channel will diverge to the full hydrofoil width.

Experiments with dye injection confirmed this behavior. Referring to Figure A-5, when dye was injected near the surface between points A and B the dye passed over the top of the hydrofoil. When dye was injected at any depth outside this range it passed under the hydrofoil. The width W_1 between points A and B was found to be a function of submergence. For deep submer-

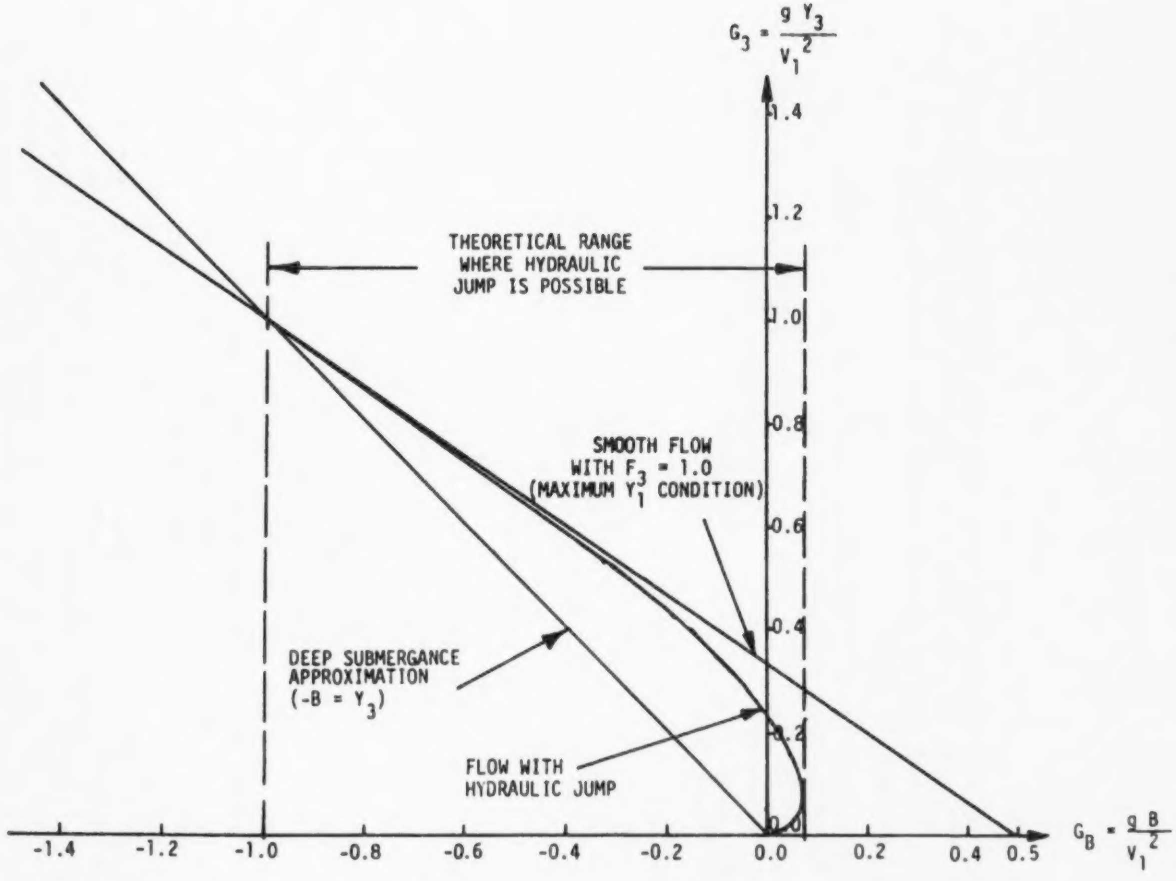

Figure A-3. Theoretical Correlation G_3 vs. G_B

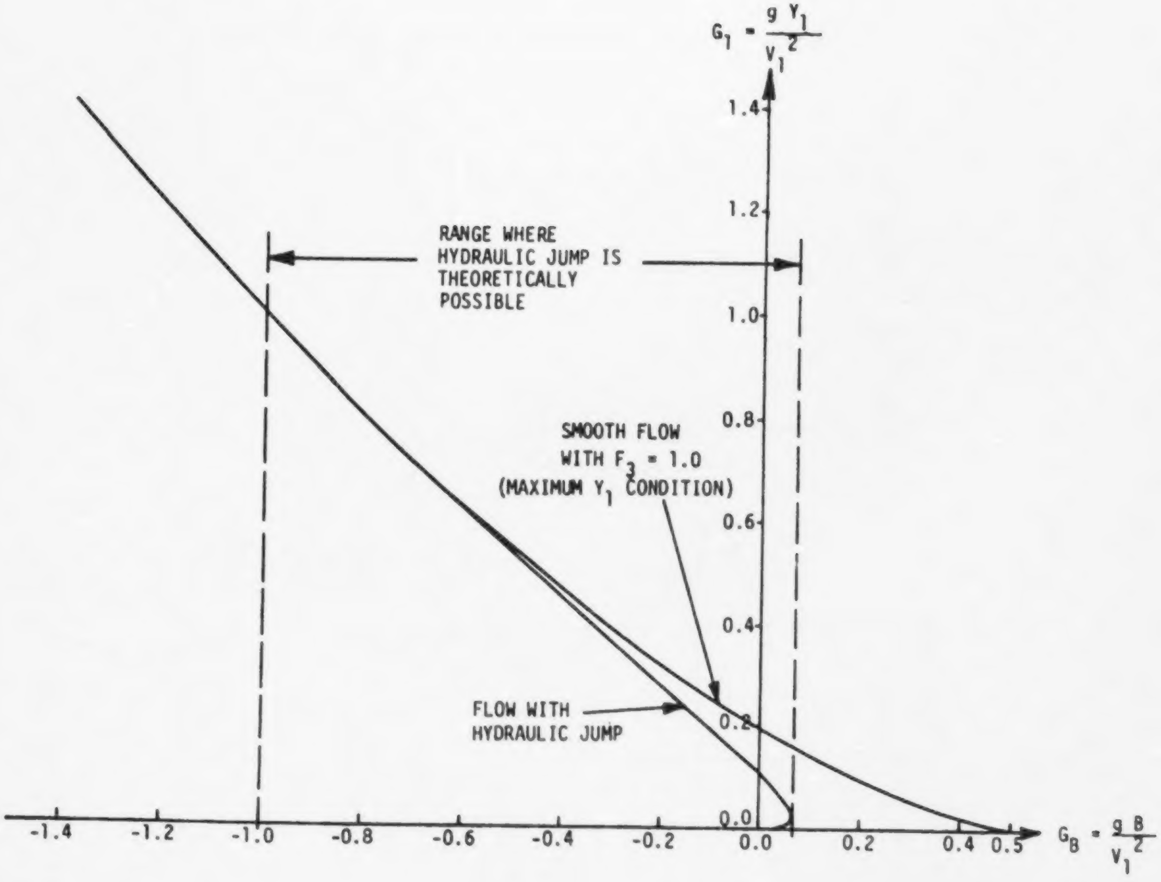

Figure A-4. Theoretical Correlation G_1 vs. G_B

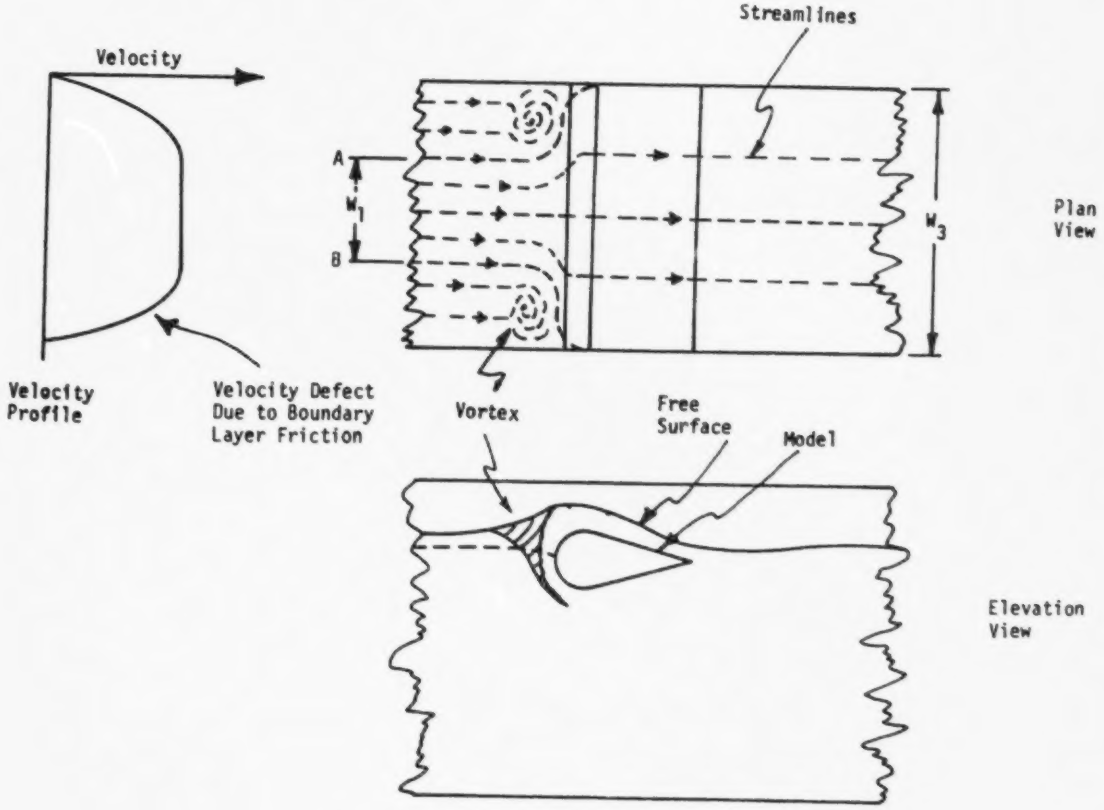
Velocity
Streamlines
A
W1
B
W3
Plan View
Velocity Profile
Velocity Defect Due to Boundary Layer Friction
Vortex
Free Surface
Model
Elevation View

Figure A-5. Three-Dimensional Flow Over Model gence, with little conversion from kinetic to potential energy, W_1 was essentially equal to the total hydrofoil width W_3. As the freeboard was increased the width W_1 decreased and the corner vortices became more pronounced.

The phenomenological theory was extended to describe these three dimensional effects by assuming that the flow passing over the hydrofoil was contained in a diverging channel of width W_1 upstream and W_3 over the top of the hydrofoil and downstream. The continuity equation for the turbulent and smooth bow wave analyses were then modified as follows:

(16) Turbulent Bow Wave Continuity:

$$V_1 \; Y_1 \; W_1 = V_2 \; Y_2 \; W_1 = V_3 \; Y_3 W_3 = QW_3$$

(17) Smooth Bow Wave Continuity:

$$V_1 \; Y_1 \; W_1 = V_3 \; Y_3 \; W_3 = QW_3$$

where Q is the flowrate per unit hydrofoil width.

The equations can be reduced in the same manner as the two-dimensional analyses and give the same results if G_1 is generalized to $G_1{}^*$ as follows:

$$(18) \quad G_1{}^* = \frac{W_3}{W_1} \; G_1$$

and the flowrate Q becomes:

$$(19) \quad Q = G_1{}^* \; \frac{V_1{}^3}{g} \left(\frac{W_1}{W_3}\right)^2$$

The relationship between G_3 and G_B remains unchanged independent of W_1/W_3. Thus if there are no three-dimensional effects, the results revert to the two-dimensional case:

$$W_1/W_3 = 1.0$$

Figure A-6 shows a comparison of data from the dolphin-nose hydrofoil model with the phenomenological theory correlations neglecting three-dimensional effects. As expected, the data points for $gY_3/V_1{}^2$ are close to the theoretical model and the data points for $gY_1/V_1{}^2$ are substantially above theoretical predictions due to three-dimensional effects.

The ratio W_1/W_3 was measured for several data points by dye injection and G_1^* was calculated directly. Thin plastic sideplates were also attached to the model to isolate the flow in the model's center (with uniform velocity) from the low velocity flow near the channel walls. Data points measured on this configuration and those corrected for vortices are shown in Figure A-7 where G_1^* is plotted against G_B. The agreement is quite close.

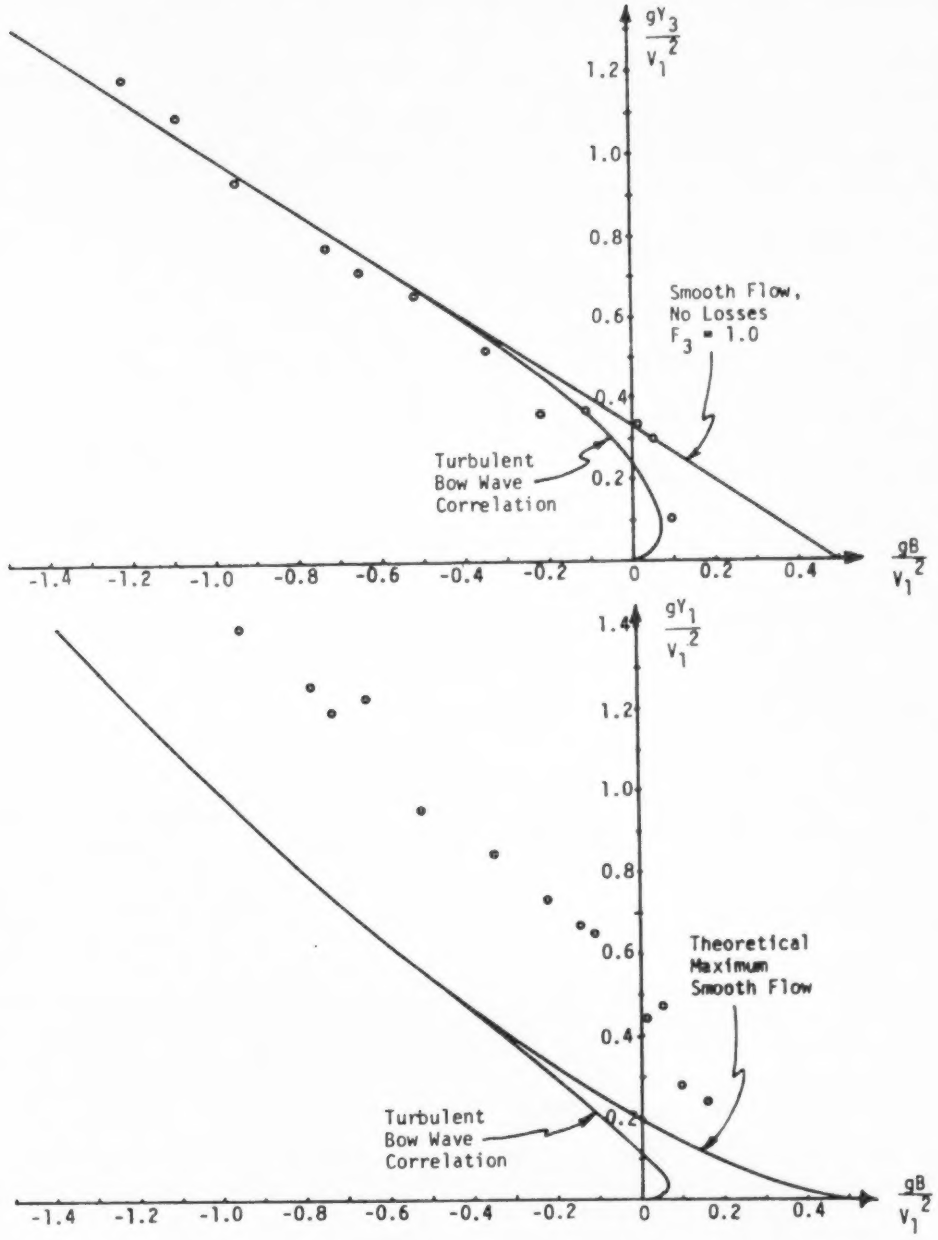

Figure A-6. Dolphin Nose Model - Correlations

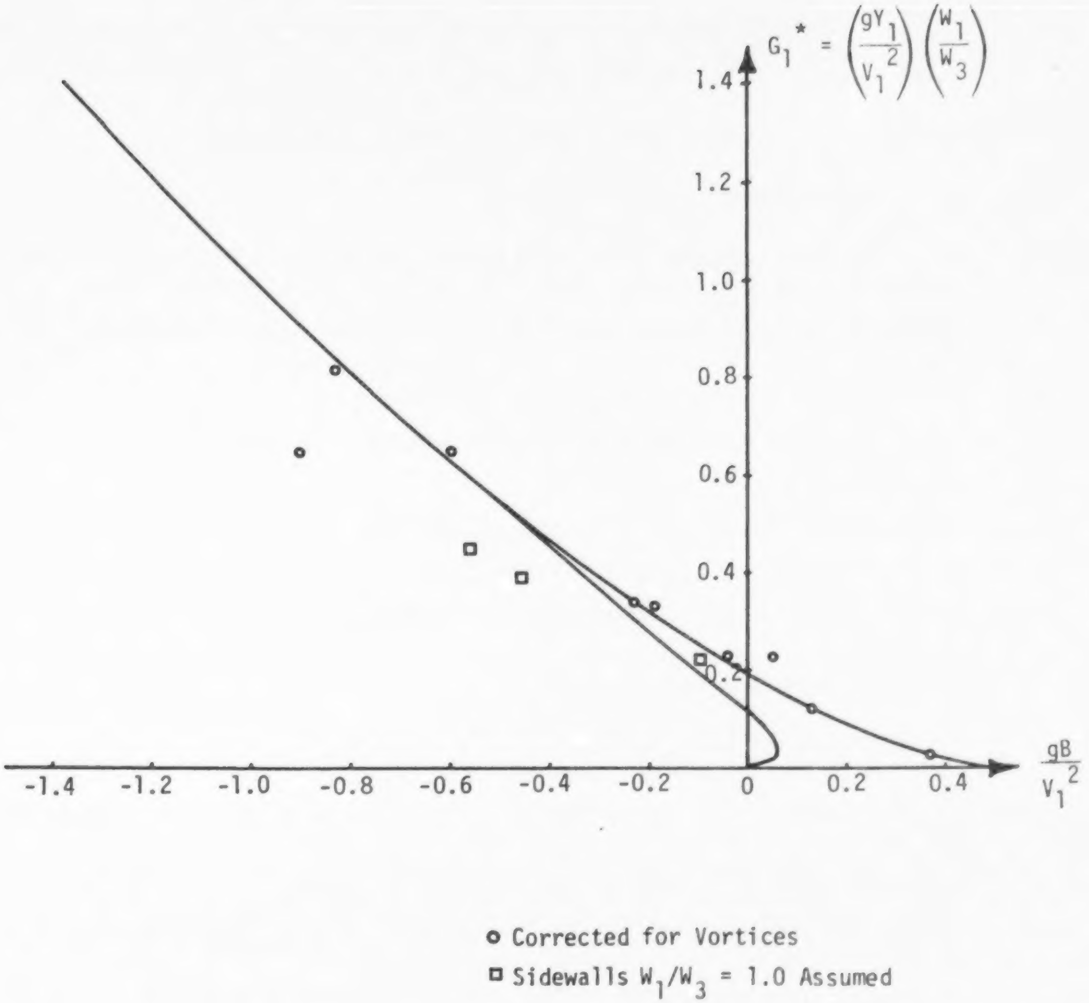

Figure A-7. Dolphin Nose Model Data Corrected For Vortices And Data Taken With Sidewalls

APPENDIX B

DETAILED TEST PROCEDURES - OHMSETT SYSTEM INTEGRATION TESTS

Stability Test Procedure

(1) Test director obtains test number and parameters from Ultrasystems personnel and gives test conditions to control room operator.

(2) Recovered oil from previous test is decanted, sampled measured and then discarded.

(3) ALL residual oil is cleaned from the channel.

(4) Catamaran personnel adjust boom parameters as required.

(5) The skimmer bar is raised.

(6) Test director verifies test conditions with Ultrasystems' personnel.

(7) Wave generator is started, if required.

(8) All test personnel assume their positions.

    (a) Test director
    (b) Photographer
    (c) Control room operator
    (d) Catamaran personnel
    (e) Instrumentation specialist

(9) Test director gives three blasts on the air horn to signal ready for test.

(10) Instrumentation specialist starts wave recorder.

(11) Test director gives one blast on the air horn to signal the start of test.

(12) Test director checks with control room operator for obtaining test speed.

(13) Test director signals when full test speed has been reached.

(14) Catamaran personnel adjust streamlined oil boom parameters if required.

(15) Catamaran personnel record hydrodynamic data.

(16) When bridge nears end of channel, control room operator is notified to bring bridge to a stop.

(17) Wave generator is stopped.

(18) Wave recorder is stopped.

Stability Test Procedure (Continued)

(19) Catamaran personnel raise model stern for return trip.

(20) Bridge is returned to starting position.

(21) All test data is recorded

(22) System is prepared for next test.

Holding Test Procedure

(1) Test director obtains test number and parameters from Ultrasystems personnel and gives test conditions to control room operator.

(2) The recovered oil from previous test is decanted, sampled, measured and then discarded.

(3) ALL residual oil is cleaned from the channel.

(4) Catamaran personnel adjust boom parameters as required.

(5) The oil preload to be used for the test is measured and deposited in the primary sump.

(6) The skimmer bar is raised.

(7) Test director verifies test conditions with Ultrasystems personnel.

(8) Wave generator is started.

(9) All test personnel assume their positions.

    (a) Test director
    (b) Photographer
    (c) Control room operator
    (d) Catamaran personnel
    (e) Instrumentation specialist

(10) Test director gives three blasts on the air horn to signal ready for test.

(11) Instrumentation specialist starts videotape and wave recorder.

(12) Test director gives one blast on the air horn to signal the start of test.

(13) Test director checks with control room operator for obtaining test speed.

(14) Test director signals when full test speed has been reached

(15) Catamaran personnel adjust streamlined oil boom parameters if required.

(16) Catamaran personnel record hydrodynamic data.

(17) When bridge nears end of channel, control room operator is notified to bring bridge to a stop.

Holding Test Procedure (Continued)

(18) As bridge slows to a stop, catamaran personnel lower front dam, hold automatic weir upright and close rear slot as required to hold oil sump.

(19) Wave generator is stopped.

(20) Videotape and wave recorder are stopped.

(21) Skimmer bar is lowered.

(22) Firehose pumps and air compressor are started.

(23) Firehose and recovery pumps are operated as required to pump all oil in main sump and weir into recovery barrels.

(24) Firehose and recovery pumps are stopped on Ultrasystems' command.

(25) Catamaran crew raises model stern for the return trip.

(26) Bridge is returned to starting position skimming any oil not previously recovered.

(27) All test data is recorded on bridge data sheet.

(28) System is prepared for next test.

System Test Procedure

(1) Test director obtains test number and parameters from Ultrasystems personnel and gives test conditions to:

  (a) Control room operator
  (b) Distribution pump operator

(2) The recovered oil from previous test is decanted, sampled, measured and then discarded.

(3) ALL residual oil is cleaned from the channel.

(4) Catamaran personnel adjust boom parameters as required.

(5) Recovery pumps are operated pumping until hoses, etc. are fully filled with water.

(6) The oil preload to be used for the test is measured and deposited in the primary sump.

(7) The oil distribution pumping rate, and the oil recovery pumping rate, are calibrated as required for the test and the flowmeter reading is recorded.

(8) The skimmer bar is raised.

(9) The air compressor used to drive the recovery pumps is started.

(10) Test director verifies test conditions with Ultrasystems personnel.

(11) Wave generator is started.

(12) All test personnel assume their positions.

  - (a) Test director
  - (b) Distribution pump operator
  - (c) Recovery pump operator
  - (d) Recovery hose operator
  - (e) Photographer
  - (f) Control room operator
  - (g) Catamaran personnel
  - (h) Instrumentation specialist

(13) Test director gives three blasts on the air horn to signal ready for test

(14) Instrumentation specialist starts videotape and wave recorder.

(15) Test director gives one blast on the air horn to signal the start of test.

(16) Test director checks with control room operator for obtaining test speed

(17) When test speed is obtained, test director signals to start oil distribution.

(18) Oil distribution operator distributes oil for time period specified in testing matrix as measured with stopwatch.

(19) Oil distribution operator records final flowmeter reading and distribution time from stopwatch.

(20) Oil recovery pump operator starts recovery pumps and stopwatch when first portion of deposited slick reaches sump inlet.

(21) When last of oil slick reach sump inlet:

  - (a) Oil recovery pump operator stops pumps and stopwatch and records time.
  - (b) Test director starts timing post distribution running time.

(22) At end of post distribution running time, test director signals control room operator to slowly stop bridge motion.

(23) As bridge slows to a stop, catamaran personnel lower front dam, hold automatic weir upright and close rear slot as required to hold oil in sump.

(24) Wave generator is stopped.

(25) Videotape and wave recorder are stoped.

(26) Recovery hose operator measures total volume recovered in collection barrels.

(27) Skimmer is lowered.

(28) Firehose pumps are started.

(29) Firehose water is directed into weir box and recovery pumps are operated as required to pump any oil remaining in weir box, hoses, etc. into collection barrels while holding weir upright to prevent mixing of oil in sump with oil in weir box.

System Test Procedure (Continued)

(30) Upon Ultrasystems' command, recovery pumps are stopped and recovery hose is transferred to second set of recovery drums and suction hose is used to clean inventory oil from sump.

(31) Firehose and recovery pumps are operated as required to pump all oil in main sump into second set of recovery barrels.

(32) Firehose and recovery pumps are stopped on Ultrasystems' command and suction hose to weir box is reconnected.

(33) Catamaran crew raises model stern for return trip.

(34) Bridge is returned to starting position skimming any oil not previously recovered.

(35) All test data is recorded on bridge data sheet.

(36) System is prepared for the next test.

APPENDIX C

OIL HANDLING AND EXPERIMENTAL ERRORS - OHMSETT SYSTEMS INTEGRATION TESTS

This appendix describes the oil handling procedures used in performing the oil tests and measuring the input and recovered oil volumes. It also assesses the probable source of inaccuracy and nonrepeatability due to systematic and experimental errors as opposed to variations in the streamlined oil boom's performance.

Oil Handling Procedures

The oils used for testing the streamlined oil boom were part of OHMSETT's standard oil stocks and had been used previously for testing other oil spill control equipment at OHMSETT, Following its previous use, it was skimmed from the tank and allowed to settle for several days as a preliminary oil/water separation. The emulsion on the surface of the tank was then processed through a vacuum distillation unit where nearly all of the emulsified water was removed* and then transferred to storage.

At the beginning of each testing day or as required, oil was pumped into the bridge storage tanks and a sample of the oil was withdrawn and analyzed for specific gravity, viscosity, surface tension, interfacial surface tension and water content. The values changed little from day to day and Table 4 (page 70) gives the average properties.

Handling of the oil inputs to the tests is shown schematically in Figure C-1. All hoses, pumps, etc were completely filled with oil prior to the start of the tests. The sump preload was pumped from the bridge oil tank through a positive displacement flowmeter and a 5.0 cm (2 inch) discharge hose directly into the sump. A ball valve on the dischage end of the hose was used to maintain the hose full of oil at all times and eliminate inaccuracies due to drainage and syphoning. The flowmeter was set to zero at the beginning of each pumping cycle and the ball valve and pump were started simultaneously. When the required volume had been pumped, the ball valve and pump were shut off and the flowmeter volume was recorded to the nearest 0.5 gallon.**

---

* Residual water and sediment control was approximately 0.1%

** All oil volumes were measured in gallons. One gallon is equivalent to 3.7853 liters.

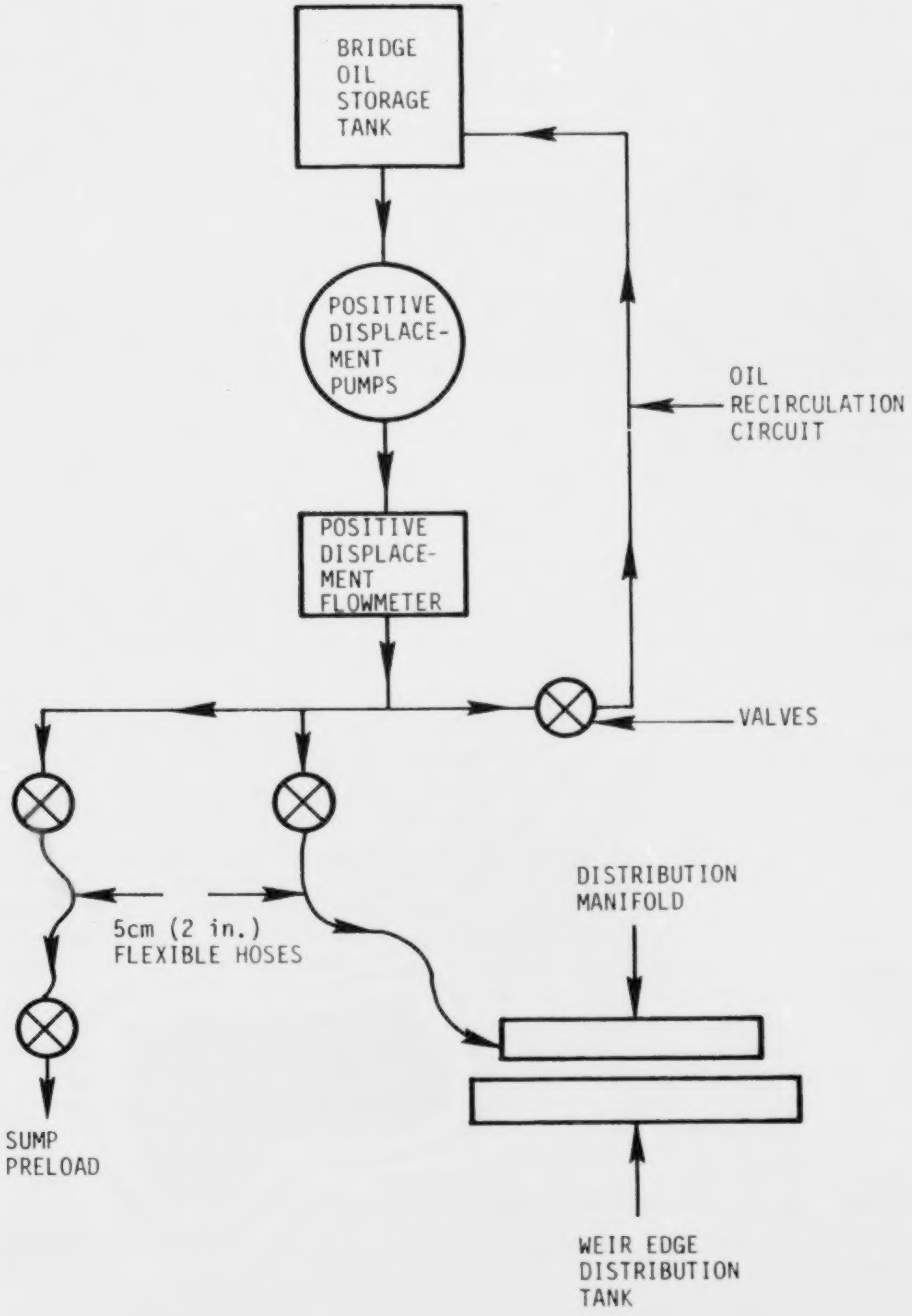
BRIDGE
OIL
STORAGE
TANK
POSITIVE
DISPLACE-
MENT
PUMPS
POSITIVE
DISPLACE-
MENT
FLOWMETER
OIL
RECIRCULATION
CIRCUIT
VALVES
5cm (2 in.)
FLEXIBLE HOSES
DISTRIBUTION
MANIFOLD
SUMP
PRELOAD
WEIR EDGE
DISTRIBUTION
TANK

Figure C-1. Oil Input - Schematic Diagram

When oil was to be distributed as a slick, the pumps were adjusted to the required flowrate by circulating the oil through the flowmeter and back to the storage tank. The pumps were then stopped, the flowmeter set to zero and the valves adjusted to distribute oil into the distribution manifold and weir edge distribution tank. During the test, the pumps were operated for a predetermined time period and the volume distributed was recorded to the nearest 0.5 gallon.

Handling of the recovered oil is shown schematically in Figure C-2. Two air operated double diapharagm pumps were used in parallel to recover the oil/water mixture from the weir skimmer.* The pump outputs were manifolded together and discharged into a series of 100-gallon recovery barrels mounted on the rear bridge. When recovery efficiency was to be measured, the pumps, hoses, etc. were preloaded with water and the total volume of oil and water pumped during the run was measured as the volume collected in the recovery barrels.

To insure that all oil was recovered from the pumps, hoses, etc., approximately 80 gallons of water were pumped through the system after the last visible oil entered the suction hoses.**

The recovered oil/water mixture was allowed to settle for at least 1/2 hour or until a clearly visible oil/water interface was visible. The excess water was then drained off and the depth of the remaining mixture was measured to the nearest 1/8-inch and converted to a volume measurement. One eighth inch corresponds to approximately 3/8 gallon. A motor driven propeller was then inserted into the mixture and operated to thoroughly mix the oil and water. One or more samples of this mixture were then withdrawn for laboratory analysis.

The percentage of water and sediment in the sample was measured according to ASTM standards*** and used to correct the recovered volumes.

Systematic Errors

The systematic errors associated with oil volume measurements can be calculated from the precision of the oil handling methods. The two main error sources are the measurement of the sample water content and the measurement of the total mixture volumes.

The ASTM method used to measure water content utilized a centrifuging technique where the oil sample was mixed with an equal volume of toluene and centrifuged in pre-calibrated pear-shaped tubes as shown in Figure C-3. The percent water and sediment in the sample was calculated by doubling the separated water volume. The accuracy of this procedure is limited by the calibration on the tube. The error in corrected oil volume associated with the minimum calibration divisions as a function of percent water in the sample as shown in Figure C-4. These errors may be interpreted as the

---

* A portion of the final sump oil volume was recovered by pumping directly out of the sump to retrieve the oil trapped underneath the stability control system float.

** The volume of the pumps and hoses was approximately 50 gallons.

*** ASTM designation D 96-73 Standard Methods of Test for Water and Sediment in Crude Oils.

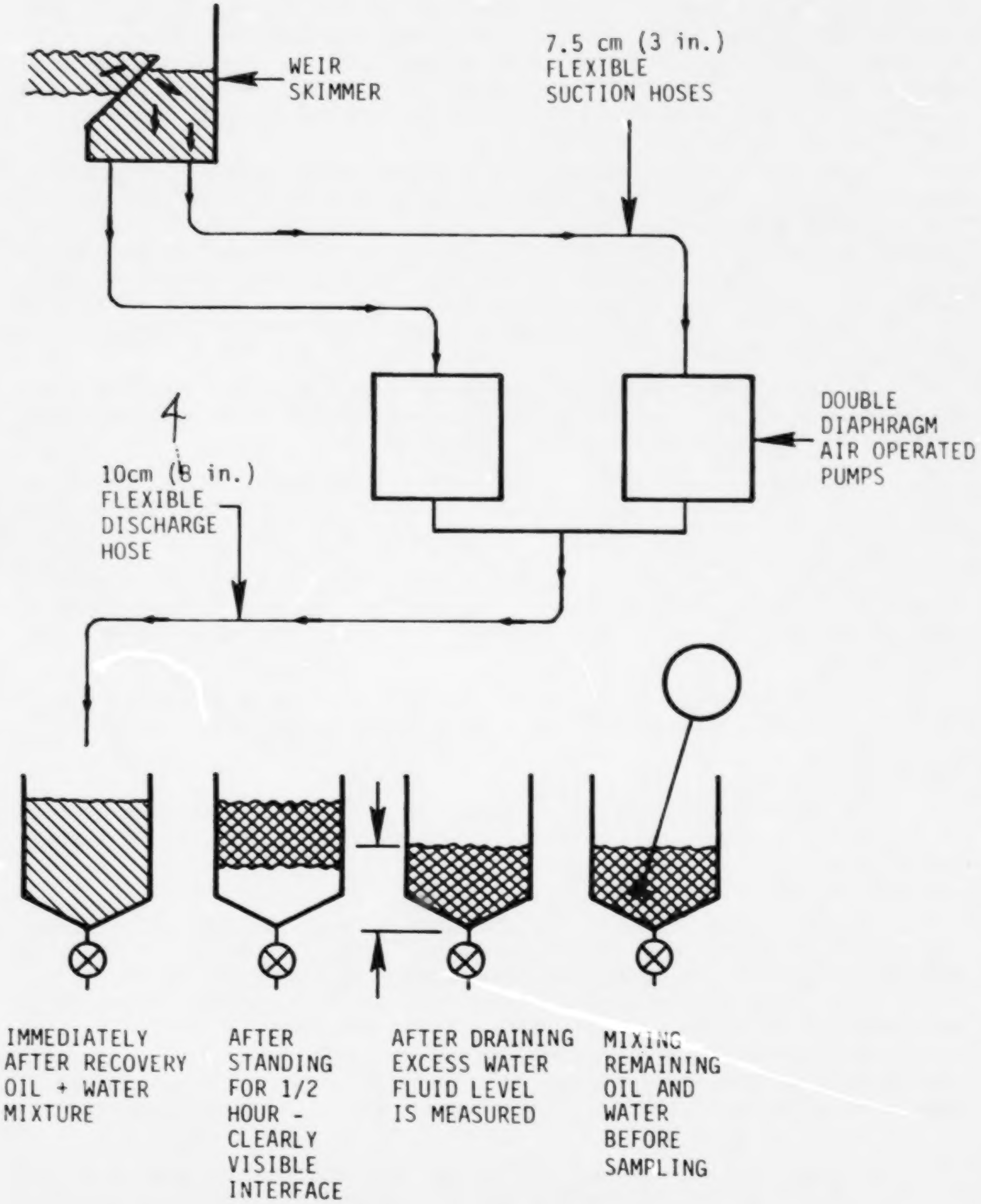
WEIR
SKIMMER
7.5 cm (3 in.)
FLEXIBLE
SUCTION HOSES
DOUBLE
DIAPHRAGM
AIR OPERATED
PUMPS
4
10cm (8 in.)
FLEXIBLE
DISCHARGE
HOSE
IMMEDIATELY
AFTER RECOVERY
OIL + WATER
MIXTURE
AFTER
STANDING
FOR 1/2
HOUR -
CLEARLY
VISIBLE
INTERFACE
AFTER DRAINING
EXCESS WATER
FLUID LEVEL
IS MEASURED
MIXING
REMAINING
OIL AND
WATER
BEFORE
SAMPLING

Figure C-2. Oil Recovery - Schematic Diagram

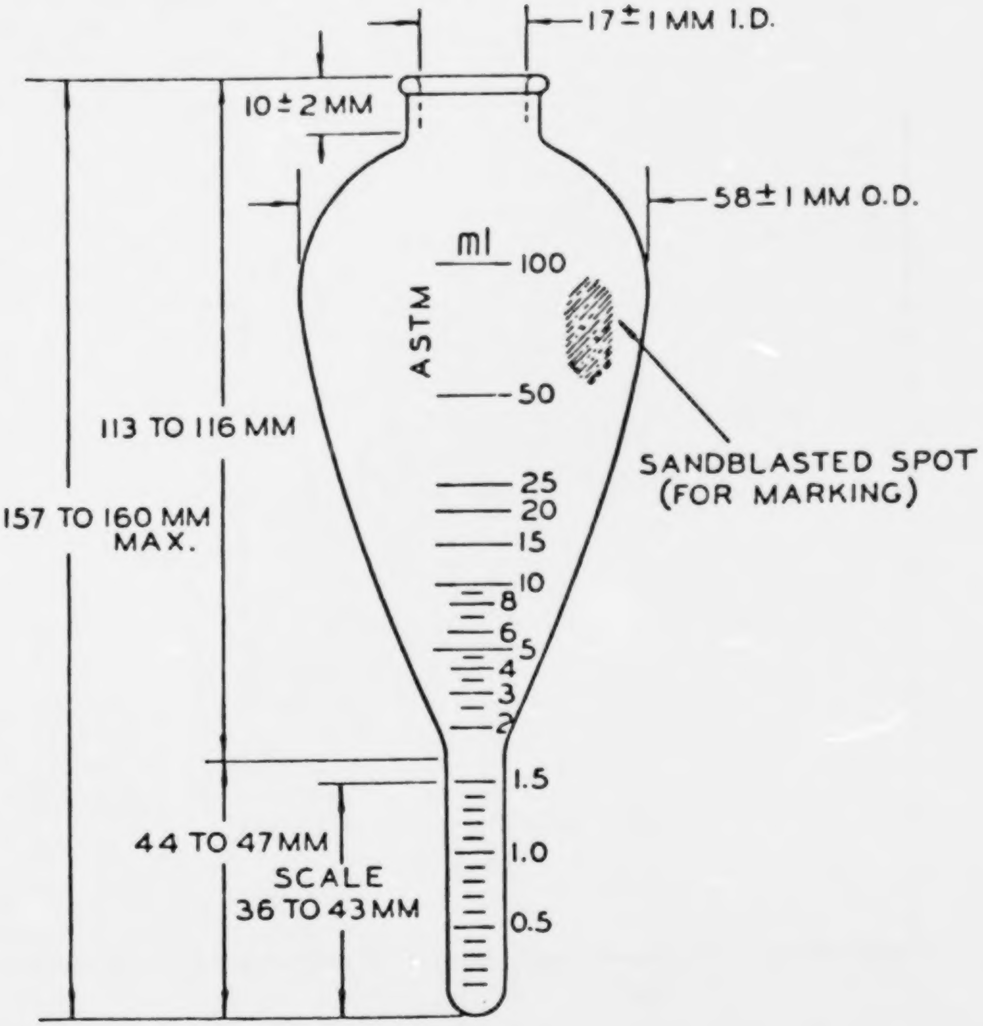
17 ± 1 MM I.D.
10 ± 2 MM
58 ± 1 MM O.D.
ml
100
ASTM
50
25
20
15
10
8
6
5
4
3
2
1.5
1.0
0.5
SANDBLASTED SPOT
(FOR MARKING)
113 TO 116 MM
157 TO 160 MM
MAX.
44 TO 47 MM
SCALE
36 TO 43 MM

Figure C-3. Pear-Shaped Centrifuge Tube from ASTM Designation D 96-73
API Standard 2542
"Standard Method Of Test For Water
And Sediment In Crude Oils"

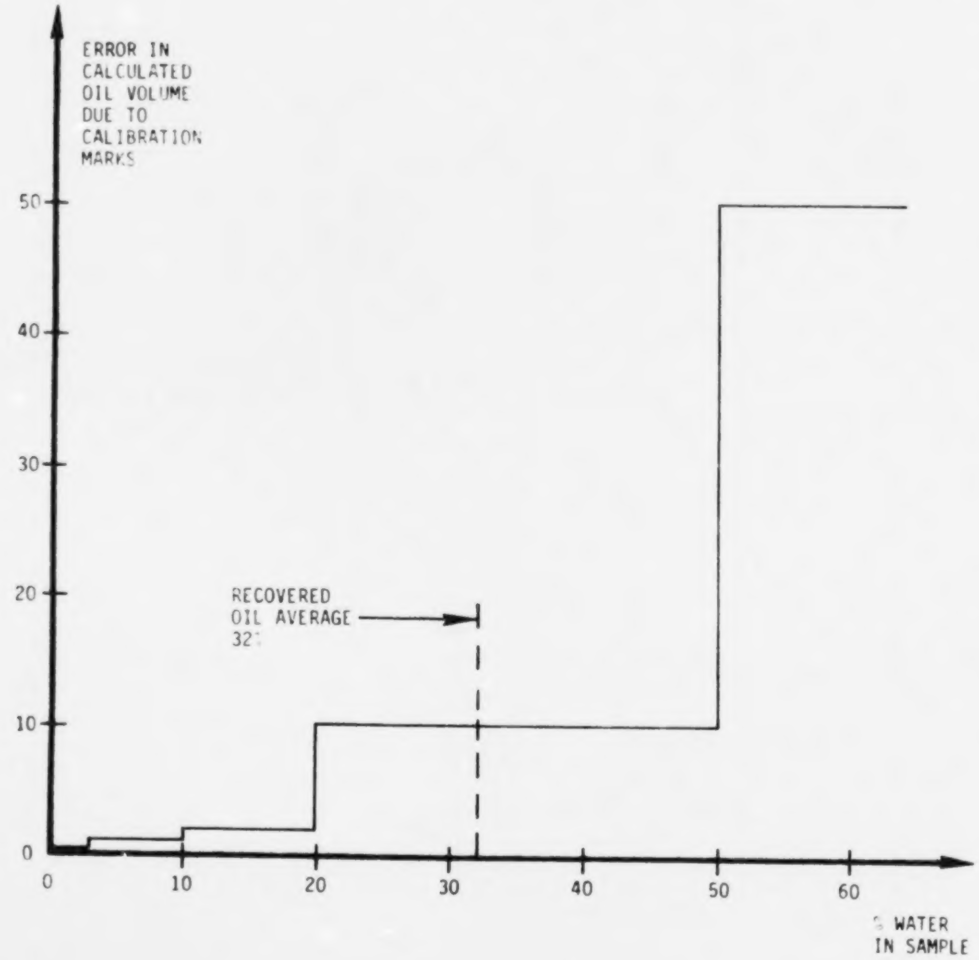

Figure C-4. Error Associated With Minimum Calibration Divisions On Centriguge Tube ASTM D96-73 maximum error due to misreading the calibrations by one of the smallest gradations. The percentage of water in the oil inputs to the tests were 0.1 percent on the average and the error associated with this water content is 0.2 percent.

Figure C-5 is a histogram showing the distribution of the percentage water in the recovered oil samples. The average water content of the 32 percent corresponds to an error in oil volume of 10 percent.

The errors associated with the measurement of oil volumes may be estimated from the precision of the volume measurements and the magnitude of the volumes measured.

The oil inputs were measured to the nearest 0.5 gallon with a positive displacement flowmeter. Two oil preload volumes were used, 40 gallons and 75 gallons with an average of 49 gallons. A range of oil slick volumes were used with a minimum of 31 gallons, a maximum of 189 gallons and an average of 94 gallons. The percentage errors in oil volumes associated with measurement errors of 0.5 gallon are shown in Figure C-6. The average error for the preload volume was 1.0 percent and for the oil slick volume it was 0.5 percent.

Recovered oil volumes were measured by recording the depth of the oil layer in 100 gallon recovery barrels* to the nearest 1/8 inch. Up to five barrels were used for each test. Figure C-7 is a histogram showing the distribution of recovered oil volumes measured. The 1/8 inch uncertainty in oil layer thickness corresponds to approximately 0.375 gallon and the percentage error as a function of sample volume is shown in Figure C-8. The average 48 gallon oil volume corresponds to an error of 0.8 percent.

Table C-1 summarizes these systematic errors for average test conditions. The majority of the total error is due to recovered oil and is primarily due to the limitations of the water content measurement procedure.

Other Errors

There are several other non-quantifiable sources of error. These include losses and uncertainty due to:

- Oil volume in weir edge distribution tank
- Oil distributed beneath the surface instead of as a slick
- Oil not encountering the streamlined oil boom

---

* A 15-gallon barrel was used for two samples and a 500-gallon barrel was used for one sample.

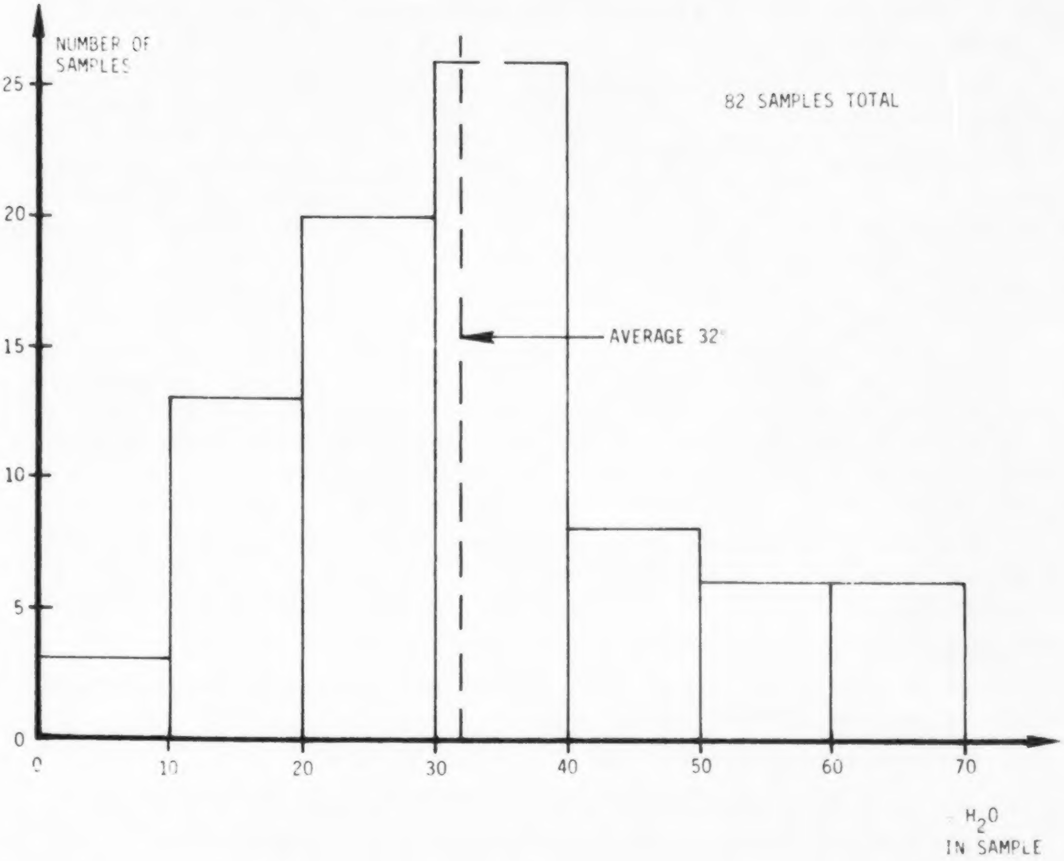

Figure C-5. Histogram of % Water In Recovered Oil Samples

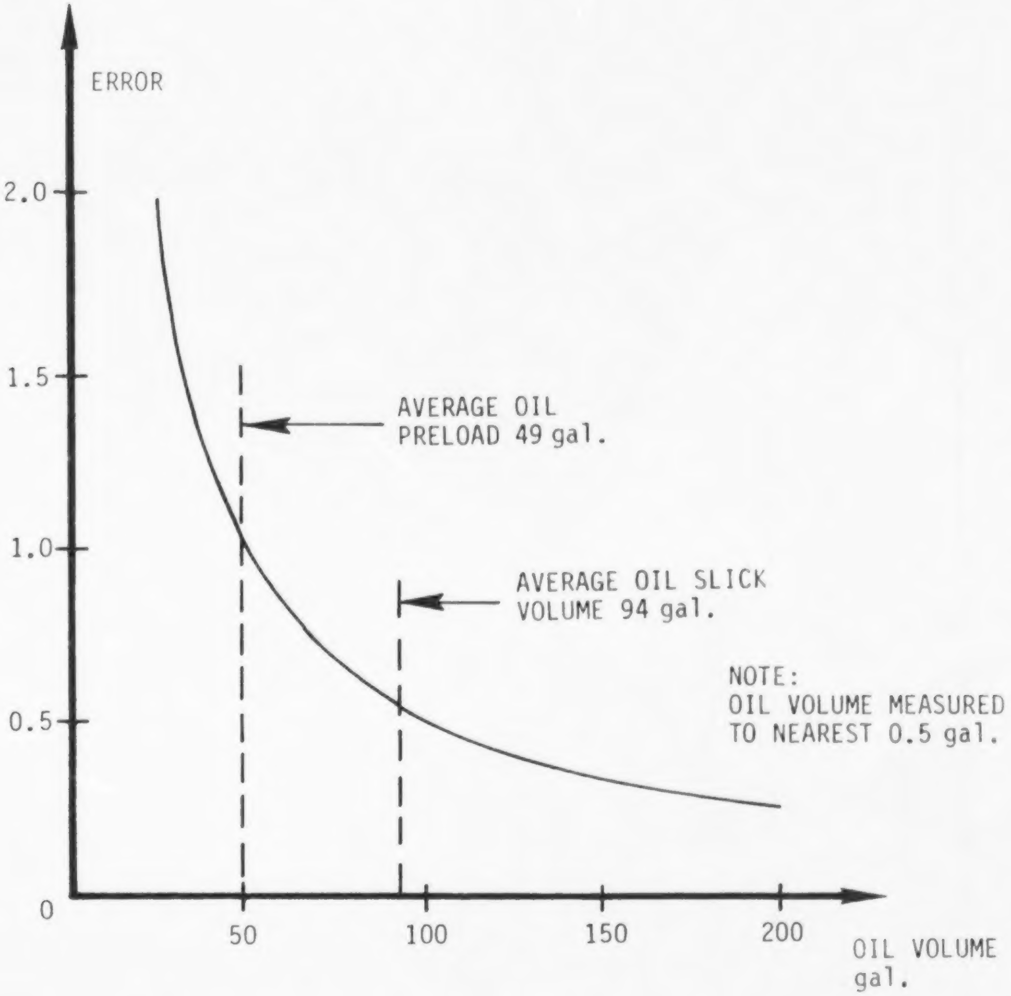

Figure C-6. Error Due To Oil Input Volume Measurement

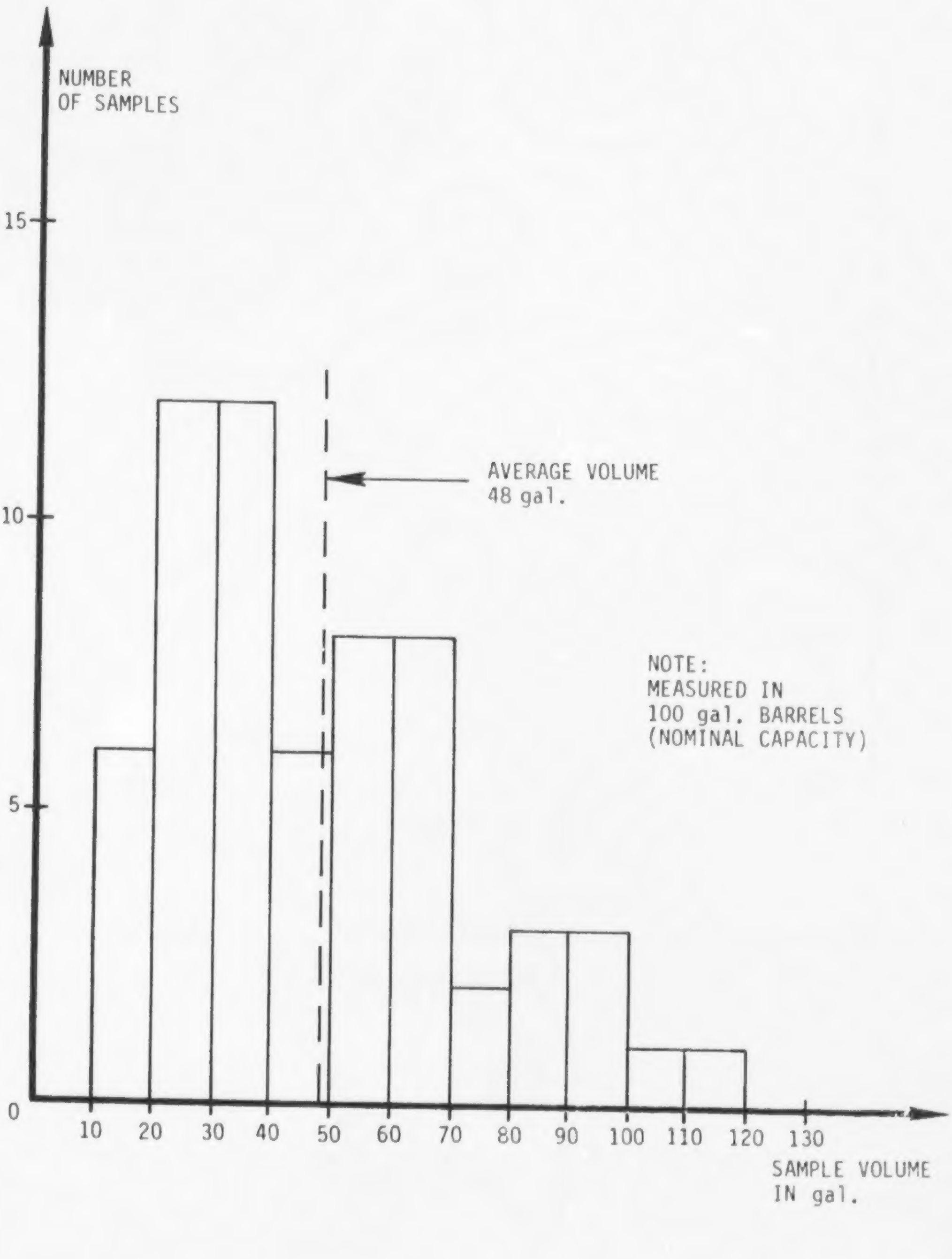

Figure C-7 Histogram Of Recovered Oil Volumes

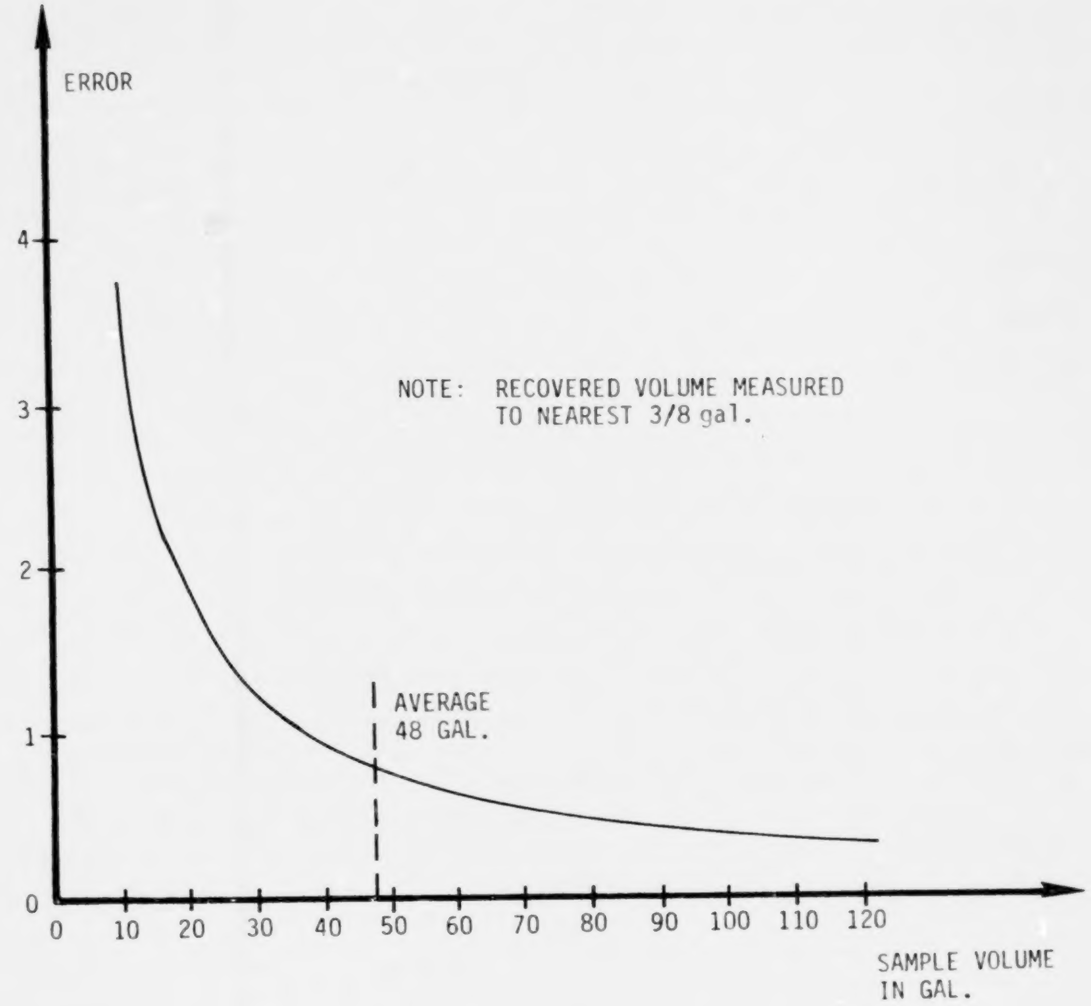

Figure C-8. Error Due To Recovered Volume Measurement

Table C-1. OIL VOLUME MEASUREMENT SUMMARY - ERRORS DUE TO MINIMUM CALIBRATION DIVISIONS

	Percent Error		
Volume	Volume Measurement	Water Content Measurement	Total
Preload	1.0	0.2	1.2
Slick	0.5	0.2	0.7
Recovered Oil	0.8	10.0	10.8

- Residual oil in the channel
- Oil coating pumps, hoses, streamlined oil boom, etc.
- Oil lost in switching recovery hose between barrels
- Start-up and shut down transients
- Oil lost in draining excess water from recovery barrels

Most of these sources of error are oil losses associated with the test procedure and as a result, the calculated values of thruput and recovery efficiencies probably tend to be lower than the actual volumes.

Considering all factors, the total probable experimental error for the thruput and recovery efficiencies is estimated to be +15 to -10 percent.